Thermodynamic Properties of Air and Mixtures of Nitrogen, Argon, and Oxygen From 60 to 2000 K at Pressures to 2000 MPa

Eric W. Lemmon[a)]
Physical and Chemical Properties Division, National Institute of Standards and Technology, 325 Broadway, Boulder, Colorado 80303

Richard T Jacobsen and Steven G. Penoncello
Center for Applied Thermodynamic Studies, College of Engineering, University of Idaho, Moscow, Idaho 83844

Daniel G. Friend
Physical and Chemical Properties Division, National Institute of Standards and Technology, 325 Broadway, Boulder, Colorado 80303

Received June 28, 1999; revised manuscript received December 2, 1999

A thermodynamic property formulation for standard dry air based upon available experimental $p-\rho-T$, heat capacity, speed of sound, and vapor–liquid equilibrium data is presented. This formulation is valid for liquid, vapor, and supercritical air at temperatures from the solidification point on the bubble-point curve (59.75 K) to 2000 K at pressures up to 2000 MPa. In the absence of reliable experimental data for air above 873 K and 70 MPa, air properties were predicted from nitrogen data in this region. These values were included in the determination of the formulation to extend the range of validity. Experimental shock tube measurements on air give an indication of the extrapolation behavior of the equation of state up to temperatures and pressures of 5000 K and 28 GPa. The available measurements of thermodynamic properties of air are summarized and analyzed. Separate ancillary equations for the calculation of dew and bubble-point pressures and densities of air are presented. In the range from the solidification point to 873 K at pressures to 70 MPa, the estimated uncertainty of density values calculated with the equation of state is 0.1%. The estimated uncertainty of calculated speed of sound values is 0.2% and that for calculated heat capacities is 1%. At temperatures above 873 K and 70 MPa, the estimated uncertainty of calculated density values is 0.5% increasing to 1.0% at 2000 K and 2000 MPa. In addition to the equation of state for standard air, a mixture model explicit in Helmholtz energy has been developed which is capable of calculating the thermodynamic properties of mixtures containing nitrogen, argon, and oxygen. This model is valid for temperatures from the solidification point on the bubble-point curve to 1000 K at pressures up to 100 MPa over all compositions. The Helmholtz energy of the mixture is the sum of the ideal gas contribution, the real gas contribution, and the contribution from mixing. The contribution from mixing is given by a single generalized equation which is applied to all mixtures used in this work. The independent variables are the reduced density and reduced temperature. The model may be used to calculate the thermodynamic properties of mixtures at various compositions including dew and bubble-point properties and critical points. It incorporates the most accurate published equation of state for each pure fluid. The mixture model may be used to calculate the properties of mixtures generally within the experimental accuracies of the available measured properties. The estimated uncertainty of calculated properties is 0.1% in density, 0.2% in the speed of sound, and 1% in heat capacities. Calculated dew and bubble-point pressures are generally accurate to within 1%. *© 2000 American Institute of Physics.* [S0047-2689(00)00103-3]

Key words: air, argon, density, equation of state, mixtures, nitrogen, oxygen, pressure, thermodynamic properties, vapor–liquid equilibrium.

[a)]Electronic mail: ericl@boulder.nist.gov

Contents

List of Tables

List of Figures

List of Symbols

Symbol	Physical quantity	Unit
A	Helmholtz energy	J
a	Molar Helmholtz energy	J/mol
B	Second virial coefficient	dm^3/mol
B_s	Adiabatic bulk modulus	MPa
C	Third virial coefficient	$(dm^3/mol)^2$
c_p	Isobaric heat capacity	J/(mol·K)
c_v	Isochoric heat capacity	J/(mol·K)
f	Fugacity	MPa
F	Mixture coefficient	
g	Gibbs energy	J/mol
h	Enthalpy	J/mol
k	Isentropic expansion coefficient	
K_T	Isothermal bulk modulus	MPa
k_T	Isothermal expansion coefficient	
M	Molar mass	g/mol
N	Coefficients of equations	
n	Number of moles	mol
p	Presssure	MPa
R	Universal gas constant ($8.314\,510 \pm 0.000\,070$)	J/(mol·K)
s	Entropy	J/(mol·K)
T	Temperature	K
u	Internal energy	J/mol
v	Molar volume	dm^3/mol
V	Total volume	dm^3
w	Speed of sound	m/s
X	Mixture composition array	
x	Mole fraction (liquid mole fraction for VLE calculations)	
y	Vapor mole fraction for VLE calculations	
Z	Compressibility factor	
α	Reduced Helmholtz energy	
β	Volume expansivity	1/K
β_s	Adiabatic compressibility	1/MPa
δ	Reduced density, $\delta = \rho/\rho_c$ or $\delta = \rho/\rho_j$	
γ	Heat capacity ratio	

κ	Isothermal compressibility	1/MPa
μ	Chemical potential	J/mol
μ_J	Joule–Thomson coefficient	K/MPa
ρ	Density	mol/dm^3
τ	Reduced temperature, $\tau=T_c/T$ or $\tau=T_j/T$	
ω	Acentric factor	
ξ	Mixture coefficient for reduced density	dm^3/mol
ζ	Mixture coefficient for reduced temperature	K
φ	Constant in melting line equation	

Superscripts

0	Ideal gas property
E	Excess-like property
f	Freezing property
idmix	Ideal solution property
r	Residual property
$'$	Liquid phase property
$''$	Vapor phase property

Subscripts

0	Reference state property
c	Critical point property
calc	Calculated point property
exp	Experimental value
i	Property of a component in the mixture
j	Maxcondentherm property
nbp	Normal boiling point property
nbpl	Normal boiling point liquid property
nbpv	Normal boiling point vapor property
o	Initial state point for shock tube calculations
p	Maxcondenbar property
r	Reduced property
red	Reducing property
s	Solidification point property
tp	Triple point property
tpl	Triple point liquid property
tpv	Triple point vapor property

Fixed Points for Air

Symbol	Quantity	Value[b]
T_j	Maxcondentherm temperature	132.6312 K
p_j	Maxcondentherm pressure	3.78502 MPa
ρ_j	Maxcondentherm density	10.4477 mol/dm^3
T_p	Maxcondenbar temperature	132.6035 K
p_p	Maxcondenbar pressure	3.7891 MPa
ρ_p	Maxcondenbar density	11.0948 mol/dm^3
T_c	Critical temperature	132.5306 K
p_c	Critical pressure	3.7860 MPa
ρ_c	Critical density	11.8308 mol/dm^3
T_s	Solidification point temperature	59.75 K
p_s	Solidification point pressure	0.005265 MPa
ρ_s	Solidification point density	33.067 mol/dm^3
T_{nbp}	Normal boiling point temperature[a]	78.903 K
ρ_{nbpl}	Normal boiling point density (liquid)[a]	30.216 mol/dm^3
M	Molar mass	28.9586 ± 0.0002 g/mol
T_0	Reference temperature	298.15 K
p_0	Reference pressure	0.101 325 MPa
h_0^0	Reference enthalpy at T_0	8649.34 J/mol
s_0^0	Reference entropy at T_0 and p_0	194.0 J/(mol·K)

[a]Normal boiling point properties are calculated on the bubble-point curve at 0.101 325 MPa.
[b]Uncertainties are reported at the 2σ confidence level; those for the critical parameters are given in Table 9.

Fixed Points for Nitrogen

Symbol	Quantity	Value[a]
T_c	Critical temperature	126.192 K
p_c	Critical pressure	3.3958 MPa
ρ_c	Critical density	11.1839 mol/dm^3
T_{tp}	Triple point temperature	63.151 K

p_{tp}	Triple point pressure	0.012 523 MPa
ρ_{tpv}	Triple point density (vapor)	0.024 07 mol/dm^3
ρ_{tpl}	Triple point density (liquid)	30.957 mol/dm^3
T_{nbp}	Normal boiling point temperature	77.355 K
ρ_{nbpv}	Normal boiling point density (vapor)	0.1646 mol/dm^3
ρ_{nbpl}	Normal boiling point density (liquid)	28.775 mol/dm^3
ω	Acentric factor	0.037
M	Molar mass	28.013 48 g/mol
T_0	Reference temperature	298.15 K
p_0	Reference pressure	0.101 325 MPa
h_0^0	Reference enthalpy at T_0	8670.0 J/mol
s_0^0	Reference entropy at T_0 and p_0	191.5 J/(mol·K)

[a]Span *et al.* (2000) report the constants given here and their associated uncertainties; temperatures for nitrogen are given on ITS-90.

Fixed Points for Argon

Symbol	Quantity	Value[a]
T_c	Critical temperature	150.687 K
p_c	Critical pressure	4.863 MPa
ρ_c	Critical density	13.407 mol/dm^3
T_{tp}	Triple point temperature	83.8058 K
p_{tp}	Triple point pressure	0.068891 MPa
ρ_{tpv}	Triple point density (vapor)	0.1015 mol/dm^3
ρ_{tpl}	Triple point density (liquid)	35.465 mol/dm^3
T_{nbp}	Normal boiling point temperature	87.302 K
ρ_{nbpv}	Normal boiling point density (vapor)	0.1445 mol/dm^3
ρ_{nbpl}	Normal boiling point density (liquid)	34.930 mol/dm^3
ω	Acentric factor	−0.002
M	Molar mass	39.948 g/mol
T_0	Reference temperature	298.15 K
p_0	Reference pressure	0.101 325 MPa
h_0^0	Reference enthalpy at T_0	6197.0 J/mol
s_0^0	Reference entropy at T_0 and p_0	154.737 J/(mol·K)

[a]Tegeler *et al.* (1999) report the constants given here and their associated uncertainties; temperatures for argon are given on ITS-90.

Fixed Points for Oxygen

Symbol	Quantity	Value[a]	Value (ITS-90)
T_c	Critical temperature	154.581 K	154.595 K
p_c	Critical pressure	5.043 MPa	
ρ_c	Critical density	13.63 mol/dm^3	
T_{tp}	Triple point temperature	54.361 K	54.359 K
p_{tp}	Triple point pressure	0.000 146 3 MPa	
ρ_{tpv}	Triple point density (vapor)	0.000 323 7 mol/dm^3	
ρ_{tpl}	Triple point density (liquid)	40.816 mol/dm^3	
T_{nbp}	Normal boiling point temperature	90.188 K	90.196 K
ρ_{nbpv}	Normal boiling point density (vapor)	0.1396 mol/dm^3	
ρ_{nbpl}	Normal boiling point density (liquid)	35.663 mol/dm^3	
ω	Acentric factor	0.022	
M	Molar mass	31.9988 g/mol	
T_0	Reference temperature	298.15 K	
p_0	Reference pressure	0.101 325 MPa	
h_0^0	Reference enthalpy at T_0	8680.0 J/mol	
s_0^0	Reference entropy at T_0 and p_0	205.043 J/(mol·K)	

[a]Schmidt and Wagner (1985) report the constants given here and their associated uncertainties; temperatures for oxygen are given on IPTS-68 consistent with the equation of state, and on ITS-90 in the last column.

1. Introduction

1.1. Background

The measurement of experimental data and the development of equations for the thermophysical properties of air and mixtures of nitrogen, argon, and oxygen has been a continuing project at the Center for Applied Thermodynamic Studies at the University of Idaho and the National Institute of Standards and Technology for more than 10 years. The experimental measurements on air are summarized by Haynes *et al.* (1998). Equations of state for air as a pseudopure fluid were published by Jacobsen *et al.* (1990a), (1992). In addition, an extended corresponding states model for calculating the thermodynamic properties of nitrogen–argon–oxygen mixtures was published by Clarke *et al.* (1994), and a Lagrangian interpolation model for calculating vapor–liquid equilibrium properties for this system was published by Lemmon *et al.* (1992). A preliminary equation of state for air valid to temperatures of 2000 K and pressures to 2000 MPa was published by Panasiti *et al.* (1999), and a new model for mixtures of nitrogen, argon, and oxygen was reported by Lemmon and Jacobsen (1998), (1999). The equations of state for air of Jacobsen *et al.* (1990a), (1992) were reported on the International Practical Temperature Scale of 1968 (IPTS-68). Version 1.0 of the NIST standard reference database for air [Lemmon (1998)] was based on the equation of state of Jacobsen *et al.* (1992). The new equation of state and mixture model presented here are based on the International Temperature Scale of 1990 (ITS-90).

Atmospheric air is a mixture of fluids including nitrogen, oxygen, argon, carbon dioxide, water vapor, and other trace elements. The standard air considered in this report is dry and contains no carbon dioxide or trace elements. The composition of air used here was reported by Olien (1987) based on the work of Jones (1978). It is consistent with that of the U.S. Standard Atmosphere (1976). Other compositions are given by Giacomo (1982) and Waxman and Davis (1978). The mole fractions of nitrogen, oxygen, argon, and carbon dioxide in air from each of the references listed above are given in Table 1.

In the analysis of Olien (1987), the values of Waxman and Davis (1978) were excluded because they are based on a purified, rather than natural, sample. The difference between the U.S. standard atmosphere (1976) and values from Jones (1978) is that Jones used a more accurate value for the composition of argon. The differences between Giacomo (1982) and the U.S. standard atmosphere are greater than those for values from Jones. Although the argon value given by Giacomo is essentially the same as that given by Jones, the carbon dioxide value given by Giacomo is for a laboratory setting in which human respiration generally increases carbon dioxide concentration and decreases oxygen concentration. Therefore, the compositions given by Giacomo were not used. Rather, the compositions given by Jones, truncated to four significant digits as indicated in Table 2, were used. In this work, the concentration of carbon dioxide is assumed negligible. The normalized values based upon this assumption are given in Table 3. An analysis of experimental measurements on air at different compositions than that reported here showed that the change caused by the difference in composition was less than the experimental error in the measurements, and hence, no effort was made to transform measurements at different air compositions to the composition reported here.

A property formulation is the set of equations used to calculate properties of a fluid at specified thermodynamic states defined by an appropriate number of independent variables. The term ''fundamental equation'' is often used in the literature to refer to empirical descriptions of one of four fundamental relations: internal energy, enthalpy, Gibbs energy, and Helmholtz energy. The formulations for fluid properties are often explicit in Helmholtz energy with independent variables of temperature and density. Pure fluids obey the Maxwell criterion (equal pressures and Gibbs energies at constant temperatures during phase changes) so that all thermodynamic properties including the vapor–liquid equilibrium may be calculated from the full expression for the Helmholtz energy without additional ancillary equations. In this work, the general term ''equation of state'' rather than the term ''fundamental equation'' is used to refer to the empirical models developed for calculating fluid properties.

Since air is not a pure fluid, general phase equilibrium calculations require consideration of phase compositions. This type of model is discussed in Sec. 5 for arbitrary mixtures of nitrogen, argon, and oxygen. For standard air at a fixed composition, two separate equations are required in addition to the equation of state to represent the dew and bubble-point pressures as functions of temperature. Densities along the dew and bubble-point curves are calculated by the solution of the equation of state and the dew or bubble-point pressure equations given in Sec. 3 at a given temperature. Ancillary equations for the dew and bubble-point densities

TABLE 1. Summary of measured compositions of air

	U.S. Std. Atmosphere (1976)	Jones (1978)	Waxman and Davis (1978)	Giacomo (1982)
N_2	0.780 840	0.781 02	0.781 20	0.781 01
O_2	0.209 476	0.209 46	0.209 20	0.209 39
Ar	0.009 340	0.009 16	0.009 30	0.009 17
CO_2	0.000 314	0.000 33	0.000 32	0.000 40
	0.999 970	0.999 97	1.000 02	0.999 97

TABLE 2. Composition of air using nitrogen, argon, oxygen, and carbon dioxide as constituents

Component	Mole fraction
N_2	0.7810
O_2	0.2095
Ar	0.0092
CO_2	0.0003
	1.0000

TABLE 3. Composition of air using nitrogen, argon, and oxygen as constituents

Component	Mole fraction
N_2	0.7812
O_2	0.2096
Ar	0.0092
	1.0000

are also given and can be used as estimating functions for iterative calculations of derived thermodynamic properties.

1.2. Prior Thermodynamic Property Formulations for Air

Several previous thermodynamic property formulations for air are referenced in Table 4. The most recent prior wide-range formulations are those of Jacobsen and co-workers [Jacobsen *et al.* (1990a); Jacobsen *et al.* (1992); Panasiti *et al.* (1999)], the first of which is based upon liquid heat capacities predicted using extended corresponding states methods and the second of which used preliminary measurements of the isochoric heat capacity from the National Institute of Standards and Technology (NIST), subsequently published by Magee (1994). The third formulation was a preliminary equation extended to temperatures and pressures of 2000 K and 2000 MPa using predicted properties above 870 K and 70 MPa calculated by corresponding states methods from experimental nitrogen data.

2. Experimental Data

The estimated uncertainty of reference equations of state for pure fluids or mixtures is generally based upon comparisons to experimental data. These data are used to determine the coefficients of the equation and to evaluate the behavior of the equation of state over the fluid surface. Data types used in this work include $p-\rho-T$, speed of sound, isochoric and isobaric heat capacities, and vapor–liquid equilibrium. The equation of state reported here was developed using least squares fitting methods described in detail in Sec. 4.3. For reference quality equations, extensive comparisons to all data types are required. In the tables included in this section, columns are included which indicate the results of statistical analyses of the comparisons of calculated values to experimental data. The details of this analysis are given in Sec. 6.

The available saturation data are summarized in Table 5 and discussed in Sec. 6.1. Data used in the fit of the ancillary equations are shown as bolded entries in the table. The values reported by Blanke (1977) were obtained by graphical methods from his $p-\rho-T$ data; several of the near critical temperature data were used in the fit of ancillary equations. Values calculated using the Leung–Griffiths model for air as reported by Jacobsen *et al.* (1990b) are also summarized in this table. Several of these values close to the critical point were used in the fit.

TABLE 4. Summary of prior formulations for the thermodynamic properties of air

Author	Year	Temperature range (K)	High pressure limit (MPa)
Hilsenrath (1955)	1955	50–3000	10
Michels *et al.* (1955)	1955	102–348	122
Din (1962)	1962	90–450	122
Baehr and Schwier (1961)	1961	60–1250	450
Vasserman and Rabinovich (1970)	1970	75–160[a]	50
Vasserman *et al.* (1971)	1971	75–1300[b]	100
Sychev *et al.* (1987)[c]	1978	70–1500	100
Jacobsen *et al.* (1990a)	1990	60–873	70
Jacobsen *et al.* (1992)	1992	60–873	70
Panasiti *et al.* (1999)	1999	60–2000	2000

[a]Liquid states only.
[b]Vapor states only.
[c]English translation of original work published in 1978.

Experimental $p-\rho-T$ data for air are illustrated in Figs. 1 and 2 and summarized in Table 6. The solid lines represent the dew and bubble-point curves. Data used in the fit of the equation of state are shown as bolded entries in the table. All available experimental data were considered in preliminary analysis, but in the final regression of the coefficients of the equation of state, only the most accurate data and data in regions where no other data were available were fitted. The air $p-\rho-T$ data sets used in the development of the equation of state for air and for the mixture model were those of Blanke (1977), Howley *et al.* (1994), Kozlov (1968), Michels *et al.* (1954a), (1954b), and Romberg (1971). The isochoric and isobaric heat capacity data are illustrated in Fig. 3 and summarized in Table 6. The speed of sound data of Younglove and Frederick (1992), Ewing and Goodwin (1993) and of Van Itterbeek and de Rop (1955) are also illustrated in Fig. 3 and summarized in Table 6. These speed of sound data and the isochoric heat capacity data of Magee (1994) were used in the fit. The critical region data of Chashkin *et al.* (1966) are not included in this table since their measurements were concerned with investigating the effect of impurities on the behavior of the isochoric heat capacity in the critical region, and the sample had a 1.2% impurity content [see Sychev *et al.* (1987)]. None of the isobaric heat capacity data summarized in Table 6 were used to develop the equation of state or mixture model because of the age of the data and the availability of other more accurate derived data (isochoric heat capacity and speed of sound) in similar regions.

A summary of sources of second virial coefficients, including those of Romberg (1971) and Michels *et al.* (1954a), (1954b), are given in Table 6. The values of Michels *et al.* were used in the fit of the equation of state. In addition to the values reported by Romberg, values of the second virial coefficients were redetermined graphically from his reported $p-\rho-T$ data. These values are given in Table 7. At the higher isotherms, data below 0.5 mol/dm^3 were not used in this graphical redetermination of the values of the second

TABLE 5. Summary and statistical analysis of saturation data for air

Author	No. of points	Temp. range (K)	Pressure range (MPa)	AAD[a]	AAD[b]
Bubble-point pressure					
Blanke (1977)	9	60–129	0.01–3.2	2.506	2.766
Jacobsen *et al*. (1990b)	18	120–133	2.10–3.8	0.049	0.207
Kuenen and Clark (1917)	14	123–133	2.54–3.8	0.663	0.839
Michels *et al*. (1954a)	3	118–132	1.96–3.7	0.069	0.212
Overall	44	60–133	0.01–3.8	0.748	1.040
Dew-point pressure					
Blanke (1977)	11	67–132	0.01–3.7	0.395	1.407
Jacobsen *et al*. (1990b)	12	122–133	2.18–3.8	0.048	0.293
Kuenen and Clark (1917)	18	123–133	2.40–3.8	0.587	0.548
Michels *et al*. (1954a)	6	118–133	1.83–3.8	0.413	0.515
Overall	47	67–133	0.01–3.8	0.382	0.680
	No. of points	Temp. range (K)	Density range (mol/dm^3)	AAD[a]	AAD[c]
Bubble-point density					
Blanke (1977)	9	60–129	17.71–33.0	0.144	0.152
Jacobsen *et al*. (1990b)	18	120–133	10.45–21.6	0.786	0.745
Kuenen and Clark (1917)	11	127–133	10.70–18.1	6.042	6.039
Michels *et al*. (1954a)	10	118–132	13.67–20.5	3.003	3.034
Overall	48	60–133	10.45–33.0	2.332	2.324
Dew-point density					
Blanke (1977)	11	67–132	0.02–8.9	0.638	0.639
Jacobsen *et al*. (1990b)	12	122–133	3.40–10.4	1.028	1.036
Kuenen and Clark (1917)	8	130–133	6.49–10.7	6.052	6.067
Michels *et al*. (1954a)	12	118–133	2.67–9.8	1.236	1.229
Overall	43	67–133	0.02–10.7	1.921	1.924

[a]Comparisons of the ancillary equations with experimental data.
[b]Comparisons of the mixture model with experimental data.
[c]Comparisons of the equation of state for air with experimental data.

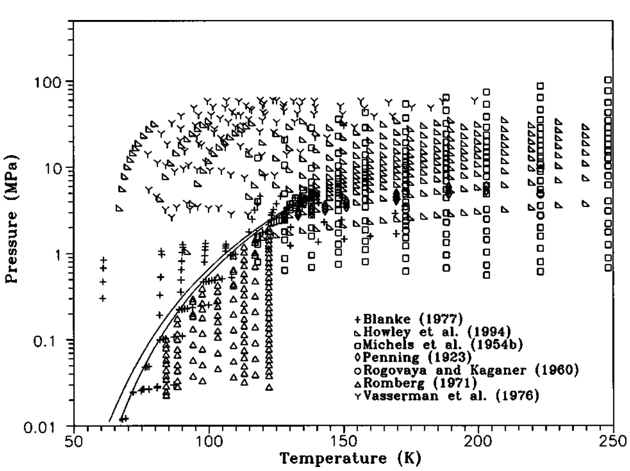

FIG. 1. Low temperature $p-\rho-T$ data for air. Solid lines represent the dew and bubble-point curves for air.

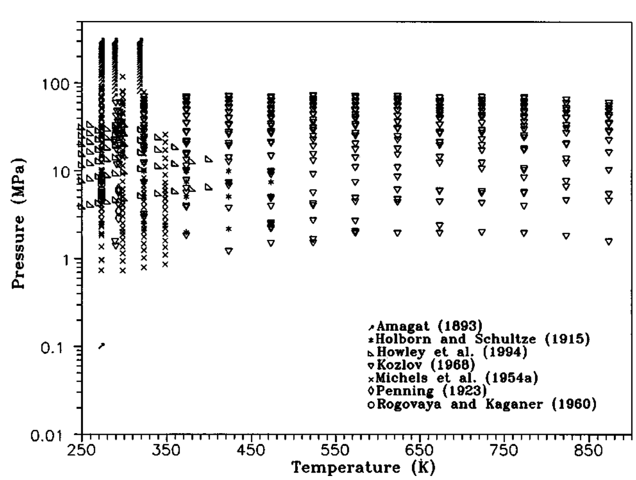

FIG. 2. High temperature $p-\rho-T$ data for air.

TABLE 6. Summary and statistical analysis of experimental data for air

Author	No. of points	Temp. range (K)	Pressure range (MPa)	Density range (mol/dm^3)	AAD[a] (air EOS)	AAD[a] (mixture model)
$p-\rho-T$						
Amagat (1893)	78	273–318	0.10–304.0	0.04–31.0	0.220	0.246
Blanke (1977)	110	61–170	0.01–4.9	0.02–33.0	0.350	0.312
Holborn and Schultze (1915)	42	273–473	1.98–10.0	0.61–4.5	0.019	0.031
Howley *et al*. (1994)	286	67–400	1.06–35.2	1.95–32.2	0.050	0.044
Kozlov (1968)	348	288–873	1.21–72.2	0.21–17.2	0.072	0.069
Michels *et al*. (1954a)	157	273–348	0.73–228.0	0.30–28.7	0.022	0.030
Michels *et al*. (1954b)	199	118–248	0.56–102.0	0.33–25.2	0.147	0.152
Penning (1923)	62	128–293	2.52–6.20	1.20–4.5	0.094	0.100
Rogovaya and Kaganer (1960)	10	273	4.71–8.6	2.12–3.9	0.091	0.102
Romberg (1971)	124	84–122	0.02–2.0	0.03–2.7	0.028	0.045
Vasserman *et al.* (1976)	109	77–199	2.62–59.8	22.82–31.4	0.078	0.080
Overall	1525	61–873	0.01–304.0	0.02–33.0	0.097	0.097
c_v						
Eucken and Hauck (1928)	16	138–165	6.72–19.6	18.08–19.0	6.571	6.063
Henry (1931)	3	288–623	0.10	0.02	0.579	0.580
Magee (1994)	227	66–299	1.71–34.6	2.04–33.0	0.373	0.493
Overall	246	66–623	0.10–34.6	0.02–33.0	0.779	0.856
c_p						
Bridgeman (1929)	51	273–553	2.03–22.3	0.44–8.6	0.920	0.916
Eucken (1913)	6	271–480	0.10	0.03	0.531	0.532
Holborn and Jakob (1917)	7	333	0.10–29.4	0.04–9.5	0.434	0.405
Jakob (1923)	47	194–523	0.10–29.4	0.02–14.6	1.083	1.083
Nesselmann (1925)	19	194–523	4.90–19.6	1.11–14.6	1.845	1.810
Poferl *et al.* (1959)	46	300–2499	0.30–1.0	0.01–0.4	3.656	3.511
Overall	176	194–2499	0.10–29.4	0.01–14.6	1.746	1.702
w						
Abbey and Barlow (1948)	6	293	<0.1	<0.04	0.388	0.389
Colwell and Gibson (1941)	7	273	<0.1	<0.04	0.100	0.100
Colwell *et al.* (1938)	9	297–299	0.10	0.04	0.063	0.062
Ewing and Goodwin (1993)	13	255	0.03–6.9	0.01–3.4	0.018	0.006
Hardy *et al.* (1942)	7	273–297	0.10	0.04	1.858	1.861
King and Partington (1930)	11	1138–1440	0.10	0.01	1.941	1.946
Quigley (1945)	29	92–259	0.10	0.05–0.1	0.313	0.306
Shilling and Partington (1928)	28	273–1572	0.10	0.01	1.405	1.407
Tucker (1943)	6	292–347	0.07–0.1	0.02	2.353	2.351
Van Itterbeek and de Rop (1955)	44	229–313	0.10–1.3	0.04–0.7	0.216	0.211
Younglove and Frederick (1992)	169	90–300	0.34–13.8	0.25–29.7	0.216	0.105
Overall	329	90–1572	<13.8	<29.7	0.446	0.387
B						
Andersen (1950)	6	273–473			1.008	0.732
Friedman (1957)	5	150–273			0.819	0.558
Hilsenrath (1955)	61	50–1501			3.779	2.719
Levelt Sengers *et al.* (1972)	54	100–1400			0.674	0.472
Michels *et al*. (1954a)	4	273–348			0.220	0.357
Michels *et al*. (1954b)	10	118–248			0.127	0.159
Romberg (1971)	39	84–473			0.240	1.130
Overall	179	50–1501			1.588	1.357

[a]AAD—Average absolute percent deviation in density for $p-\rho-T$ and average absolute difference in B (cm^3/mol) for the second virial coefficients.

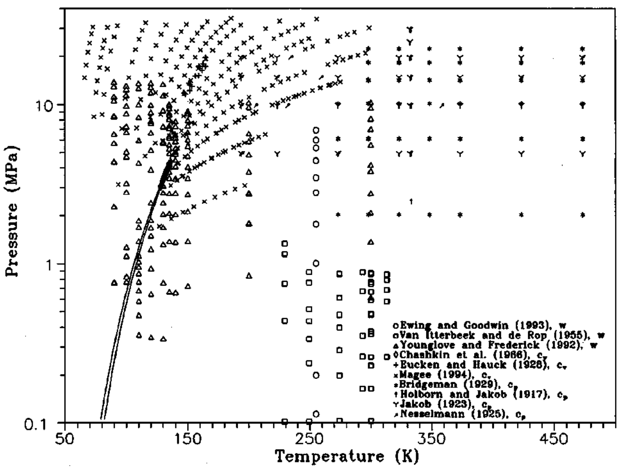

FIG. 3. Isochoric and isobaric heat capacities and speed of sound data for air. Solid lines represent the dew and bubble-point curves for air.

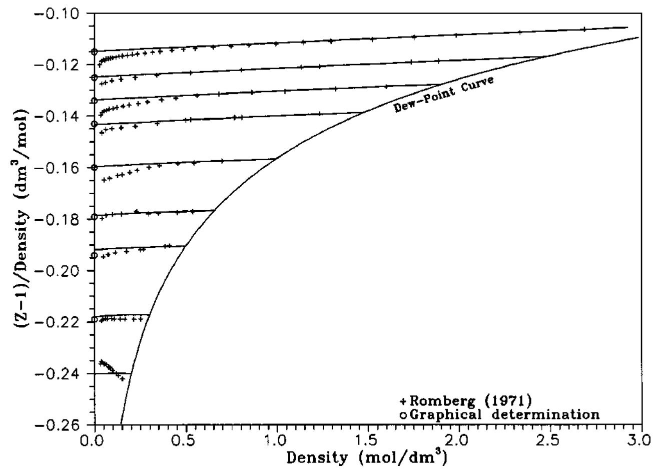

FIG. 4. Derivation of second virial coefficient data from the $p-\rho-T$ data of Romberg (1971).

virial coefficients since in many apparatus, such low density data are subject to local adsorption by the walls of the apparatus or to higher uncertainties in the measurement of extremely low pressures. No value of the second virial coefficient was determined for the 84 K isotherm. The $p-\rho-T$ data used to generate the second virial coefficients are shown in Fig. 4. The solid lines show isotherms calculated from the equation of state presented here and the solid curve represents the dew-point curve. The y intercept (zero density) represents the second virial coefficient at a given temperature, and the third virial coefficients can be taken from the slope of each line at zero density. The values of the second virial coefficient calculated from the equation of state are in good agreement with those presented in Table 7 and shown as circles in the figure. Values of the second virial coefficients and $p-\rho-T$ data from Michels *et al.* are shown in a similar fashion in Fig. 5. The circles at zero density represent the second virial coefficients reported by Michels.

Binary $p-\rho-T$ and vapor–liquid equilibrium data for mixtures containing nitrogen, argon, and oxygen are summarized in Table 8. The composition ranges listed in these tables show the composition of the first component listed. All available experimental data were considered in the preliminary analysis, but the final regression of the coefficients of the mixture model used the data sets indicated by the bolded entries in Table 8. Data of Crain and Sonntag (1966), Palavra (1979), and Kosov and Brovanov (1979) were used for the nitrogen–argon mixture, and data of Pool *et al.* (1962) were used for the nitrogen–oxygen and argon–oxygen mixtures. In addition to the limited data for the nitrogen–oxygen system, the following data sets for air were also used in the mixture modeling: Blanke (1977), Howley *et al.* (1994), Michels *et al.* (1954a), (1954b), Romberg (1971), Magee (1994), Ewing and Goodwin (1993), and Younglove and Frederick (1992). The largest impact from the addition of these data sets was on the nitrogen–oxygen parameters, however, the argon–oxygen parameters were also influenced to some degree by the air data. These data had little impact on the nitrogen–argon parameters, as there were sufficient binary data for this system to model the parameters well. The VLE data used in the model development included the nitrogen–argon data of Hiza *et al.* (1999), the nitrogen–oxygen data of Duncan and Staveley (1966), and the argon–oxygen data of Burn and Din (1962) and of Wilson *et al.* (1965). Comparisons with ternary VLE data indi-

TABLE 7. Second virial coefficients derived from the experimental $p-\rho-T$ data of Romberg (1971)

Temperature (K/ITS-90)	Graphical redetermination of the second virial coefficient (dm^3/mol)
88.27	−0.219
94.06	−0.194
97.56	−0.179
103.24	−0.160
109.10	−0.143
113.05	−0.134
117.12	−0.125
122.22	−0.115

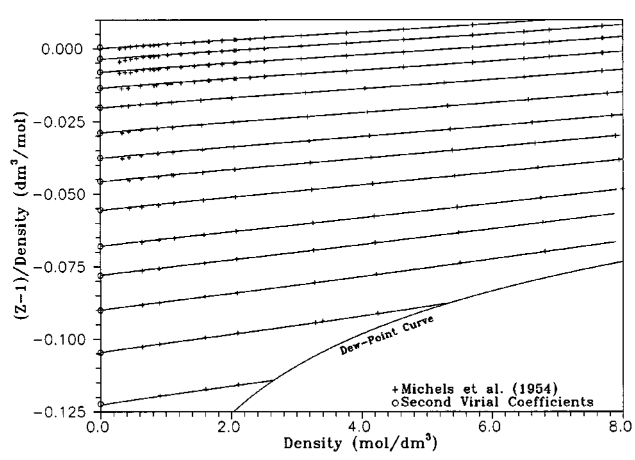

FIG. 5. Second virial coefficient data and $p-\rho-T$ data of Michels *et al.* (1954a), (1954b).

TABLE 8. Summary and statistical analysis of data for mixtures of nitrogen, argon, and oxygen

Author	No. of points	Pressure range (MPa)	Density range (mol/dm^3)	Temp. range (K)	Comp. range (mol)	AAD[a]
N_2–Ar — $p-\rho-T$						
Crain and Sonntag (1966)	264	0.19–52.5	0.08–26.6	143–273	0.20–0.80	0.209
Holst and Hamburger (1916)	41	0.01–0.2	0.01–0.2	74–90	0.31–0.80	0.193
Kosov and Brovanov (1979)	201	5.93–58.8	2.46–18.8	293–353	0.16–0.81	0.363
Maslennikova *et al.* (1979)	88	100.–800.	17.5–41.1	298–423	0.26–0.75	0.320
Massengill and Miller (1973)	6	0.27–1.3	25.7–30.2	90–113	0.50	0.409
Palavra (1979)	203	0.95–24.9	25.8–32.9	94–106	0.32–0.70	0.021
Pool *et al.* (1962)	24	0.10–0.2	28.3–33.9	84	0.18–0.89	0.502
Ricardo *et al.* (1992)	21	7.41–145.	25.8–34.7	119	0.52	0.160
Townsend (1956)	144	0.18–13.9	0.07–5.7	298–323	0.16–0.84	0.054
Zandbergen and Beenakker (1967)	55	0.76–9.6	0.55–13.1	171–293	0.19–0.74	0.097
Overall	1047	0.01–800.	0.01–41.1	74–423	0.16–0.89	0.191
N_2–Ar — VLE						
Elshayal and Lu (1975)	7	0.39–0.7		100	0.14–0.90	0.468
Fastovskii and Petrovskii (1956)	56	0.12–0.4		79–103	0.05–0.90	1.182
Hiza *et al*. (1999)	44	0.08–0.8		85–100	0.10–0.89	0.379
Jin *et al.* (1993)	13	1.48–2.8		123	0.05–0.97	0.555
Lewis and Staveley (1975)	8	0.07–0.2		85	0.23–0.81	0.840
Miller *et al.* (1973)	14	0.84–1.5		112	0.11–0.85	0.326
Narinskii (1966)	98	0.13–2.3		80–120	0.02–0.96	0.484
Pool *et al.* (1962)	12	0.07–0.2		84	0.06–0.88	0.420
Sprow and Prausnitz (1966)	17	0.08–0.2		84	0.06–0.91	0.460
Thorpe (1968)	68	0.13–1.1		81–115	0.10–0.91	0.830
Wilson *et al.* (1965)	176	0.10–2.6		72–134	0.05–1.00	0.805
Overall	513	0.07–2.8		72–134	0.02–1.00	0.708
N_2–O_2 — $p-\rho-T$						
Blagoi and Rudenko (1958)	19	[b]	30.7–38.0	67–79	0.11–0.80	0.415
Knaap *et al.* (1961)	7	[b]	29.6–34.8	77	0.29–0.91	0.097
Kuenen *et al.* (1922)	153	2.93–6.0	1.22–19.4	135–293	0.25–0.50	0.877
Pool *et al*. (1962)	7	0.09–0.2	29.8–34.1	84	0.25–0.74	0.088
Overall	186	0.09–6.0	1.22–38.0	67–293	0.11–0.91	0.771
N_2–O_2 — VLE						
Armstrong *et al.* (1955)	70	0.003–0.1		65–78	0.03–0.94	0.870
Cockett (1957)	62	0.12–0.1		81–91	0.07–0.81	1.287
Din (1960)	108	0.11–1.0		79–116	0.10–0.89	0.788
Dodge and Dunbar (1927)	49	0.06–3.0		77–125	0.05–0.91	0.903
Duncan and Staveley (1966)	11	0.002–0.01		63	0.10–0.80	1.524
Hiza *et al.* (1999)	65	0.001–0.8		63–100	0.07–0.88	0.689
Pool *et al.* (1962)	11	0.05–0.2		84	0.10–0.90	0.310
Thorogood and Haselden (1963)	13	0.10		88–90	0.002–0.08	1.320
Wilson *et al.* (1965)	138	0.10–2.6		78–136	0.05–0.99	0.540
Yorizane *et al.* (1978)	20	0.05–0.1		80	0.11–0.85	2.489
Overall	547	0.001–3.0		63–136	0.002–0.99	0.865
Ar–O_2 — $p-\rho-T$						
Blagoi and Rudenko (1958)	36	[b]	34.8–38.2	70–89	0.10–0.87	0.274
Knaap *et al.* (1961)	6	[b]	34.7–35.2	90	0.28–0.79	0.052
Pool *et al*. (1962)	15	0.05–0.1	34.7–36.3	84–90	0.17–0.86	0.025
Saji and Okuda (1965)	20	[b]	34.9–36.1	85–87	0.25–0.92	0.244
Overall	77	0.05–0.1	34.7–38.2	70–90	0.10–0.92	0.200
Ar–O_2 — VLE						
Bourbo and Ischkin (1936)	27	0.07–0.2		87–95	0.04–0.86	0.710
Burn and Din (1962)	140	0.06–1.0		85–118	0.10–0.91	0.232
Clark *et al.* (1954)	55	0.10–0.7		90–110	0.10–0.90	0.313
Fastovskii and Petrovskii (1955)	24	0.12–0.2		89–96	0.21–0.83	0.774
Hiza *et al.* (1999)	16	0.16–0.3		95–100	0.11–0.79	0.805
Narinskii (1957)	55	0.11–1.2		90–120	0.03–0.96	0.237
Parikh and Zollweg (1997)	24	0.12–0.9		92–115	0.01–0.92	1.149
Pool *et al.* (1962)	24	0.05–0.1		84–90	0.10–0.90	0.168
Wang (1960)	35	0.12–0.2		90–96	0.02–1.00	1.393
Wilson *et al*. (1965)	200	0.10–2.6		87–139	0.003–0.98	0.403
Yorizane *et al.* (1978)	58	0.10		89–92	<0.76	0.857
Overall	568	0.05–2.6		84–139	<1.00	0.493
N_2–Ar–O_2 — VLE						
Fastovskii and Petrovskii (1957)	14	0.1		81–88	0.13–0.68	0.555
Funada *et al.* (1982)	60	0.1		90	<0.004	0.278
Narinskii (1969)	115	0.13–2.2		82–120	0.04–0.86	0.489
Weishaupt (1948)	41	0.1		81–92	0.01–0.89	1.613
Wilson *et al.* (1965)	1427	0.10–2.6		78–136	0.001–0.99	0.561
Overall	1657	0.10–2.6		78–136	<0.99	0.572

[a]AAD—Average absolute deviation in density for $p-\rho-T$ and average absolute deviation in bubble-point pressure for VLE.
[b]No pressure reported, bubble-point pressure assumed.

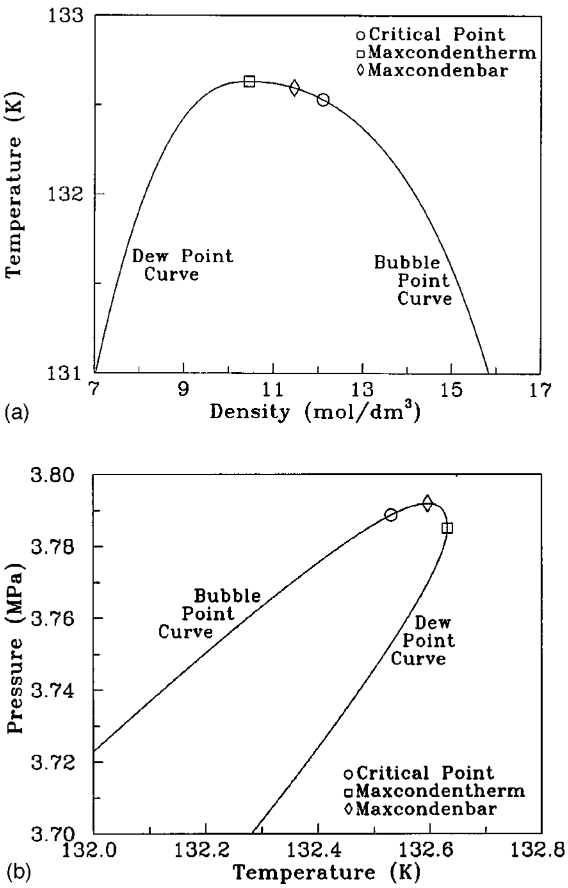

FIG. 6. Critical region phase boundaries for air.

cated that the binary mixture parameters were sufficient for modeling the ternary mixture interactions.

3. Vapor–Liquid Equilibria for Air

The maxcondentherm (state point of maximum temperature along the saturation line), maxcondenbar (state point of maximum pressure along the saturation line), and critical point for air used in this work were reported by Jacobsen *et al.* (1990b). These values were determined using a modified Leung–Griffiths model to represent the high-pressure VLE data for ternary systems of nitrogen, argon, and oxygen. The values of the properties at the maxcondentherm (T_j, p_j, ρ_j) were used as reducing parameters for the equation of state reported here so that the dew-point pressure and density equations will not be double-valued at any given temperature above the critical temperature as illustrated in Fig. 6; thus, for these temperature dependent equations, the dew-point line is represented by the bubble-point equation between the maxcondentherm point and the critical point. The fixed point properties for air used in this work are given in Table 9.

TABLE 10. Coefficients for the dew and bubble-point pressure and density equations for air

i	N_i	i	N_i
	Bubble-point pressure, Eq. (1)		**Dew-point pressure, Eq. (1)**
1	0.226 072 4	1	−0.156 726 6
2	−7.080 499	2	−5.539 635
3	5.700 283	5	0.756 721 2
4	−12.440 17	8	−3.514 322
5	17.819 26		
6	−10.813 64		
	Bubble-point density, Eq. (2)		**Dew-point density, Eq. (3)**
1	44.3413	1	−2.0466
2	−240.073	2	−4.7520
3	285.139	3	−13.259
4	−88.3366	4	−47.652
5	−0.892 181		

3.1. Ancillary Equations

The ancillary equations were developed using linear and nonlinear regression algorithms with the experimental database discussed in Sec. 2 and calculated data discussed in Sec. 6.1. The equation for the dew and bubble-point pressures is

$$\ln\left(\frac{p}{p_j}\right)=\left(\frac{T_j}{T}\right)\sum_{i=1}^{8} N_i\theta^{i/2}, \tag{1}$$

where the N_i are the coefficients given in Table 10 for either the dew or bubble-point pressure equation and $\theta=1-T/T_j$. Values of N_i are zero for the coefficients not listed in the table. Densities along the dew and bubble lines can be calculated from the Helmholtz energy formulation given in Sec. 4 at any temperature and the corresponding pressure calculated from Eq. (1). Ancillary equations for the densities

TABLE 9. Maxcondentherm, maxcondenbar, and critical point for air

	Pressure[a] (MPa)	Temperature[a,c] (K)	Density (mol/dm³)
Maxcondentherm[b]	**3.785 02±0.004±Δ*p***	**132.6312±0.002±Δ*T***	**10.4477±0.05**
Maxcondenbar	3.7891±0.002±Δ*p*	132.6035±0.004±Δ*T*	11.0948±0.05
Critical point	3.7860±Δ*p*	132.5306±Δ*T*	11.8308±0.05

[a]$\Delta p=0.02$ MPa, $\Delta T=0.02$ K; the uncertainties in the maxcondentherm and maxcondenbar pressure and temperature comprise components related to the value associated with the critical parameters and smaller components related to the uncertainty in the distance from the critical point.
[b]Values used for the reducing parameters in the equation of state.
[c]Temperature on ITS-90.

along the saturation lines are given here for convenience in certain calculations such as estimation routines. The equation for the bubble-point density is

$$\frac{\rho}{\rho_j}-1=N_1\theta^{0.65}+N_2\theta^{0.85}+N_3\theta^{0.95}+N_4\theta^{1.1}+N_5\ln\frac{T}{T_j}, \tag{2}$$

and the equation for the dew-point density is

$$\ln\left(\frac{\rho}{\rho_j}\right)=N_1\theta^{0.41}+N_2\theta^{1.0}+N_3\theta^{2.8}+N_4\theta^{6.5}, \tag{3}$$

where the coefficients are also given in Table 10. In these equations, T_j, p_j, and ρ_j are values at the maxcondentherm. Comparisons of these equations to experimental data are given in Sec. 6.1. These ancillary equations are valid for temperatures from the solidification point (59.75 K) to the maxcondentherm (132.6312 K). Values for the dew-point pressure and density between the critical point and the maxcondentherm, shown in Fig. 6, are calculated by the bubble-point equations.

3.2. Freezing Liquid Line

A freezing liquid line for air was estimated using the melting curves for pure nitrogen, argon, and oxygen due to the lack of experimental information for the mixture. The solidification temperature T_s of air along the bubble line given by Blanke (1973) is 59.75 K. The solidification pressure p_s corresponding to this temperature was calculated from the bubble-point pressure equation, Eq. (1), as 0.005 265 MPa. The freezing liquid line for air was assumed to have the same general pressure dependence as the freezing liquid line for pure nitrogen. This can be expressed as

$$p^f_{r_{\mathrm{Air}}}=\varphi p^f_{r_{\mathrm{N_2}}}, \tag{4}$$

where the reduced freezing pressures are defined as

$$p^f_r=\frac{p^f(T_r)}{p_{\mathrm{tp}}}-1 \tag{5}$$

for nitrogen, argon, or oxygen, and

$$p^f_r=\frac{p^f(T_r)}{p_s}-1 \tag{6}$$

for air. In these equations, $p^f(T_r)$ is the freezing liquid pressure at the reduced temperature, T_r is the reduced temperature (T/T_{tp} or T/T_s), and the subscript tp indicates the triple point for nitrogen, argon, or oxygen. The value of φ was determined at a reduced temperature of 2 from

$$x_{\mathrm{N_2}}\ln p^f_{r_{\mathrm{N_2}}}(2)+x_{\mathrm{Ar}}\ln p^f_{r_{\mathrm{Ar}}}(2)+x_{\mathrm{O_2}}\ln p^f_{r_{\mathrm{O_2}}}(2)$$
$$=\ln p^f_{r_{\mathrm{Air}}}(2)=\ln \varphi p^f_{r_{\mathrm{N_2}}}(2), \tag{7}$$

where the mole fractions x are taken from the composition of air used in this work, and the pure fluid melting pressures were taken from Span *et al.* (2000), Tegeler *et al.* (1999), and Schmidt and Wagner (1985). The value φ calculated from this equation is 2.773 234. Although values of the freezing liquid line for air could have been calculated from a generalization of Eq. (7), Eq. (4) was selected instead since its extrapolation behavior to very high temperatures was known. The resulting equation for the freezing liquid pressure of air is

$$\frac{p}{p_s}-1=35\,493.5\left[\left(\frac{T}{T_s}\right)^{1.789\,63}-1\right], \tag{8}$$

derived using the melting pressure equation of nitrogen [Span *et al.* (2000)].

TABLE 11. Averaged molar composition of standard air at specified temperatures

T(K)	Composition			
	N_2	Ar	O_2	NO
1500	0.7804	0.0093	0.2089	0.0014
1600	0.7802	0.0093	0.2083	0.0022
1700	0.7797	0.0093	0.2078	0.0032
1800	0.7790	0.0094	0.2071	0.0045
1900	0.7780	0.0094	0.2063	0.0063
2000	0.7768	0.0094	0.2056	0.0082

4. Equation of State for Air

4.1. Effects of Dissociation

The details included in this and the following section are taken from Panasiti (1996) with some modifications. At high temperatures, air and its constituents dissociate, and the composition changes to include various atomic and ionic species and new compounds including oxides of nitrogen. Hilsenrath and Klein (1965) report the extent of dissociation in the temperature range from 1500 to 15000 K. They considered the equilibrium between atoms, molecules, and ions for the elements nitrogen, oxygen, argon, carbon, and neon. In all, 28 species were considered by Hilsenrath and Klein. For the temperature range of current interest, the amount of nitric oxide (NO) in equilibrium at 2000 K formed from the dissociation of oxygen and nitrogen was large enough that it might be expected to cause a noticeable change in the thermodynamic properties of the mixture. No other constituents were considered in the current study due to their small concentrations. Table 11 lists averaged values of composition, derived from Hilsenrath and Klein, for a mixture of nitrogen, argon, oxygen, and nitric oxide at various temperatures. Although Hilsenrath and Klein consider a pressure dependence, the effect on calculated properties is small, and the composition of air is assumed to be constant over all pressures at a given temperature.

Several methods were considered to determine the effects of dissociation on the thermodynamic properties of air. These methods include calculations using cubic equations, extended corresponding states predictions [Clarke *et al.* (1994); Lemmon (1996)], and mixture equations of state of the form developed by Bender (1973). Use of extended corresponding states models with accurate pure fluid information is one of the most accurate methods for obtaining mixture properties. However, the equation of state for oxygen [Schmidt and Wagner (1985)] has limited temperature and pressure ranges (less than 300 K and 82 MPa), and the accuracy of properties calculated beyond these limits is uncertain. In addition, there is no published equation of state for nitric oxide. Therefore, the Peng–Robinson (1976) equation of state was used with standard mixing rules to determine the effect of dissociation of air and its constituents. The acentric factors ω required in the Peng–Robinson model and the critical parameters for nitrogen, argon, and oxygen are listed in the fixed point tables. The critical temperature of nitric oxide is 180.15 K, the critical pressure is 6.48 MPa, and the acentric factor is 0.6. The values of the critical parameters and the acentric factor for nitric oxide were taken from Prasad and Viswanath (1974).

Although cubic equations generally cannot be used to calculate values of density with high accuracy over a wide range of temperature and pressure, the purpose here was to compare the differences in density between two mixtures: the three-component N_2–Ar–O_2 model of fixed composition for air used in this work, and a four-component N_2–Ar–O_2–NO model which accounted for dissociation by the addition of the NO component. Errors associated with the calculation of density differences should be much smaller than those calculated for the overall value of density. The highest deviation at 2000 K and 2000 MPa is approximately 0.1%, which is less than the expected uncertainty of experimental measurements at these high temperatures and pressures. The differences in calculated heat capacities between the two mixtures is approximately 0.8%, also within the estimated uncertainty. Based on this analysis, it was concluded that dissociation effects are small enough at temperatures up to 2000 K and pressures to 2000 MPa that they were not explicitly considered in the development of the new equation of state for air.

4.2. Calculation of Air Properties from Experimental Data for Nitrogen

A modified extended corresponding states technique was used to predict properties of air corresponding to states defined by measurements of nitrogen properties. Experimental $p-\rho-T$ measurements for nitrogen extend to 1800 K and 2220 MPa. Air properties were calculated from high-pressure and high-temperature nitrogen data using the assumption that the compressibility factors are equal

$$Z_{\mathrm{Air}}(T_{\mathrm{Air}},\rho_{\mathrm{Air}})=Z_{\mathrm{N_2}}(T_{\mathrm{N_2}},\rho_{\mathrm{N_2}}) \tag{9}$$

at corresponding states defined by

$$T_{\mathrm{Air}}=(1.038\,128+0.000\,054\,933T_{\mathrm{N_2}})T_{\mathrm{N_2}} \tag{10}$$

and

$$\rho_{\mathrm{Air}}=1.043\,492\rho_{\mathrm{N_2}}, \tag{11}$$

for T in kelvin. The pressure was calculated from Eq. (9) for air using nitrogen data

$$p_{\mathrm{Air}}=\frac{T_{\mathrm{Air}}}{T_{\mathrm{N_2}}}\frac{\rho_{\mathrm{Air}}}{\rho_{\mathrm{N_2}}}p_{\mathrm{N_2}}. \tag{12}$$

The numerical constants in Eqs. (10) and (11) were obtained by fitting selected $p-\rho-T$ nitrogen data of Jaeschke and Hinze (1991), Klimeck *et al.* (1998), Michels *et al.* (1936), and Nowak *et al.* (1997) in the range from 200 to 520 K at pressures to 67 MPa to a preliminary version of the air equation of state. The data of Nowak *et al.* represent the most reliable high temperature, high pressure data available for nitrogen. This fitting procedure minimized deviations between air properties estimated from nitrogen data and values calculated from the preliminary equation of state for air. The average absolute deviations for values calculated from the nitrogen equation of state of Span *et al.* (2000) were 0.01% for the data of Jaeschke and Hinze, 0.002% for the data of Klimeck *et al.*, 0.02% for the data of Michels *et al.*, and 0.001% for the data of Nowak *et al.* In comparison, the average absolute deviations for values calculated from the air equation of state as compared with the transformed data were 0.02% for the data of Jaeschke and Hinze and of Klimeck *et al.*, 0.04% for the data of Michels *et al.*, and 0.03% for the data of Nowak *et al.* Using Eqs. (10)–(12), high temperature, high pressure $p-\rho-T$ nitrogen data of Robertson and Babb (1969) and Saurel (1958) were transformed to predict state points for air and were used in subsequent fitting of the equation of state for air. The data of Robertson and Babb were used in the final regression of the coefficients. The estimated uncertainty of calculated air properties is 1.0% in density at the highest temperatures and pressures of 2000 K and 2000 MPa.

4.3. Fitting Procedures

The equation of state was developed using selected experimental pressure–density–temperature ($p-\rho-T$) data, isochoric heat capacity data, speed of sound data, and second virial coefficients as indicated in Table 6 and discussed in Sec. 2. The units adopted for this work are megapascals for pressure, moles per cubic decimeter for density, kelvins for temperature, and joules for energy. Units of the experimental data were converted as necessary from those of the original publications to these units. All temperatures were converted to the International Temperature Scale of 1990 (ITS-90) based on temperature differences given by Preston-Thomas (1990).

The functional forms of preliminary equations for the residual part of the Helmholtz energy were optimized with the algorithm developed by Wagner (1974). The fitting process was used to select an optimal set of terms for representing the selected data from a large bank of terms of the form given in Eq. (25) below. The exponents i_k, j_k, and l_k were selected in this process. The exponents j_k in Eq. (25) are generally considered to be greater than or equal to zero so that only ideal gas terms contribute as T goes to infinity, and

i_k and l_k are integers greater than zero. Each data point used in the least-squares determination of the coefficients of the equation of state was assigned a weighting factor. The weights used in the fitting process were calculated using the error propagation formula (sometimes called the theorem of propagation of variance). The functions for weighting were calculated by making use of a preliminary equation of state for the partial derivatives required for estimating variances by the error propagation formula. In several instances, the error propagation weights were modified by the assignment of arbitrary multiplicative factors to increase or lessen the effect of a particular data set on the overall representation of the surface.

The isobaric heat capacity and speed of sound data are not linearly related to the coefficients in the Helmholtz energy formulation and must first be linearized before being used in the fitting process. The isobaric heat capacity is linearized by calculating the density at the experimental pressure and temperature and reducing the isobaric heat capacities to an equivalent isochoric heat capacity using

$$c_v=c_p-R\frac{\left(1+\delta\frac{\partial\alpha^r}{\partial\delta}-\delta\tau\frac{\partial^2\alpha^r}{\partial\delta\partial\tau}\right)^2}{1+2\delta\frac{\partial\alpha^r}{\partial\delta}+\delta^2\frac{\partial^2\alpha^r}{\partial\delta^2}}. \tag{13}$$

The speed of sound is linearized by calculating the density and the ratio of the heat capacities γ from a preliminary equation of state. To improve the representation of the speed of sound data and of the available shock tube data for air, the final functional form was developed using nonlinear regression techniques. Using a combination of linear and nonlinear techniques, a functional form was obtained which yielded the best representation of the selected experimental data. Details of the nonlinear fitting procedures are given by Lemmon and Jacobsen (2000).

4.4. Ideal Gas Heat Capacity

The ideal gas heat capacity for air is given by the mole fraction average of the ideal gas heat capacities for nitrogen, argon, and oxygen

$$\frac{c_p^0(T)}{R}=x_{N_2}\left(\frac{c_p^0(T)}{R}\right)_{N_2}+x_{Ar}\left(\frac{c_p^0(T)}{R}\right)_{Ar}+x_{O_2}\left(\frac{c_p^0(T)}{R}\right)_{O_2}. \tag{14}$$

The ideal gas heat capacity for nitrogen taken from Span *et al.* (2000) is

$$\frac{c_p^0}{R}=\sum_{i=1}^{4}N_iT^{i-1}+\frac{N_5u^2e^u}{(e^u-1)^2}, \tag{15}$$

where $u=N_6/T$. The ideal gas heat capacity for argon is

$$\frac{c_p^0}{R}=\frac{5}{2}. \tag{16}$$

The ideal gas heat capacity for oxygen taken from Schmidt and Wagner (1985) is

TABLE 12. Coefficients for the ideal gas expressions

i	N_i	i	N_i
	c_p^0 of nitrogen, Eq. (15)		**c_p^0 of oxygen, Eq. (17)**
1	3.5	1	3.500 42
2	$0.306\,646\,9\times10^{-5}$	2	$0.166\,961\times10^{-7}$
3	$0.470\,124\,0\times10^{-8}$	3	1.067 78
4	$-0.398\,798\,4\times10^{-12}$	4	1.012 58
5	1.012 941	5	0.944 365
6	3364.011	6	2242.45
		7	11 580.4
	c_p^0 of air, Eq. (18)		**α^0 of air, Eq. (24)**
1	3.490 888 032	1	$0.605\,719\,400\times10^{-7}$
2	$2.395\,525\,583\times10^{-6}$	2	$-0.210\,274\,769\times10^{-4}$
3	$7.172\,111\,248\times10^{-9}$	3	$-0.158\,860\,716\times10^{-3}$
4	$-3.115\,413\,101\times10^{-13}$	4	$-13.841\,928\,076$
5	0.223 806 688	5	17.275 266 575
6	0.791 309 509	6	$-0.195\,363\,420\times10^{-3}$
7	0.212 236 768	7	2.490 888 032
8	0.197 938 904	8	0.791 309 509
9	3364.011	9	0.212 236 768
10	2242.45	10	$-0.197\,938\,904$
11	11 580.4	11	25.363 65
		12	16.907 41
		13	87.312 79

$$\frac{c_p^0}{R}=N_1+N_2T^2+\frac{N_3}{T^{1.5}}+\frac{N_4v^2e^v}{(e^v-1)^2}+\frac{(2/3)N_5w^2e^{-w}}{[(2/3)e^{-w}+1]^2}, \tag{17}$$

where $v=N_6/T$ and $w=N_7/T$. The coefficients for Eqs. (15) and (17) are given in Table 12.

The ideal gas heat capacity c_p^0 for air, calculated by combining the ideal gas heat capacity equations for nitrogen, argon, and oxygen, according to Eq. (14), is given by the following expression:

$$\frac{c_p^0}{R}=\sum_{i=1}^{4}N_iT^{i-1}+\frac{N_5}{T^{1.5}}+\frac{N_6u^2e^u}{(e^u-1)^2}+\frac{N_7v^2e^v}{(e^v-1)^2}+\frac{(2/3)N_8w^2e^{-w}}{((2/3)e^{-w}+1)^2}, \tag{18}$$

where $u=N_9/T$, $v=N_{10}/T$, and $w=N_{11}/T$. The coefficients of this equation are given in Table 12; note that different values for the coefficients N_i are used in Eqs. (15), (17), and (18)

4.5. Ideal Gas Helmholtz Energy

The ideal gas contribution to the Helmholtz energy of air is given by

$$a^0=-RT+\sum_{i=1}^{3}x_i(h_i^0-Ts_i^0+RT\ln x_i), \tag{19}$$

where x_i is the mole fraction of component i in air, and h_i^0 and s_i^0 are the ideal gas enthalpy and entropy of component i at the specified temperature. The ideal gas enthalpy is given by

$$h_i^0 = h_{0i}^0 + \int_{T_0}^{T} c_{pi}^0 dT, \tag{20}$$

where h_{0i}^0 is the enthalpy datum value at the reference temperature (T_0) for component i, based upon a zero reference point for the ideal crystal at absolute zero temperature. The ideal gas entropy is given by

$$s_i^0 = s_{0i}^0 + \int_{T_0}^{T} \frac{c_{pi}^0}{T} dT - R \ln\left(\frac{p^0}{p_0}\right), \tag{21}$$

where s_{0i}^0 is the entropy datum value at the reference temperature and pressure (T_0 and p_0) for component i, also based upon a zero reference point of the ideal crystal at absolute zero temperature. The variable p^0 is the ideal gas pressure at the fluid density and temperature. Combining Eqs. (19)–(21) results in the following expression for the ideal gas Helmholtz energy

$$a^0 = -RT + \sum_{i=1}^{3} x_i \left(RT \ln \frac{\rho T}{\rho_0 T_0} + h_{0i}^0 - T s_{0i}^0 + \int_{T_0}^{T} c_{pi}^0 dT - T \int_{T_0}^{T} \frac{c_{pi}^0}{T} dT + RT \ln x_i \right), \tag{22}$$

where p^0/p_0 has been replaced with $\rho T/\rho_0 T_0$. Dividing Eq. (22) by RT and replacing the temperatures with T_{ci}/τ and the densities with $\delta \rho_{ci}$ results in

$$\alpha^0 = \frac{a^0}{RT} = -1 + \sum_{i=1}^{3} x_i \left(\ln \frac{\delta \tau_0}{\delta_0 \tau} + \frac{h_{0i}^0 \tau}{RT_c} - \frac{s_{0i}^0}{R} - \frac{\tau}{R} \int_{\tau_0}^{\tau} \frac{c_{pi}^0}{\tau^2} d\tau + \frac{1}{R} \int_{\tau_0}^{\tau} \frac{c_{pi}^0}{\tau} d\tau + \ln x_i \right), \tag{23}$$

where $\tau_0 = T_{ci}/T_0$, $\delta_0 = \rho_0/\rho_{ci}$ is the reduced ideal gas density at p_0 and T_0, T_0 is the reference temperature (298.15 K), and p_0 is the reference pressure (0.101 325 MPa). T_{ci} and ρ_{ci} are the critical parameters of the pure fluids. Values of h_{0i}^0 and s_{0i}^0 for nitrogen, argon, and oxygen are taken from Cox *et al.* (1989) and are given in the fixed point tables.

The following expression for α^0 is obtained by combining Eqs. (18) and (23):

$$\alpha^0 = \ln \delta + \sum_{i=1}^{5} N_i \tau^{i-4} + N_6 \tau^{1.5} + N_7 \ln \tau + N_8 \ln[1 - \exp(-N_{11}\tau)] + N_9 \ln[1 - \exp(-N_{12}\tau)] + N_{10} \ln[2/3 + \exp(N_{13}\tau)], \tag{24}$$

where $\delta = \rho/\rho_j$ and $\tau = T_j/T$, as given by Eq. (25) in the Sec. 4.6, and T_j and ρ_j are parameters at the maxcondentherm of air. The coefficients of this equation are given in Table 12.

4.6. Equation of State for Air

The equation of state for air was developed using experimental data for pressure–density–temperature ($p-\rho-T$), isochoric heat capacity, speed of sound, and second virial coefficients, along with calculated air properties at high temperatures and pressures as described in Sec. 4.2. Values of $p-\rho-T$ on the dew and bubble-point curves calculated using Eqs. (1), (2), and (3) were used to define the vapor–liquid equilibrium boundaries. To expand the range of the equation beyond 2000 K and 2000 MPa, data published by Nellis *et al.* (1991), determined using a shock tube apparatus, were included in the fitting process as discussed in Sec. 4.8 below. The equation of state for air used in this work is explicit in the nondimensional Helmholtz energy

TABLE 13. Coefficients and exponents for the equation of state for air

k	N_k	i_k	j_k	l_k
1	0.118 160 747 229	1	0	0
2	0.713 116 392 079	1	0.33	0
3	$-0.161\,824\,192\,067 \times 10^{1}$	1	1.01	0
4	$0.714\,140\,178\,971 \times 10^{-1}$	2	0	0
5	$-0.865\,421\,396\,646 \times 10^{-1}$	3	0	0
6	0.134 211 176 704	3	0.15	0
7	$0.112\,626\,704\,218 \times 10^{-1}$	4	0	0
8	$-0.420\,533\,228\,842 \times 10^{-1}$	4	0.2	0
9	$0.349\,008\,431\,982 \times 10^{-1}$	4	0.35	0
10	$0.164\,957\,183\,186 \times 10^{-3}$	6	1.35	0
11	$-0.101\,365\,037\,912$	1	1.6	1
12	$-0.173\,813\,690\,970$	3	0.8	1
13	$-0.472\,103\,183\,731 \times 10^{-1}$	5	0.95	1
14	$-0.122\,523\,554\,253 \times 10^{-1}$	6	1.25	1
15	$-0.146\,629\,609\,713$	1	3.6	2
16	$-0.316\,055\,879\,821 \times 10^{-1}$	3	6	2
17	$0.233\,594\,806\,142 \times 10^{-3}$	11	3.25	2
18	$0.148\,287\,891\,978 \times 10^{-1}$	1	3.5	3
19	$-0.938\,782\,884\,667 \times 10^{-2}$	3	15	3

$$\alpha(\delta, \tau) = \frac{a(\rho, T)}{RT} = \alpha^0(\delta, \tau) + \alpha^r(\delta, \tau), \tag{25}$$

where α^0 is the ideal-gas contribution to the Helmholtz energy given in the previous section, α^r is the residual contribution to the Helmholtz energy, $\delta = \rho/\rho_j$ is the reduced density, $\tau = T_j/T$ is the reciprocal reduced temperature, ρ_j is the density at the maxcondentherm, and T_j is the temperature at the maxcondentherm.

The residual Helmholtz energy contribution to the equation of state is given by

$$\alpha^r(\delta, \tau) = \sum_{k=1}^{10} N_k \delta^{i_k} \tau^{j_k} + \sum_{k=11}^{19} N_k \delta^{i_k} \tau^{j_k} \exp(-\delta^{l_k}). \tag{26}$$

The coefficients N_k of the equation of state are given in Table 13. The values of i_k, j_k, and l_k were determined from the fitting procedures described in Sec. 4.3. For the nonexponential terms in Eq. (26), i_k ranges from 1 to 6 and j_k ranges from 0 to 1.35. The thermodynamic properties can be calculated from the Helmholtz energy using differentiation with respect to density and temperature as described in Sec. 4.7.

4.7. Calculation of Thermodynamic Properties

The functions used for calculating pressure, compressibility factor, internal energy, enthalpy, entropy, Gibbs energy, isochoric heat capacity, isobaric heat capacity, and the speed of sound from Eq. (25) are given as Eqs. (27)–(34). These functions were used in calculating the tables of thermodynamic properties of air given in the Appendix. The densities for the dew and bubble-point states are determined by the simultaneous solution of the dew or bubble-point pressure equation (1) and the equation of state for a given temperature. The derived properties for saturation states are calculated as functions of temperature and density using the standard thermodynamic relations given in Eqs. (27)–(34).

$$Z=\frac{p}{\rho RT}=1+\delta\left(\frac{\partial\alpha^r}{\partial\delta}\right)_\tau \tag{27}$$

$$\frac{u}{RT}=\tau\left[\left(\frac{\partial\alpha^0}{\partial\tau}\right)_\delta+\left(\frac{\partial\alpha^r}{\partial\tau}\right)_\delta\right] \tag{28}$$

$$\frac{h}{RT}=\tau\left[\left(\frac{\partial\alpha^0}{\partial\tau}\right)_\delta+\left(\frac{\partial\alpha^r}{\partial\tau}\right)_\delta\right]+\delta\left(\frac{\partial\alpha^r}{\partial\delta}\right)_\tau+1 \tag{29}$$

$$\frac{s}{R}=\tau\left[\left(\frac{\partial\alpha^0}{\partial\tau}\right)_\delta+\left(\frac{\partial\alpha^r}{\partial\tau}\right)_\delta\right]-\alpha^0-\alpha^r \tag{30}$$

$$\frac{g}{RT}=1+\alpha^0+\alpha^r+\delta\left(\frac{\partial\alpha^r}{\partial\delta}\right)_\tau \tag{31}$$

$$\frac{c_v}{R}=-\tau^2\left[\left(\frac{\partial^2\alpha^0}{\partial\tau^2}\right)_\delta+\left(\frac{\partial^2\alpha^r}{\partial\tau^2}\right)_\delta\right] \tag{32}$$

$$\frac{c_p}{R}=\frac{c_v}{R}+\frac{\left[1+\delta\left(\frac{\partial\alpha^r}{\partial\delta}\right)_\tau-\delta\tau\left(\frac{\partial^2\alpha^r}{\partial\delta\partial\tau}\right)\right]^2}{\left[1+2\delta\left(\frac{\partial\alpha^r}{\partial\delta}\right)_\tau+\delta^2\left(\frac{\partial^2\alpha^r}{\partial\delta^2}\right)_\tau\right]} \tag{33}$$

$$\frac{w^2M}{RT}=\frac{c_p}{c_v}\left[1+2\delta\left(\frac{\partial\alpha^r}{\partial\delta}\right)_\tau+\delta^2\left(\frac{\partial^2\alpha^r}{\partial\delta^2}\right)_\tau\right] \tag{34}$$

Equations for the second and third virial coefficients are given in Eqs. (35)–(36).

$$B(T)=\frac{1}{\rho_j}\left(\left.\frac{\partial\alpha^r}{\partial\delta}\right|_\tau\right)_{\delta=0} \tag{35}$$

$$C(T)=\frac{1}{\rho_j^2}\left(\left.\frac{\partial^2\alpha^r}{\partial\delta^2}\right|_\tau\right)_{\delta=0} \tag{36}$$

Other derived properties, given in Eqs. (37)–(47), include the first derivative of pressure with respect to density $(\partial p/\partial\rho)_T$, second derivative of pressure with respect to density $(\partial^2 p/\partial\rho^2)_T$, first derivative of pressure with respect to temperature $(\partial p/\partial T)_\rho$, Joule–Thomson coefficient (μ_J), isentropic expansion coefficient (k), isothermal expansion coefficient (k_T), volume expansivity (β), adiabatic compressibility (β_s), adiabatic bulk modulus (B_s), isothermal compressibility (κ), and isothermal bulk modulus (K_T).

$$\left(\frac{\partial p}{\partial\rho}\right)_T=RT\left[1+2\delta\left(\frac{\partial\alpha^r}{\partial\delta}\right)_\tau+\delta^2\left(\frac{\partial^2\alpha^r}{\partial\delta^2}\right)_\tau\right] \tag{37}$$

$$\left(\frac{\partial^2 p}{\partial\rho^2}\right)_T=\frac{RT}{\rho}\left[2\delta\left(\frac{\partial\alpha^r}{\partial\delta}\right)_\tau+4\delta^2\left(\frac{\partial^2\alpha^r}{\partial\delta^2}\right)_\tau+\delta^3\left(\frac{\partial^3\alpha^r}{\partial\delta^3}\right)_\tau\right] \tag{38}$$

$$\left(\frac{\partial p}{\partial T}\right)_\rho=R\rho\left[1+\delta\left(\frac{\partial\alpha^r}{\partial\delta}\right)_\tau-\delta\tau\left(\frac{\partial^2\alpha^r}{\partial\delta\partial\tau}\right)\right] \tag{39}$$

$$\mu_J=\left(\frac{\partial T}{\partial p}\right)_h=\frac{T\beta-1}{\rho c_p} \tag{40}$$

$$k=-\frac{v}{p}\left(\frac{\partial p}{\partial v}\right)_s=\frac{w^2\rho M}{p} \tag{41}$$

$$k_T=-\frac{v}{p}\left(\frac{\partial p}{\partial v}\right)_T=\frac{\rho}{p}\left(\frac{\partial p}{\partial\rho}\right)_T \tag{42}$$

$$\beta=\frac{1}{v}\left(\frac{\partial v}{\partial T}\right)_p=\frac{1}{\rho}\left(\frac{\partial p}{\partial T}\right)_\rho\left(\frac{\partial\rho}{\partial p}\right)_T \tag{43}$$

$$\beta_s=\frac{1}{kp}=-\frac{1}{v}\left(\frac{\partial v}{\partial p}\right)_s \tag{44}$$

$$B_s=kp=-v\left(\frac{\partial p}{\partial v}\right)_s \tag{45}$$

$$\kappa=\frac{1}{k_Tp}=-\frac{1}{v}\left(\frac{\partial v}{\partial p}\right)_T \tag{46}$$

$$K_T=k_Tp=-v\left(\frac{\partial p}{\partial v}\right)_T \tag{47}$$

The derivatives of the ideal gas Helmholtz energy, Eq. (24), are given in Eqs. (48)–(49).

$$\left.\frac{\partial\alpha^0}{\partial\tau}\right|_\delta=\sum_{i=1}^{5}(i-4)N_i\tau^{i-5}+1.5N_6\tau^{0.5}+N_7/\tau+\frac{N_8N_{11}}{e^{N_{11}\tau}-1}+\frac{N_9N_{12}}{e^{N_{12}\tau}-1}+\frac{N_{10}N_{13}}{(2/3)e^{-N_{13}\tau}+1}\tag{48}$$

$$\left.\frac{\partial^2\alpha^0}{\partial^2\tau}\right|_\delta=\sum_{i=1}^{5}(i-4)(i-5)N_i\tau^{i-6}+0.75N_6\tau^{-0.5}-N_7/\tau^2-\frac{N_8N_{11}^2e^{N_{11}\tau}}{(e^{N_{11}\tau}-1)^2}-\frac{N_9N_{12}^2e^{N_{12}\tau}}{(e^{N_{12}\tau}-1)^2}+\frac{(2/3)N_{10}N_{13}^2e^{-N_{13}\tau}}{[(2/3)e^{-N_{13}\tau}+1]^2}\tag{49}$$

The derivatives of the residual Helmholtz energy, Eq. (26), are given in Eqs. (50)–(55).

$$\left.\frac{\partial\alpha^r}{\partial\delta}\right|_\tau=\sum_{k=1}^{10}i_kN_k\delta^{i_k-1}\tau^{j_k}+\sum_{k=11}^{19}N_k\delta^{i_k-1}\tau^{j_k}\times\exp(-\delta^{l_k})(i_k-l_k\delta^{l_k})\tag{50}$$

$$\left.\frac{\partial^2\alpha^r}{\partial\delta^2}\right|_\tau=\sum_{k=1}^{10}i_k(i_k-1)N_k\delta^{i_k-2}\tau^{j_k}+\sum_{k=11}^{19}N_k\delta^{i_k-2}\tau^{j_k}\times\exp(-\delta^{l_k})[(i_k-l_k\delta^{l_k})(i_k-1-l_k\delta^{l_k})-l_k^2\delta^{l_k}]\tag{51}$$

$$\left.\frac{\partial^3\alpha^r}{\partial\delta^3}\right|_\tau=\sum_{k=1}^{10}i_k(i_k-1)(i_k-2)N_k\delta^{i_k-3}\tau^{j_k}+\sum_{k=11}^{19}N_k\delta^{i_k-3}\tau^{j_k}\exp(-\delta^{l_k})\{i_k(i_k-1)(i_k-2)+\delta^{l_k}[-2l_k+6i_kl_k-3i_k^2l_k-3i_kl_k^2+3l_k^2-l_k^3]+(\delta^{l_k})^2[3i_kl_k^2-3l_k^2+3l_k^3]-l_k^3(\delta^{l_k})^3\}\tag{52}$$

$$\left.\frac{\partial\alpha^r}{\partial\tau}\right|_\delta=\sum_{k=1}^{10}j_kN_k\delta^{i_k}\tau^{j_k-1}+\sum_{k=11}^{19}j_kN_k\delta^{i_k}\tau^{j_k-1}\exp(-\delta^{l_k})\tag{53}$$

$$\left.\frac{\partial^2\alpha^r}{\partial\tau^2}\right|_\delta=\sum_{k=1}^{10}j_k(j_k-1)N_k\delta^{i_k}\tau^{j_k-2}+\sum_{k=11}^{19}j_k(j_k-1)\times N_k\delta^{i_k}\tau^{j_k-2}\exp(-\delta^{l_k})\tag{54}$$

$$\frac{\partial^2\alpha^r}{\partial\tau\partial\delta}=\sum_{k=1}^{10}i_kj_kN_k\delta^{i_k-1}\tau^{j_k-1}+\sum_{k=11}^{19}j_kN_k\delta^{i_k-1}\tau^{j_k-1}\times\exp(-\delta^{l_k})(i_k-l_k\delta^{l_k})\tag{55}$$

4.8. Hugoniot Curve

Data measured with a shock tube apparatus [Nellis *et al.*, (1991)] were included in the optimization of the equation of state for air to improve the extrapolation behavior beyond 2000 K and 2000 MPa. One method used to demonstrate the extrapolation behavior of an equation of state is the examination of the Hugoniot curve. The conservation relations for fluid properties before and after the shock wave taken from Nellis *et al.* and the equation of state presented here were used to generate the Hugoniot curve for air. The Hugoniot curve is the locus of states accessible to a fluid after a shock wave which occur at a specified initial state. The equations for the conservation of mass, momentum, and energy across the shock wave are

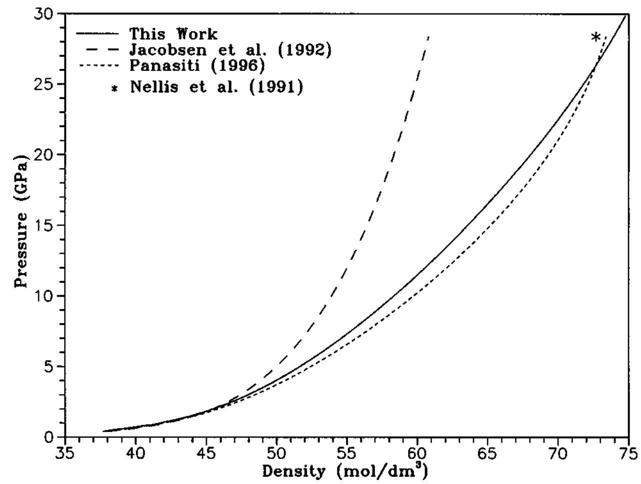

FIG. 7. Calculated Hugoniot curve for air.

$$p-p_0=\rho_0(w_s-w_0)(w_p-w_0),\tag{56}$$

$$v=v_0\left[1-\frac{(w_p-w_0)}{(w_s-w_0)}\right],\tag{57}$$

and

$$u-u_0=0.5(p+p_0)(v_0-v),\tag{58}$$

where p_0 is the initial pressure, ρ_0 is the initial mass density, u_0 is the initial molar internal energy, v_0 is the initial molar volume, w_0 is the initial velocity of the material ahead of the shock front, p is the final shock pressure, v is the final molar volume, and u is the final molar internal energy. The velocity of the shock wave is w_s and the velocity of the material downstream from the shock front is w_p. Combining Eqs. (56) and (57) results in

$$v=v_0\left(1-\frac{p-p_0}{\rho_0w_s^2}\right).\tag{59}$$

Rearrangement of Eq. (58) results in

$$v=\frac{-2(u-u_0)}{p+p_0}+v_0.\tag{60}$$

To calculate a point on the Hugoniot curve for air for a specified upstream state (p_0,T_0) and downstream pressure (p), Eqs. (59) and (60) are solved simultaneously by iterating on the unknown value for the shock wave velocity w_s. The calculated molar volume from Eq. (59) is used with the known value of p to calculate the temperature and internal energy u from the air equation of state. Figure 7 shows the

TABLE 14. Pure fluid equations of state used in the mixture model

Fluid	Author	Temperature range (K)	Maximum pressure (MPa)
Nitrogen	Span *et al.* (2000)	63.151–1000	2200
Argon	Tegeler *et al.* (1999)	83.806–700	1000
Oxygen	Schmidt and Wagner (1985)	54.361–300	82

Hugoniot curve for air calculated using this process for an initial state on the bubble line at 77.1 K as specified by Nellis *et al.* The data point on the plot is the lowest measured shock tube point from Nellis *et al.* The reported shock tube points above 30 GPa were not included because, according to Nellis *et al.*, nitrogen spontaneously dissociates above 30 GPa.

As shown in Fig. 7, the Hugoniot curve approaches the shock tube point of Nellis *et al.* (1991) indicating that the extrapolation behavior of the equation of state presented here is reasonable. However, the extrapolation behavior of the formulation should not be based solely on Fig. 7. To further assess the extrapolation behavior of the formulation, other techniques, such as determining the isothermal behavior at extreme pressures and densities, were used. These techniques are described in Sec. 7.1.

5. Mixture Model for the Nitrogen–Argon–Oxygen System

5.1. Mixture Model

The model used in this work to calculate the thermodynamic properties of nitrogen–argon–oxygen mixtures is based on the Helmholtz energy of the mixture using a corresponding states theory that was originally developed by Lemmon (1996) and Lemmon and Jacobsen (1998), (1999). The Helmholtz energy of the mixture is calculated as the sum of an ideal gas contribution, a real gas contribution, and a contribution from mixing. The Helmholtz energy for an ideal solution (the first two contributions) is determined at the reduced density and temperature of the mixture using accurate pure fluid equations of state for the mixture components. The contribution from mixing, a modified excess function, is given by a single generalized empirical equation which is applied to all mixtures considered. Reducing parameters, which are dependent on the mole fraction, are used to modify values of density and temperature. The model may be used to calculate thermodynamic properties of mixtures at various compositions, including dew and bubble-point properties and critical points. It incorporates the most accurate published equation of state for each pure fluid as given in Table 14. Additional information concerning the model is given by Lemmon and Tillner-Roth (1999).

An excess property of a mixture is defined as the actual mixture property at a given condition minus the value for an ideal solution at the same condition. In most other work dealing with excess properties, the mixing condition is defined at constant pressure and temperature. Because the independent variables for the pure fluid Helmholtz energy equations are density and temperature, properties are calculated here at the density and temperature of the mixture. Since this model deals with the entire fluid surface, reduced values of density and temperature are used rather than the physical values to ensure that properties of the constituents are calculated for the same phase as the mixture. While this approach is arbitrary and different from the usual excess property format, it results in an accurate representation of the phase boundaries for pure fluids and their mixtures.

The formulation for nitrogen–argon–oxygen mixtures given here is a modification of the generalized model developed by Lemmon (1996) for a wide range of fluids including hydrocarbons and cryogens. It preserves the general nature of the previous work, but is more accurate at low temperatures for the calculation of nitrogen–argon–oxygen mixture properties than the prior formulation. By restricting the application to a particular class of fluids, the model was designed to represent the unique characteristics of this system. The model represents available measured data in all parts of the thermodynamic surface within their estimated experimental accuracy.

An advantage of the approach used here is that the behavior of the Helmholtz energy contribution from mixing is the same for the nitrogen–oxygen, nitrogen–argon, and argon–oxygen binary systems. Relatively simple scaling factors are used to determine its magnitude for each pair. This generalization makes it possible to extend the limits of the model for the argon–oxygen mixture, for which there are few experimental single-phase data. In addition, all vapor and liquid thermodynamic properties, including energy, entropy, heat capacity, sound speed, and the mixture critical temperature, pressure, and density, can be calculated using this approach.

Preliminary equations for the mixture model based on the Helmholtz energy have incorporated equations with 7–10 terms in the excess contribution [Lemmon and Jacobsen, (1998), (1999)]. Many of these terms were included to account for deficiencies in the pure fluid equations, especially in the extrapolation behavior to high temperatures and pressures, and at temperatures below the triple points of the pure fluids. The equation presented here uses only two terms and is more predictive in nature, and results calculated for the argon–oxygen system should generally be more accurate than the preliminary models.

The Helmholtz energy for mixtures of nitrogen, argon, and oxygen can be calculated using

$$a = a^{\mathrm{idmix}} + a^{E}. \tag{61}$$

The Helmholtz energy for the ideal mixture is

$$a^{\mathrm{idmix}} = \sum_{i=1}^{3} x_i [a_i^0(\rho,T) + a_i^r(\delta,\tau) + RT \ln x_i], \tag{62}$$

In these equations, ρ and T are the mixture density and temperature, a_i^0 is the ideal gas Helmholtz energy for component i, and $a_i^r(=\alpha_i^r RT)$ is the pure-fluid residual Helmholtz energy of component i evaluated at a reduced density and temperature defined below. Equations for the ideal gas Helm-

TABLE 15. Parameters of the mixture model

	F_{ij}	ζ_{ij} (K)	ξ_{ij}(dm^3/mol)
Nitrogen–Argon	1.121 527	−1.237 713	−0.000 760 31
Nitrogen–Oxygen	1.	−0.856 350	−0.000 418 47
Argon–Oxygen	0.597 203	−2.115 126	0.000 412 32

holtz energy and residual Helmholtz energy for the pure fluids are given in the references shown in Table 14.

The excess contribution to the Helmholtz energy from mixing used in this work is

$$\frac{a^E}{RT} = \alpha^E(\delta,\tau,\mathbf{x}) = \left\{\sum_{i=1}^{2}\sum_{j=i+1}^{3} x_i x_j F_{ij}\right\}[-0.001\,952\,45\delta^2\tau^{-1.4} + 0.008\,713\,34\delta^2\tau^{1.5}], \tag{63}$$

where the coefficients and exponents were obtained from nonlinear regression of experimental mixture data. Values of F_{ij} are given in Table 15. All single phase thermodynamic properties can be calculated from the Helmholtz energy as described in Sec. 4.7 using the relations

$$\alpha^0 = \sum_{i=1}^{3} x_i\left[\frac{a_i^0(\rho,T)}{RT} + \ln x_i\right] \tag{64}$$

and

$$\alpha^r = \sum_{i=1}^{3} x_i \alpha_i^r(\delta,\tau) + \alpha^E(\delta,\tau,\mathbf{x}), \tag{65}$$

where the derivatives are taken at constant composition. Calculations of two-phase properties are described in Sec. 5.2. The reduced values of density and temperature for the mixture used in Eqs. (63) and (65) are

$$\delta = \rho/\rho_{\mathrm{red}} \tag{66}$$

and

$$\tau = T_{\mathrm{red}}/T, \tag{67}$$

where ρ and T are the mixture density and temperature, and ρ_{red} and T_{red} are the reducing values

$$\rho_{\mathrm{red}} = \left(\sum_{i=1}^{3}\frac{x_i}{\rho_{c_i}} + \sum_{i=1}^{2}\sum_{j=i+1}^{3} x_i x_j \xi_{ij}\right)^{-1} \tag{68}$$

and

$$T_{\mathrm{red}} = \sum_{i=1}^{3} x_i T_{c_i} + \sum_{i=1}^{2}\sum_{j=i+1}^{3} x_i x_j \zeta_{ij}. \tag{69}$$

The parameters ζ_{ij} and ξ_{ij} are used to define the shapes of the reducing temperature lines and reducing density lines. These reducing parameters are not the same as the critical parameters of the mixture and are determined simultaneously in the nonlinear fit of experimental data with the other parameters of the mixture model. The generalized factors and mixture parameters F_{ij}, ζ_{ij} and ξ_{ij} are given in Table 15.

If equations for the ideal gas Helmholtz energy in the nondimensional form $\alpha_i^0(\delta,\tau)$, similar to Eq. (24), are used rather than equations in the dimensional form $a_i^0(\rho,T)$ as indicated by Eq. (64), the reducing variables for δ and τ in the ideal gas equation are

$$\delta = \rho/\rho_{c_i} \tag{70}$$

and

$$\tau = T_{c_i}/T, \tag{71}$$

rather than the reducing values defined by Eqs. (66) and (67). This only applies to the ideal gas part of the equation, not to the residual Helmholtz energy. The residual and excess terms $\alpha_i^r(\delta,\tau)$ and $\alpha^E(\delta,\tau,\mathbf{x})$ in Eq. (65) must be evaluated at the reduced state point of the mixture defined by Eqs. (66) and (67). This complication is avoided though the use of dimensional equations of the form given in Eq. (22) or dimensionless equations of the form given in Eq. (23) where the critical properties cancel out of the equation. Equations of the form given in Eq. (24) are derived from dimensional equations, and the critical parameters of the pure fluids are built into the coefficients of the equations.

5.2. Vapor–Liquid Equilibrium (VLE) Properties

In a two-phase nonreacting mixture, the thermodynamic constraints for vapor–liquid equilibrium (VLE) are

$$T' = T'' = T, \tag{72}$$

$$p' = p'' = p, \tag{73}$$

and

$$\mu_i' = \mu_i'', \quad i = 1,2,\ldots,q, \tag{74}$$

where the superscripts $'$ and $''$ refer to the liquid and vapor phases, respectively, and q is the number of components in the mixture. Equation (74) is identical to equating the fugacities of the liquid and vapor phases for each component in the mixture

$$f_i' = f_i''. \tag{75}$$

The chemical potential of component i in a mixture is

$$\mu_i(\rho,T) = \left(\frac{\partial A}{\partial n_i}\right)_{T,V,n_j} = \mu_i^c(T) + RT\ln(f_i), \tag{76}$$

where $\mu_i^c(T)$ is a function of temperature only and the notation n_j indicates that all mole numbers are held constant except n_i. The chemical potential in an ideal gas mixture is

$$\mu_i^0 = \left(\frac{\partial A^0}{\partial n_i}\right)_{T,V,n_j} = \mu_i^c(T) + RT\ln(f_i^0), \tag{77}$$

where f_i^0 is the ideal gas partial pressure of constituent i, $x_i p^0 = x_i \rho RT$. Subtracting these equations results in

TABLE 16. Different types of VLE calculations

Calculation type	Specified quantities	Calculated quantities
BUBL p	T and the x_i	p and the y_i
DEW p	T and the y_i	p and the x_i
BUBL T	p and the x_i	T and the y_i
DEW T	p and the y_i	T and the x_i
FLASH	T and p	x_i and y_i

$$f_i = x_i \rho RT \exp\left(\frac{\partial(n\alpha^r)}{\partial n_i}\right)_{T,V,n_j}, \tag{78}$$

where α^r was defined in Eq. (65). The partial derivative at constant temperature, total volume (not molar volume), and mole number of all constituents except i is generally evaluated numerically.

Five common VLE calculations are listed in Table 16. The VLE conditions for these five calculations can be determined iteratively. The x_i represent the mole fractions in the liquid phase, and the y_i represent the mole fractions in the vapor phase. Details of the iterative processes can be found in Van Ness and Abbott (1982) or Smith and Van Ness (1975).

5.3. Critical Locus

In the development of the mixture model, equations for the reducing parameters were given for the calculation of the reduced density and temperature δ and τ. These parameters are equal to the critical parameters in the pure fluid limits. For a mixture, the reducing parameters are not the same as the critical parameters, but are empirical functions designed to minimize the deviations between experimental data and the mixture model.

The criteria for the critical point of a binary mixture are

$$\left(\frac{\partial^2 g}{\partial x^2}\right)_{p,T} = \left(\frac{\partial^3 g}{\partial x^3}\right)_{p,T} = 0, \tag{79}$$

where g is the molar Gibbs energy of the mixture. Near the critical point, this equation can be expanded in terms of the numerical differences

$$\Delta\left(\frac{\partial^2 g}{\partial x^2}\right)_{p,T} \approx \frac{\partial}{\partial T}\left(\frac{\partial^2 g}{\partial x^2}\right)_{p,T} \Delta T + \frac{\partial}{\partial p}\left(\frac{\partial^2 g}{\partial x^2}\right)_{p,T} \Delta p \tag{80}$$

and

$$\Delta\left(\frac{\partial^3 g}{\partial x^3}\right)_{p,T} \approx \frac{\partial}{\partial T}\left(\frac{\partial^3 g}{\partial x^3}\right)_{p,T} \Delta T + \frac{\partial}{\partial p}\left(\frac{\partial^3 g}{\partial x^3}\right)_{p,T} \Delta p, \tag{81}$$

where ΔT and Δp are the differences from the critical point temperature and pressure in an iterative algorithm for finding the critical point, and the left sides of these equations represent the deviations from the zero value at the critical point indicated in Eq. (79). Solving these equations for ΔT and Δp results in

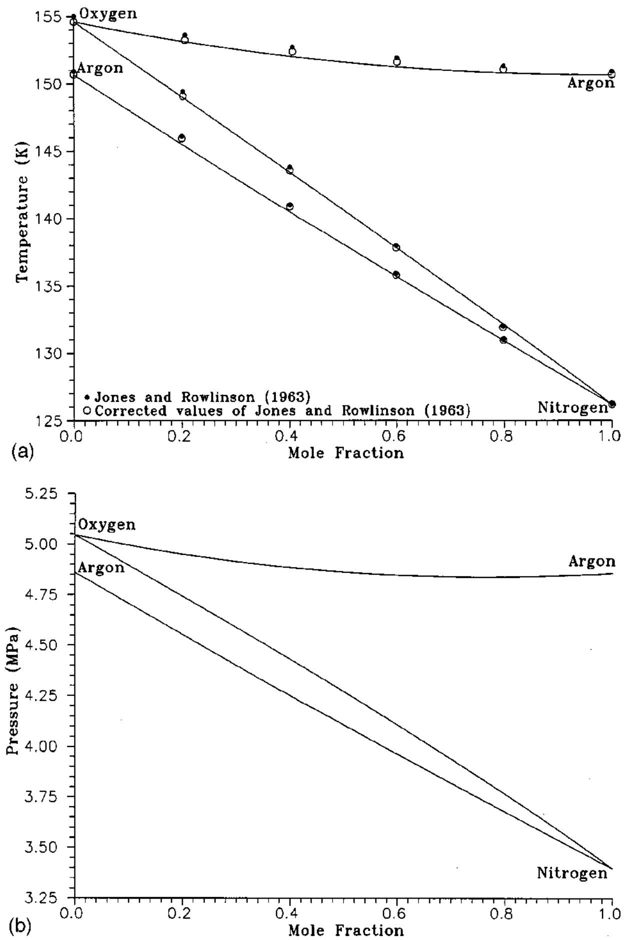

FIG. 8. Critical lines for nitrogen–argon, nitrogen–oxygen, and argon–oxygen binary mixtures.

$$\Delta T \approx \frac{\left(\frac{\partial^2 g}{\partial x^2}\right)_{p,T} \frac{\partial}{\partial p}\left(\frac{\partial^3 g}{\partial x^3}\right)_{p,T} - \left(\frac{\partial^3 g}{\partial x^3}\right)_{p,T} \frac{\partial}{\partial p}\left(\frac{\partial^2 g}{\partial x^2}\right)_{p,T}}{\frac{\partial}{\partial T}\left(\frac{\partial^3 g}{\partial x^3}\right)_{p,T} \frac{\partial}{\partial p}\left(\frac{\partial^2 g}{\partial x^2}\right)_{p,T} - \frac{\partial}{\partial T}\left(\frac{\partial^2 g}{\partial x^2}\right)_{p,T} \frac{\partial}{\partial p}\left(\frac{\partial^3 g}{\partial x^3}\right)_{p,T}} \tag{82}$$

and

$$\Delta p \approx \frac{-\left(\frac{\partial^2 g}{\partial x^2}\right)_{p,T} - \frac{\partial}{\partial T}\left(\frac{\partial^2 g}{\partial x^2}\right)_{p,T} \Delta T}{\frac{\partial}{\partial p}\left(\frac{\partial^2 g}{\partial x^2}\right)_{p,T}}, \tag{83}$$

from which an estimate of the location of the critical point can be obtained. The reducing parameters can be used as initial estimates for the critical pressure and temperature and the values of T and p are repeatedly incremented according to Eqs. (82) and (83) until the second and third derivatives of the Gibbs energy are both simultaneously near zero.

The critical lines for the nitrogen–argon, nitrogen–oxygen, and argon–oxygen binary mixtures are shown in Fig. 8 along with experimental values of the critical temperature from Jones and Rowlinson (1963). The value of T_c for oxygen reported by Jones and Rowlinson is 0.3% different from the value given by Schmidt and Wagner (1985). Likewise, the value for argon is 0.2% different from that given by Tegeler *et al.* (1999). To account for these differences, the experimental values of Jones and Rowlinson were corrected for each (i,j) binary pair using

$$T_c = T_{c,\mathrm{Jones}} + x_i(T_{c,i} - T_{c,i,\mathrm{Jones}}) + x_j(T_{c,j} - T_{c,j,\mathrm{Jones}}). \tag{84}$$

The adjusted values are also shown in Fig. 8.

6. Comparisons of Calculated Properties to Experimental Data

The uncertainty of the equation of state and the mixture model was determined by statistical comparisons of property values calculated with the equation of state or mixture model to experimental data. These statistics are based on the percent deviation in any property X defined as

$$\%\Delta X = 100\left(\frac{X_{\mathrm{exp}} - X_{\mathrm{calc}}}{X_{\mathrm{exp}}}\right), \tag{85}$$

where X_{exp} is the measured or predicted data, and X_{calc} is computed from the equation of state. Using this definition, the average absolute deviation (AAD) is defined as

$$\mathrm{AAD} = \frac{1}{n}\sum_{i=1}^{n} |\%\Delta X_i|, \tag{86}$$

where n is the number of data points. For the second virial coefficient, the difference in B (in cm^3/mol) is used rather than the percent difference since the percent difference can become very large near $B=0$.

6.1. Comparisons of the Ancillary Equations for Air with Experimental Data

Comparisons of dew and bubble-point properties calculated using Eqs. (1), (2), and (3) to the experimental data of Blanke (1977), Michels *et al.* (1954a), Kuenen and Clark (1917) and the calculated data reported by Jacobsen *et al.* (1990b) are shown in Fig. 9 and the average absolute deviations are given in Table 6.

For the bubble-point pressure equation, the Blanke data below 110 K are not in agreement with values calculated from the mixture model given in Sec. 5, with differences approaching 15% in pressure at the lowest temperature. The Blanke values are the only available low-temperature data for the properties of air on the phase boundaries, however, they were determined graphically from $p-\rho-T$ data. Because of the large deviations mentioned above, they were not used to develop the ancillary equations where they conflicted with values calculated from the mixture model. To maintain consistency between the mixture model and the ancillary equation reported here, the bubble-point pressures from the mixture model were used for temperatures below 100 K in developing the ancillary equations. At higher temperatures, the data of Michels *et al.* and Blanke between 120 and 130 K and the Leung-Griffiths calculations from Jacobsen *et al.* between 131.8 and 132.5 K were used.

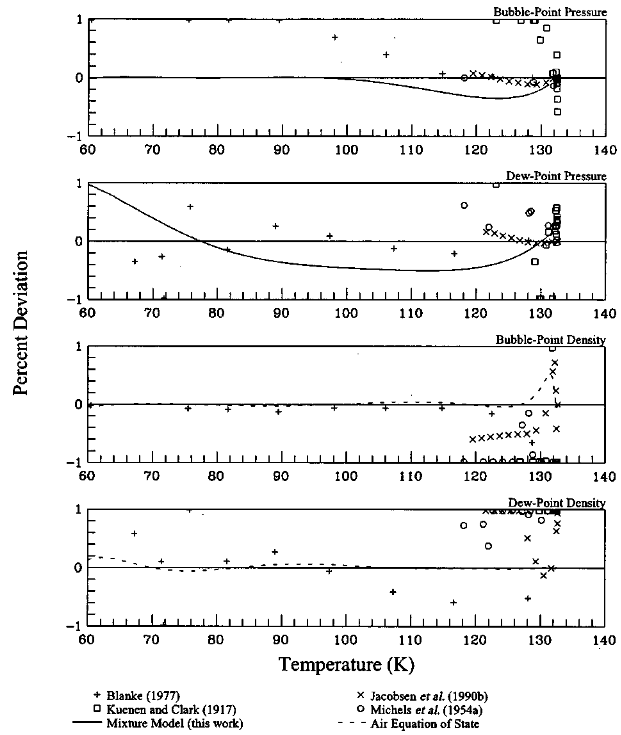

FIG. 9. Comparisons of dew and bubble-point properties calculated with the ancillary equations toexperimental and calculated data for air.

For the dew-point pressure equation, values below 66 K from the mixture model were used in the absence of experimental data. Most of the data of Blanke are represented within 0.3%. The Leung–Griffiths calculations from Jacobsen *et al.* (1990b) between 130.4 and 132.6 K were fitted in the critical region. For both the dew and bubble-point pressures, the first term of Eq. (1) ensures that the first derivative of pressure with respect to temperature is infinite at the maxcondentherm, as shown in Fig. 6.

Below 118 K, the data of Blanke are the only available saturated density data for air. For the bubble-point densities, both the air equation of state and the mixture model of this work agree with the density data of Blanke to within 0.1%. The single-phase liquid surface is represented well by accurate experimental data, and the uncertainty of density values calculated from the equation of state should be less than 0.1% even at the lowest temperatures. For the dew-point densities, the average absolute deviation of the data of Blanke was 0.6%. These data have not been represented well by previous equations of state for air [Jacobsen *et al.* (1990a); Jacobsen *et al.* (1992); Panasiti *et al.* (1999)] nor with preliminary equations developed using second virial coefficients, and these data show deviations of up to 2% from all of these equations. Calculated density values from the equation of state were used in the development of the dew and bubble-point ancillary equations for consistency.

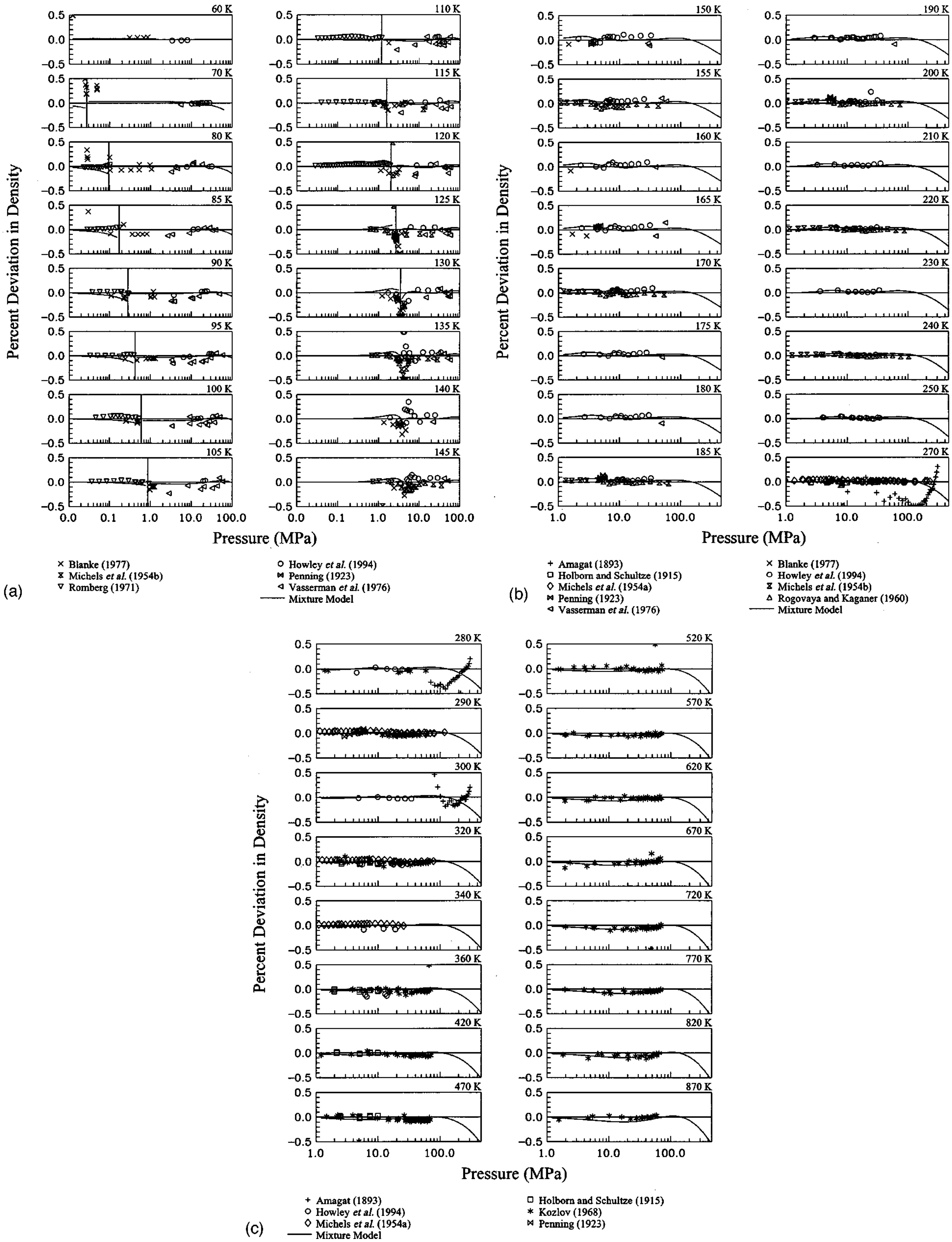

FIG. 10. Comparisons of densities calculated with the equation of state to experimental data for air.

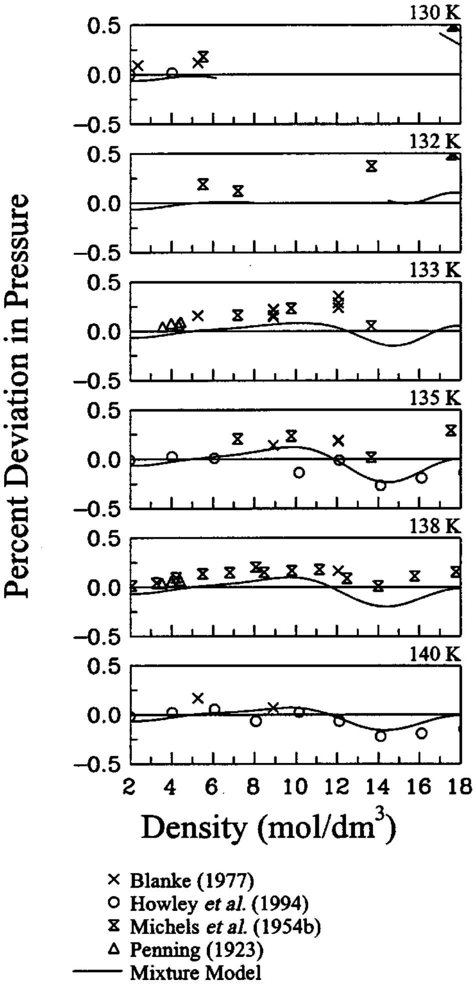

FIG. 11. Comparisons of pressures calculated with the equation of state to experimental data for air in the critical region.

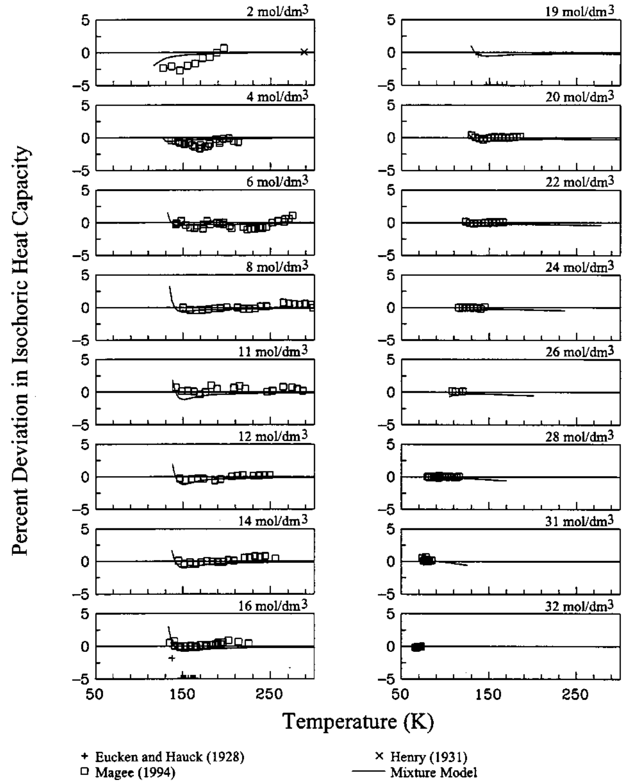

FIG. 12. Comparisons of isochoric heat capacities calculated with the equation of state to experimental data for air.

6.2. Comparisons of the Equation of State for Air and the Mixture Model with Experimental and Calculated Data for Air

Table 6 shows the statistical analysis of comparisons to experimental data sets for $p-\rho-T$, isochoric and isobaric heat capacities, speed of sound, and second virial coefficients for air. Comparisons to all available experimental data are given in Figs. 10–15. The vertical lines in these figures show the locations of the phase boundaries at the indicated temperature. Deviations between the mixture model at the composition of standard air and the air equation of state are shown as solid lines at the indicated isotherms or isochores. These comparisons are quite useful in determining the consistency of data sets and the uncertainty of the equation of state, since the mixture model has very few adjustable parameters, and only a very limited set of data was used to determine the parameters. Equations of state can be overfit due to the large number of adjustable parameters. For the mixture model, this is not a problem, and deviations between experimental data, the equation of state, and the mixture model are useful in showing various trends and inconsistencies.

Figure 10 shows comparisons of densities calculated with the equation of state to experimental $p-\rho-T$ data. Several inconsistencies can be seen in the data used in the fit. At 290 K, the data of Michels *et al.* (1954a) and of Kozlov (1968) differ by an average of 0.1% in density. This offset is also seen between the data of Kozlov and the equation of state throughout most of the data of Kozlov. The data of Howley *et al.* (1994) are generally consistent with the data of Michels *et al.*, except at temperatures below 200 K. At 155 K, these two data sets differ by 0.1%. Although used in the fit, the scatter in the data of Blanke is within 0.2% in the liquid, and within 0.5% in the vapor. Differences between the overlapping vapor phase data of Romberg (1971) and the equation of state are less than 0.1%, as compared with 0.5% for the data of Blanke. There are no overlapping data in the liquid. Despite the age of the data of Amagat (1893), the equation of state (which was not fit to these data) agrees on average to within 0.3% at pressures between 200 and 300 MPa and temperatures from 270 to 300 K. The only other data in a comparable range are the data of Michels *et al.* at 270 K up to 228 MPa. The equation of state agrees within 0.1% with these data. Differences between the mixture model and the Amagat data are larger at the highest pressures, however, these pressures are well beyond the limits of the oxygen equation of state.

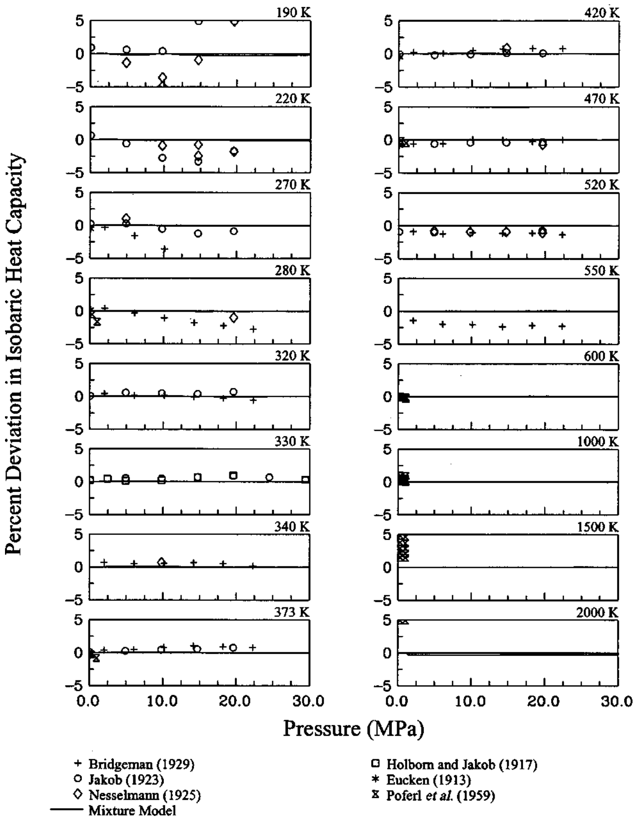

FIG. 13. Comparisons of isobaric heat capacities calculated with the equation of state to experimental data for air.

The deviations of data in the critical region between 130 and 140 K are shown in Fig. 11. Since density deviations tend to be large in the critical region for any substance (because $\partial\rho/\partial p$ at constant temperature approaches infinity at the critical point), this figure shows comparisons of pressures calculated with the equation of state to experimental $p-\rho-T$ data. The scatter between different data sets is within $\pm 0.3\%$ in pressure throughout most of the critical region, with deviations tending to be positive for the data of Blanke (1977) and Michels *et al.* (1954b), and negative or near zero for comparisons with the data of Howley *et al.* (1994). Deviations between the mixture model and the equation of state tend to be less than that with the experimental data, with the mixture model agreeing best with the data of Howley *et al.*

Comparisons of values calculated from the equation of state are shown for isochoric heat capacities in Fig. 12, isobaric heat capacities in Fig. 13, and the speed of sound in Fig. 14. The equation of state agrees very well with the c_v data of Magee (1994) except at the lowest density isochore, 2 mol/dm^3, where the uncertainty of the isochoric heat capacity data tend to be highest. Comparisons with the mixture model are quite good, except for the upturns in the vapor phase near the saturation boundaries. Deviations with the isobaric heat capacity data in the vapor phase are generally within 2%, however, both the uncertainty and the scatter in these data are higher than that for the isochoric heat capacity data. Deviations between the equation of state and the mixture model are nearly negligible, even at 2000 K. Comparisons between the equation of state and the speed of sound data of Ewing and Goodwin (1993) and the data of Younglove and Frederick (1992) are very good at temperatures above 200 K and below 120 K. Near the saturation boundaries and in the critical regions, the deviations tend to be somewhat higher but generally within 1%. The mixture model follows the data of Younglove and Frederick more closely than does the equation of state in these regions.

The differences in the second virial coefficients are shown in Fig. 15. Differences between the data of Romberg (1971) at low temperatures with the equation of state tend to be positive, whereas differences between the graphically determined data from Romberg given here in Table 7 tend to be more scattered, generally within ± 1 cm^3/mol (about 0.5% at 90 K) except at the lowest temperature. This scatter is due to the difficulty of determining the second virial coefficient as the uncertainty of $p-\rho-T$ data increases at low pressures and temperatures as shown in Fig. 4. The second virial coefficients calculated from the mixture model are not as accurate as those calculated from the air equation of state. Values of the second virial coefficient for oxygen calculated from the equation of state of Schmidt and Wagner (1985) show a minimum at 75 K, and calculated values become positive at temperatures below 58 K. This low temperature behavior is unrealistic and reduces the accuracy of virial coefficients calculated using the mixture model in spite of the fact that the calculated values from Schmidt and Wagner are within the uncertainty of available experimental data.

Figure 16 shows calculated dew and bubble-line densities in the critical region reported by Jacobsen *et al.* (1990b) determined using a Leung–Griffiths model for ternary systems. As shown in Fig. 16, the equation of state developed in this work represents the calculated data of Jacobsen *et al.* (1990b) more accurately than the previous equation of Jacobsen *et al.* (1992). Densities were calculated from each equation of state at the temperature and bubble or dew-point pressure of the equation. This pressure was calculated from the respective ancillary equation for each equation of state. Dew and bubble-point states at the air composition calculated from the mixture model as described in Sec. 5.2. are also shown in the figure.

Figure 17 shows the percent deviation in density between values calculated with the equation of state for air and the properties of air predicted from nitrogen data by the methods described in Sec. 4.2 and used in the development of the air equation of state. At temperatures above 1000 K where deviations between the nitrogen equation of state and the experimental data for nitrogen exceed 2%, the equation of state for air mimics the trends set by the equation of state for nitrogen [Span *et al.* (2000)] as shown by the calculated data points in Fig. 17.

6.3. Comparisons of the Mixture Model with Experimental Single Phase Data

Summary comparisons of values calculated using the mixture model to $p-\rho-T$ data for mixtures of nitrogen, argon,

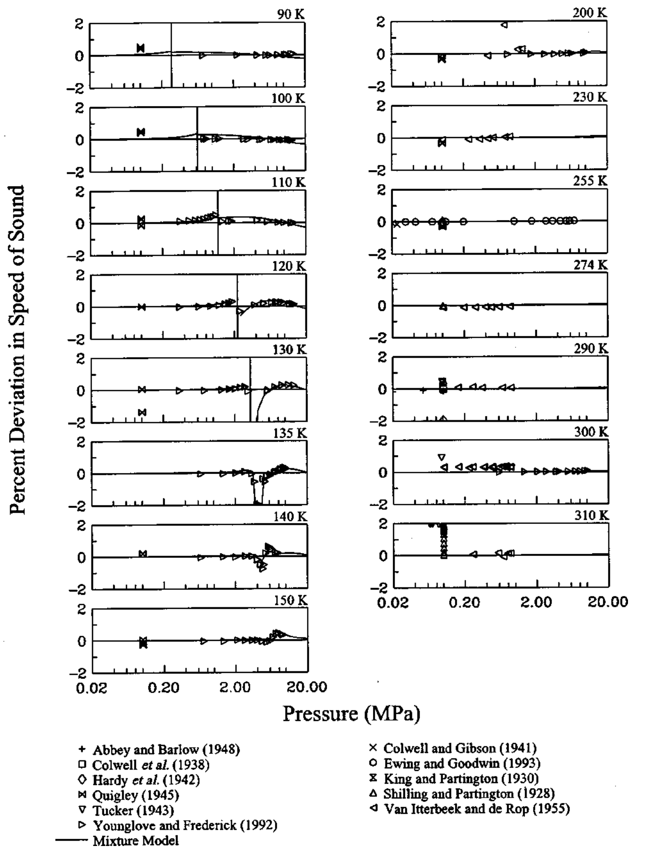

FIG. 14. Comparisons of speeds of sound calculated with the equation of state to experimental data for air.

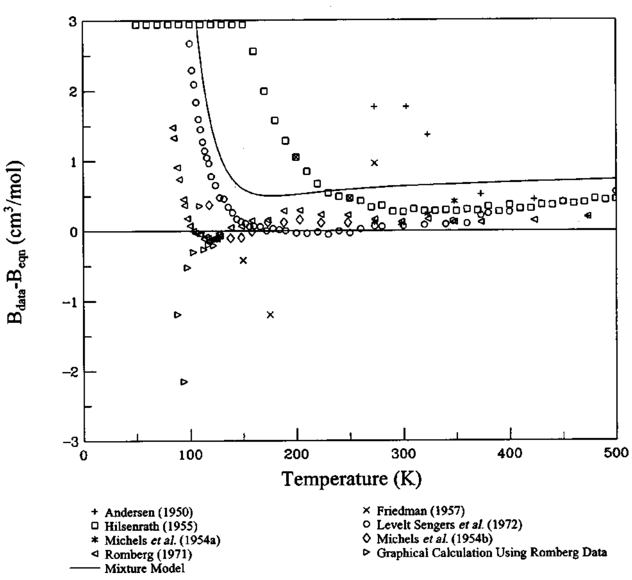

FIG. 15. Comparisons of second virial coefficients calculated with the equation of state to experimental data for air.

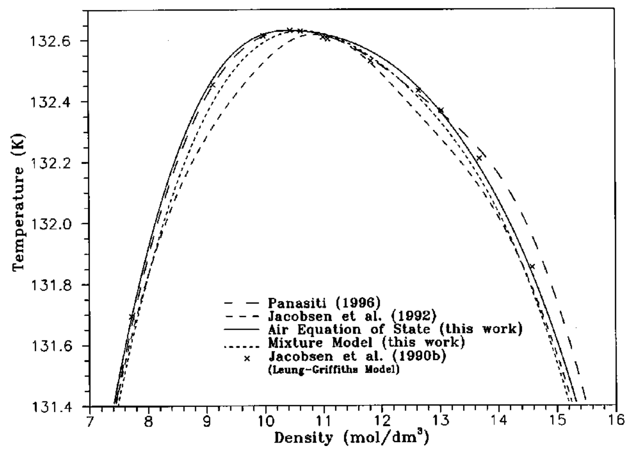

FIG. 16. Comparisons of critical region phase boundaries calculated with the equation of state to predicted data for air.

and oxygen are given in Table 8; this table indicates the temperature range and composition range for the first component listed for each data set. The bubble-point pressures, calculated from the model, were assumed for several data sets for the nitrogen–oxygen and argon–oxygen systems where the pressures were not included in the published data. Comparisons of densities calculated from the mixture model to experimental data are shown in Fig. 18 for the nitrogen–argon binary mixture and in Fig. 19 for the nitrogen–oxygen and argon–oxygen binary mixtures.

The Maslennikova *et al.* (1979) data for the nitrogen–argon mixture extend to 800 MPa and deviations are on average within 0.3%. From this and because of the generalized nature of the model, calculated densities should be within 1.0% up to 800 MPa for the nitrogen–oxygen and argon–oxygen systems where no data exist. The magnitudes of the deviations for most of the nitrogen–argon data are similar to those for the extended corresponding states models of Clarke *et al.* (1994) and version 9.08 of the NIST14 database [Friend (1992)].

Very few data exist for the nitrogen–oxygen and argon–oxygen mixtures. For the nitrogen–oxygen mixture, air data and the data of Pool *et al.* (1962) were used to determine the parameters for the mixture model. Although the temperature range of experimental $p-\rho-T$ data for the argon–oxygen system is only 70–90 K with pressures up to 0.2 MPa in the liquid phase, the model should be valid for all temperatures and pressures for argon–oxygen mixtures within the ranges of experimental data for the nitrogen–oxygen and nitrogen–argon systems due to the predictive nature of the model. From these comparisons, we estimate that the uncertainty of $p-\rho-T$ calculations in the extended range for argon–oxygen mixtures is within 0.5%. This estimate is based additionally on comparisons to the large amount of VLE data available over the entire two-phase range for this mixture.

6.4. Comparisons of the Mixture Model with Experimental VLE Data

Comparisons of bubble-point pressures calculated with the mixture model to experimental data are shown in Fig. 20 for

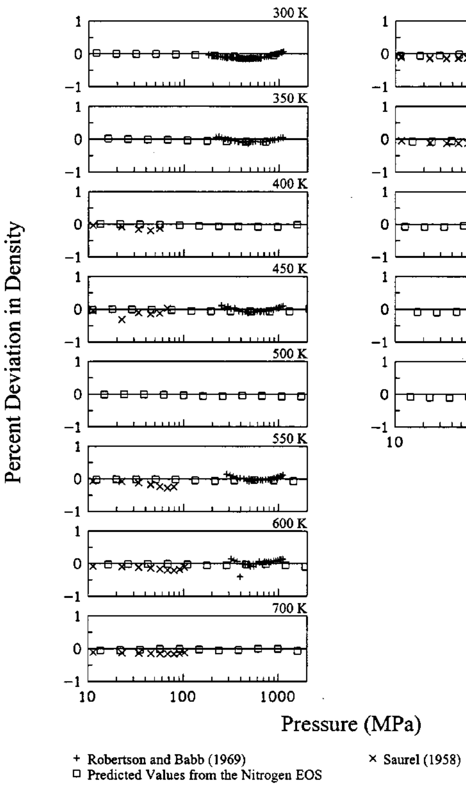

FIG. 17. Comparisons of densities calculated with the equation of state to calculated $p-\rho-T$ data estimated from nitrogen data.

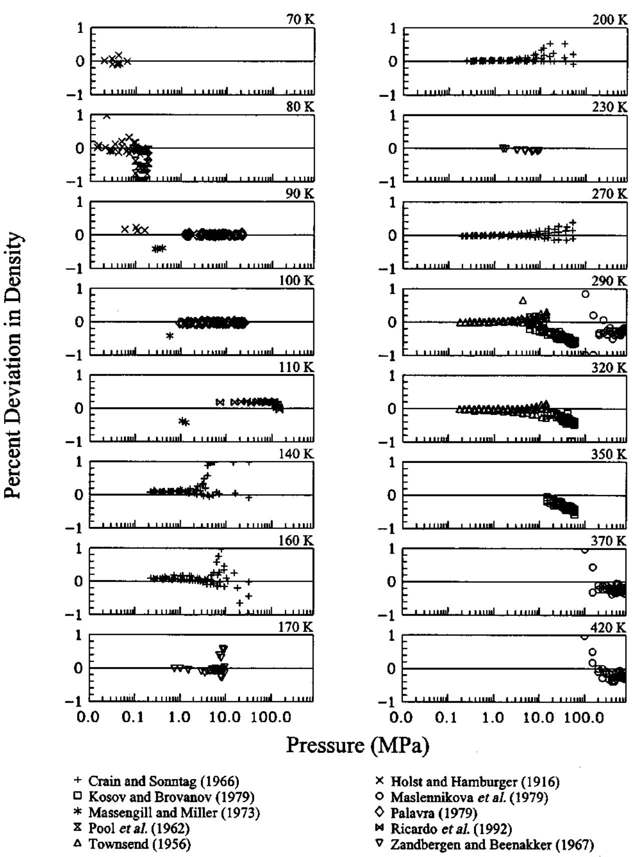

FIG. 18. Comparisons of densities calculated with the mixture model to experimental data for the nitrogen–argon binary mixture.

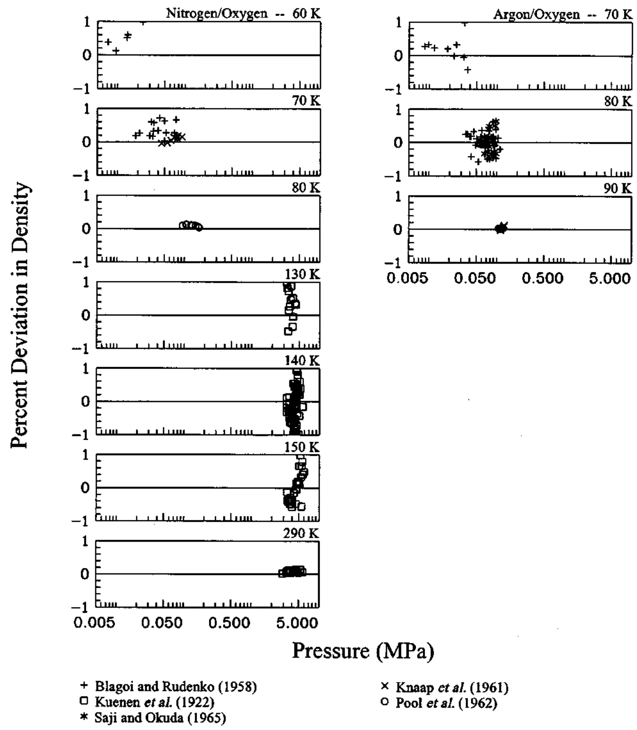

FIG. 19. Comparisons of densities calculated with the mixture model to experimental data for the nitrogen–oxygen and argon–oxygen binary mixtures.

the nitrogen–argon binary mixture, Fig. 21 for the nitrogen–oxygen binary mixture, Fig. 22 for the argon–oxygen binary mixture, and Fig. 23 for the nitrogen–argon–oxygen ternary mixture. The average deviations in bubble-point pressure for the VLE data of Wilson *et al.* (1965) for the nitrogen–argon, nitrogen–oxygen, argon–oxygen, and nitrogen–argon–oxygen mixtures are within 0.8% and are nearly the same as those for the model developed by Lemmon (1996). However, the deviations between the mixture model and the lower temperature nitrogen–oxygen data of Duncan and Staveley (1966) and Armstrong *et al.* (1955) are substantially lower in the new model reported here, and the average deviations for these data sets are about 1.6% and 0.8%, respectively, about 50% smaller than those for the model of Lemmon (1996).

7. Estimated Uncertainty of Calculated Properties

7.1. Characteristic Curves of Air

Plots of constant property lines on various thermodynamic coordinates are useful in assessing the behavior of the equation of state in regions where there are no accurate experimental results for the corresponding property. The equation of state for air developed here was used to produce plots of temperature against isochoric heat capacity (Fig. 24), isobaric heat capacity (Fig. 25), and speed of sound (Fig. 26). As mentioned in Sec. 4.8, analytical methods in addition to calculating the Hugoniot curve are needed to determine the extrapolation behavior of an equation of state. Figure 27

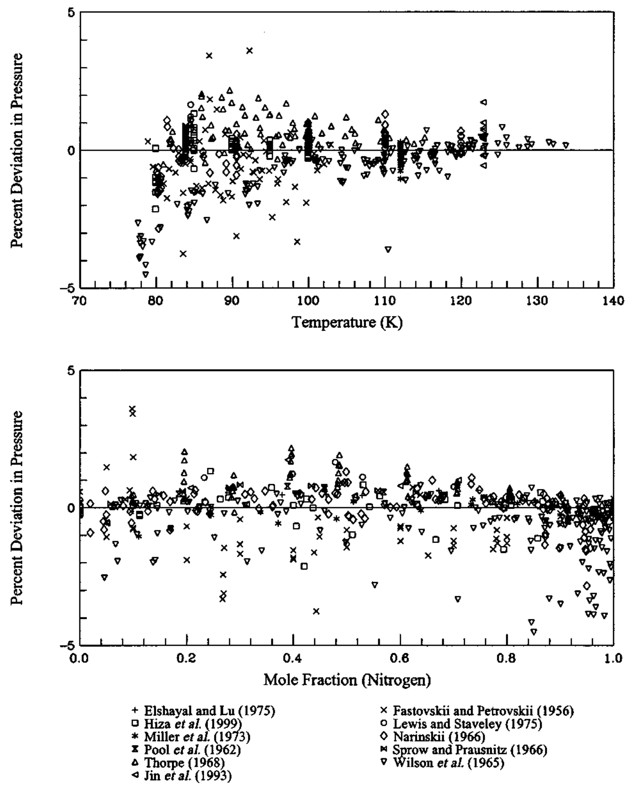

FIG. 20. Comparisons of bubble-point pressures calculated with the mixture model to experimental data for the nitrogen–argon binary mixture.

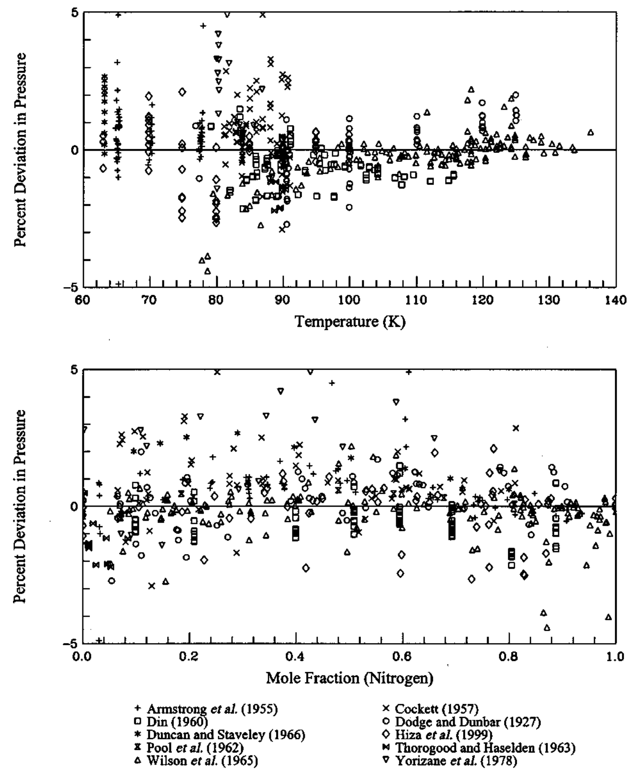

FIG. 21. Comparisons of bubble-point pressures calculated with the mixture model to experimental data for the nitrogen–oxygen binary mixture.

shows a pressure versus density plot along isotherms. This plot indicates that the equation of state presented here exhibits reasonable extrapolation behavior at high pressures and densities.

Plots of certain ''ideal curves'' are useful in assessing the behavior of an equation of state [Deiters and de Reuck (1997), Span and Wagner (1997), Span (2000)]. The characteristic curves considered in this work are the Boyle curve, given by the equation

$$\left(\frac{\partial Z}{\partial v}\right)_T = 0, \tag{87}$$

the Joule–Thomson inversion curve,

$$\left(\frac{\partial Z}{\partial T}\right)_p = 0, \tag{88}$$

or

$$\left(\frac{\partial T}{\partial p}\right)_h = 0, \tag{89}$$

and the Joule inversion curve

$$\left(\frac{\partial Z}{\partial T}\right)_v = 0. \tag{90}$$

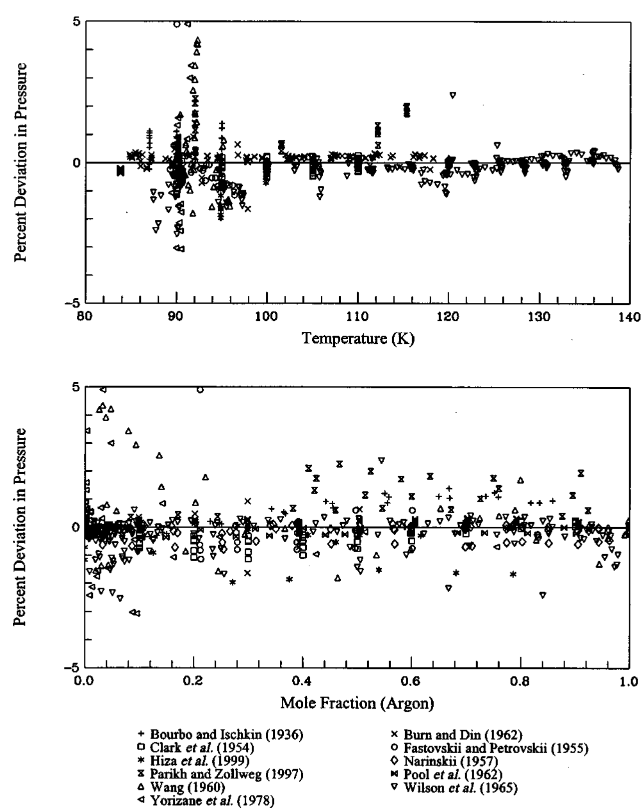

FIG. 22. Comparisons of bubble-point pressures calculated with the mixture model to experimental data for the argon-oxygen binary mixture.

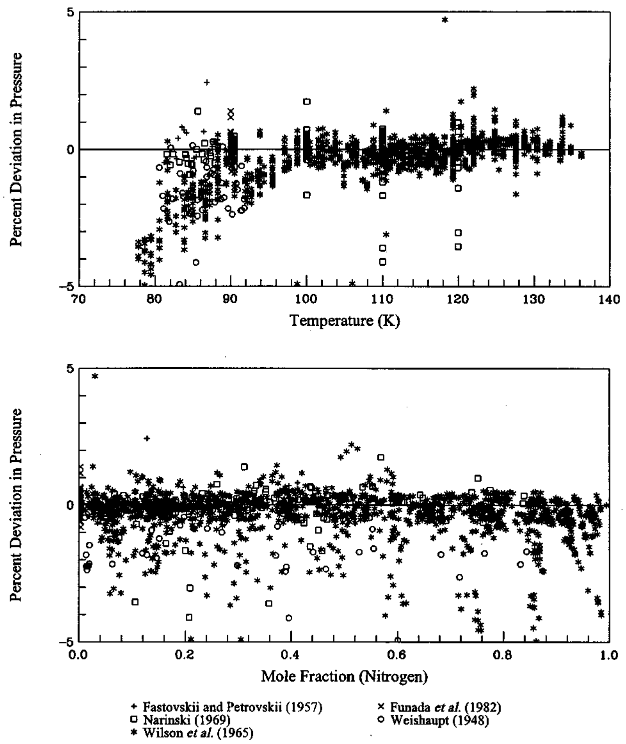

FIG. 23. Comparisons of bubble-point pressures calculated with the mixture model to experimental data for the nitrogen-argon-oxygen ternary mixture.

Figure 28 illustrates these characteristic curves for the equation of state for air. Although the curves in Fig. 28 do not provide numerical information, reasonable shapes of these curves as shown indicate qualitatively correct extrapolation behavior of the equation of state.

7.2. Uncertainty of the Equation of State for Air and of the Mixture Model

The uncertainties of the models presented here have been estimated by comparing calculated results with experimental data, as summarized in Sec. 6, and assessing the data them-

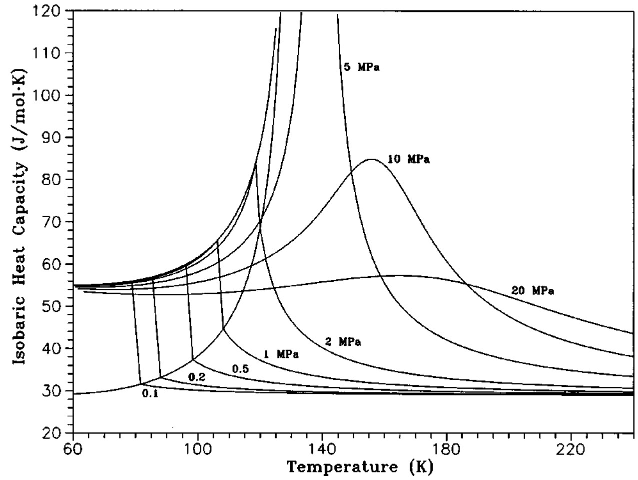

FIG. 25. Isobaric heat capacity versus temperature diagram for air.

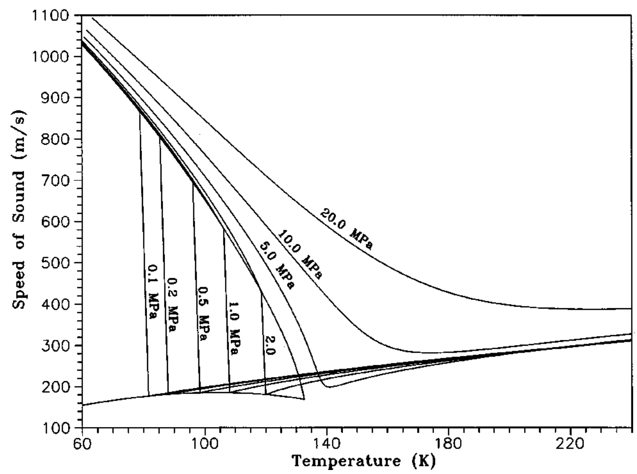

FIG. 26. Speed of sound versus temperature diagram for air.

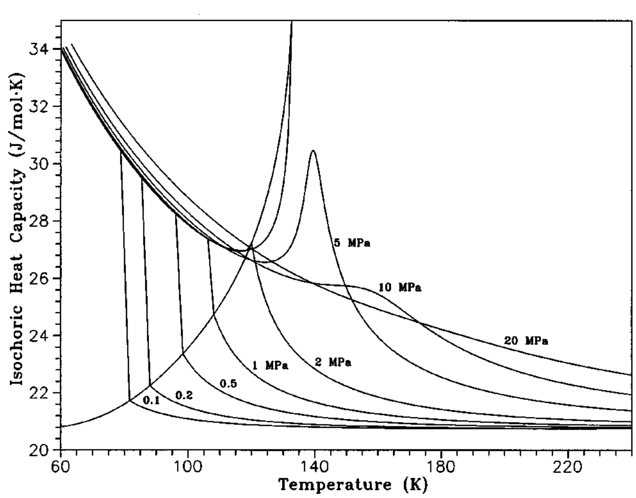

FIG. 24. Isochoric heat capacity versus temperature diagram for air.

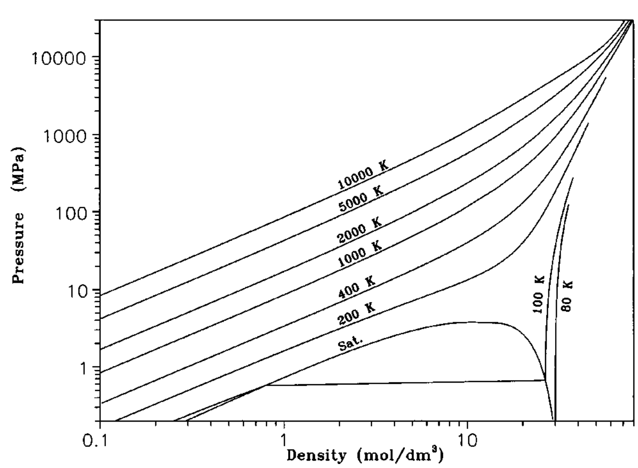

FIG. 27. Pressure versus density diagram for air.

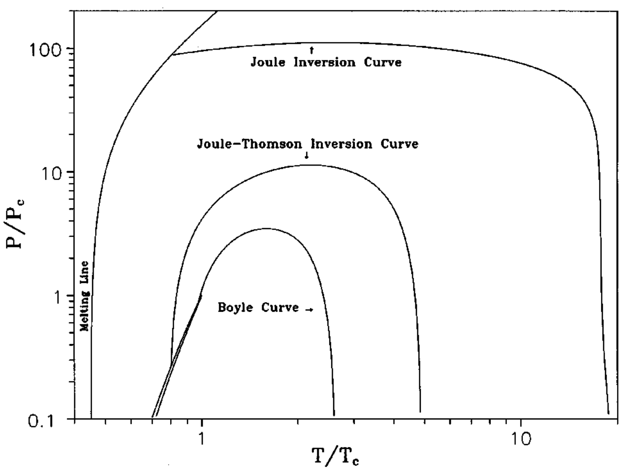

FIG. 28. Characteristic curves for air.

selves according to the quoted experimental uncertainties and the mutual consistency of data obtained from different sources. A general knowledge of the behavior of thermodynamic surfaces and substantial experience with other correlating equations for well-studied fluids have also been applied in the estimation of uncertainties. The uncertainties represent expanded combined uncertainties where a normal distribution of errors is assumed and a coverage factor of 2 has been applied (equivalent to a confidence level of about 95%). This means that if a uniform distribution of state points is considered within the range specified below, no more than 2% of values for a given property will deviate from the physical value by more than the specified uncertainty.

For the equation of state of standard air, the region for which sufficient data are available to establish reliable uncertainty estimates ranges from the solidification point to 873 K at pressures up to 70 MPa, except in the critical region from 130 to 134 K and 9 to 13 mol/dm^3. The estimated uncertainty of density values calculated using the equation of state for air is 0.1%. The estimated uncertainty of speed of sound values is within 0.2% based on comparisons with the data of Younglove and Frederick (1992), Van Itterbeek and de Rop (1955), and Ewing and Goodwin (1993). The estimated uncertainty is 1% for calculated values of heat capacity based upon comparisons to the experimental data of Magee (1994). In the critical region defined above, the uncertainty in pressure calculations is estimated to be 0.3%. Outside the range of the primary experimental data for air ($T > 870$ K, $p > 70$ MPa) and at temperatures less than 2000 K and pressures less than 2000 MPa, the estimated uncertainty in predicted densities is 1.0%. Without experimental data, the uncertainty of extrapolated properties cannot be verified.

The uncertainty of the mixture model reported here for arbitrary compositions of nitrogen, oxygen, and argon is within 0.1% in density, 0.2% for the speed of sound, and 1% in heat capacity for both binary and ternary mixtures in the same range given for the air equation of state. The uncertainty of calculated dew and bubble-point pressures is within 1%. The mixtures and ranges for which calculated properties have been verified by experimental data to have deviations within these limits are listed in Table 17. In regions where there are no binary mixture data, the uncertainty is estimated to be of the same magnitude. However, these estimates cannot be verified until experimental data are available to support these estimates.

TABLE 17. Regions of stated uncertainty of the mixture model

Mixture	Temperature range (K)	Maximum pressure (MPa)
Nitrogen–Argon	70–420	800
Nitrogen–Oxygen and Air	60–870	100
Argon–Oxygen	70–90	0.2
	70–400[a]	100[a]

[a]No data are available to verify this range, however, the uncertainty of the equation should be at least 0.5% in density for the range stated due to the predictive nature of the model.

Because of the generalized and predictive nature of the mixture model, calculated densities of mixtures of nitrogen, argon, and oxygen extrapolated to temperatures up to 1000 K and pressures to 100 MPa have an estimated uncertainty of 0.5%. Although the equation of state for oxygen by Schmidt and Wagner (1985) is valid only to temperatures of 300 K, the original work of Lemmon (1996) demonstrated that the oxygen equation extrapolates to temperatures up to 1000 K within 0.5% in density through comparisons with the Kozlov (1968) data. As new measurements become available, they will refine the uncertainty estimates in regions not covered by experimental data, and will enable continued evaluation and optimization of the mixture model.

8. References

Abbey, R. L. and G. E. Barlow, Aust. J. Sci. Res. **A1**, 175 (1948).
Amagat, E. A., Ann. Chem. Phys. **29**, 68 (1893).
Andersen, J. R., Trans. ASME **72**, 759 (1950).
Armstrong, G. T., J. M. Goldstein, and D. E. Roberts, J. Res. Natl. Bur. Stand. **55**(5), 265 (1955).
Baehr, H. D. and K. Schwier, *The Thermodynamic Properties of Air for Temperatures Between* −210 °C *and* 1250 °C *up to Pressures of 4500 Bar*, Thermodynamische Eigenschaften der Gase und Flussigkeiten (Springer-Verlag, Berlin, 1961).
Bender, E., Cryogenics **11**, 11 (1973).
Blagoi, Yu. P. and N. C. Rudenko, Izv. Vyssh. Uchebn. Zaved. Fiz. **6**, 145 (1958).
Blanke, W., ''Messung der thermischen Zustandsgrossen von Luft im Zweiphasengebiet und seiner Umgebung,'' Dissertation for Dr. Ing., Ruhr-Universitat Bochum, Germany, 1973.
Blanke, W., *Proceedings 7th Symposium Thermophysics Properties*, edited by A. Cezairlizan (The American Society of Mechanical Engineers, New York, 1977), p. 461.
Bourbo, P. and I. Ischkin, Physica **3**(10), 1067 (1936).
Bridgeman, O. C., Phys. Rev. **34**, 527 (1929).
Burn, I. and F. Din, Trans. Faraday Soc. **58**(475), 1341 (1962).
Chashkin, Y. R., V. G. Gorbunova, and A. V. Voronel, Sov. Phys. JETP **22**, 304 (1966).
Clark, A. M., F. Din, and J. Robb, Proc. R. Soc. London **A221**, 517 (1954).
Clarke, W. P., R. T Jacobsen, E. W. Lemmon, S. G. Penoncello, and S. W. Beyerlein, Int. J. Thermophys. **15**(6), 1289 (1994).
Cockett, A. H., Proc. R. Soc. London **A239**, 76 (1957).
Colwell, R. C. and L. H. Gibson, J. Acoust. Soc. Am. **12**, 436 (1941).

Colwell, R. C., A. W. Friend, and D. A. McGraw, J. Franklin Inst. **225**, 579 (1938).

Cox, J. D., D. D. Wagman, and V. A. Medvedev, *CODATA Key Values for Thermodynamics* (Hemisphere, New York, 1989).

Crain, R. W., Jr. and R. Sonntag, Adv. Cryo. Eng. **11**, 379 (1966).

Deiters, U. K. and K. M. de Reuck, Pure Appl. Chem. **69**(6), 1237 (1997).

Din, F., Trans. Faraday Soc. **56**, 668 (1960).

Din, F., *Thermodynamic Functions of Gases*, Volume 1: Ammonia, Carbon Dioxide, and Carbon Monoxide; Volume 2: Air, Acetylene, Ethylene, Propane and Argon, Volume 3. Ethane, Methane, and Nitrogen (Butterworths, London, 1962).

Dodge, B. F. and A. K. Dunbar, J. Am. Chem. Soc. **49**, 591 (1927).

Duncan, A. G. and L. A. K. Staveley, Trans. Faraday Soc. **62**, 548 (1966).

Elshayal, I. M. and B. C.-Y. Lu, Can. J. Chem. Eng. **53**, 83 (1975).

Eucken, A., Phys. Z. **14**, 324 (1913).

Eucken, A. and F. Hauck, Z. Phys. Chem. **134**, 161 (1928).

Ewing, M. B. and A. R. H. Goodwin, J. Chem. Thermodyn. **25**, 423 (1993).

Fastovskii, V. G. and Yu. V. Petrovskii, Russ. J. Phys. Chem. **29**, 1311 (1955).

Fastovskii, V. G. and Yu. V. Petrovskii, Russ. J. Phys. Chem. **30**, 76 (1956).

Fastovskii, V. G. and Yu. V. Petrovskii, Russ. J. Phys. Chem. **31**, 836 (1957).

Friedman, A. S., J. Res. Natl. Bur. Stand. **58**(2), 93 (1957).

Friend, D. G., *NIST Standard Reference Database 12*, NIST Thermophysical Properties of Pure Fluids, Version 3.0 (National Institute of Standards and Technology, Standard Reference Data Program, Gaithersburg, 1992).

Funada, I., S. Yoshimura, H. Masuoka, and M. Yorizane, Adv. Cryo. Eng. **27**, 893 (1982).

Giacomo, P., Metrologia **18**, 33 (1982).

Hardy, H. C., D. Telfair, and W. H. Peilemeier, J. Acoust. Soc. Am. **13**, 226 (1942).

Haynes, W. M., E. W. Lemmon, R. T Jacobsen, and D. G. Friend, Rev. High Pressure Sci. Technol. **7**, 1171 (1998).

Henry, P. S. H., Proc. R. Soc. London **A133**, 492 (1931).

Hilsenrath, J., *Tables of Thermal Properties of Gases*; Chapter 2: The Thermodynamic Properties of Air; Chapter 7: The Thermodynamic Properties of Nitrogen, NBS Circular 564 (1955).

Hilsenrath, J. and M. Klein, *Tables of Thermodynamic Properties of Air in Chemical Equilibrium Including Second Virial Corrections from 1500 °K to 15000 °K* (National Bureau of Standards, Gaithersburg, 1965), AEDC-TR-65-58.

Hiza, M. J., A. J. Kidnay, and W. M. Haynes, Int. J. Thermophys. (submitted 1999).

Holborn, L. and M. Jakob, J. Soc. German Eng. **61**, 146 (1917).

Holborn, L. and H. Schultze, Ann. Phys. **47**, 1089 (1915).

Holst, G. and L. Hamburger, Z. Phys. Chem. **91**, 513 (1916).

Howley, J. B., J. W. Magee, and W. M. Haynes, Int. J. Thermophys. **15**(5), 801 (1994).

Jacobsen, R. T, W. P. Clarke, S. G. Penoncello, and R. D. McCarty, Int. J. Thermophys. **11**(1), 169 (1990a).

Jacobsen, R. T, W. P. Clarke, S. W. Beyerlein, M. F. Rousseau, L. J. Van Poolen, and J. C. Rainwater, Int. J. Thermophys. **11**(1), 179 (1990b).

Jacobsen, R. T, S. G. Penoncello, S. W. Beyerlein, W. P. Clarke, and E. W. Lemmon, Fluid Phase Equilib. **79**, 113 (1992).

Jaeschke, M. and H. M. Hinze, Fortschr.-Ber. VDI **3**, 262 (1991).

Jakob, M., Z. Tech. Phys. **4**, 460 (1923).

Jin, Z.-Li, K.-Y. Liu, and W.-W. Sheng, J. Chem. Eng. Data **38**, 353 (1993).

Jones, F. E., J. Res. Natl. Bur. Stand. **83**(5), 419 (1978).

Jones, I. W. and J. S. Rowlinson, Trans. Faraday Soc. **59**(488), 1702 (1963).

King, F. E. and J. R. Partington, Philos. Mag. **9**(60), 1020 (1930).

Klimeck, J., R. Kleinrahm, and W. Wagner, J. Chem. Thermodyn. **30**, 1571 (1998).

Knaap, H. F. P., M. Knoester, and J. J. M. Beenakker, Physica **27**, 309 (1961).

Kozlov, A., ''Experimental investigation of the specific volumes of air in the 20–600 °C temperature range and 20–700 bar pressure range,'' Dissertation for Candidate of Technical Science, Moscow Power Engineering Institute, 1968.

Kosov, N. D. and I. S. Brovanov, Inz.-Fiz. Zh. **36**(4), 627 (1979).

Kuenen, J. P. and A. L. Clark, Communs. Phys. Lab. Univ. Leiden **150**, 55 (1917).

Kuenen, J. P., T. Verschoyle, and A. T. Van Urk, Proc. R. Acad. Amsterdam **26**, 49 (1922).

Lemmon, E. W., ''A generalized model for the prediction of the thermodynamic properties of mixtures including vapor-liquid equilibrium,'' Ph.D. dissertation, University of Idaho, Moscow, 1996.

Lemmon, E. W., *NIST Standard Reference Database 72: NIST Thermophysical Properties of Air and Air Component Mixtures*, Version 1.0 (National Institute of Standards and Technology, Standard Reference Data Program, Gaithersburg, 1998).

Lemmon, E. W. and R. T Jacobsen, Adv. Cryo. Eng. **43**, 1281 (1998).

Lemmon, E. W. and R. T Jacobsen, Int. J. Thermophys. **20**, 825 (1999).

Lemmon, E. W. and R. T Jacobsen, *An International Standard Formulation for the Thermodynamic Properties of 1,1,1-Tr; Triflluoroethane (HFC-143a) for Temperatures from 161 to 450 K and Pressures to 50 MPa*, J. Phys. Chem. Ref. Data. (in press, 2000).

Lemmon, E. W. and R. Tillner-Roth, Fluid Phase Equilib. **165**, 1 (1999).

Lemmon, E. W., R. T Jacobsen, and S. W. Beyerlein, Adv. Cryo. Eng. **37**, 1107 (1992).

Levelt Sengers, J. M. H., M. Klein, and J. S. Gallagher, *Pressure-Volume-Temperature Relationships of Gases. Virial Coefficients, American Institute of Physics Handbook*, 3rd ed. (McGraw Hill, New York, 1972).

Lewis, K. L. and L. A. K. Staveley, J. Chem. Thermodyn. **7**(9), 855 (1975).

Magee, J. W., Int. J. Thermophys. **15**(5), 849 (1994).

Maslennikova, V. Ya., A. N. Egorov, and D. S. Tsiklis, Russ. J. Phys. Chem. **53**(6), 919 (1979).

Massengill, D. R. and R. C. Miller, J. Chem. Thermodyn. **5**, 207 (1973).

Michels, A., T. Wassenaar, and G. J. Wolkers, Appl. Sci. Res. **5**, 121 (1955).

Michels, A., T. Wassenaar, and W. van Seventer, Appl. Sci. Res. **4**, 52 (1954a).

Michels, A., T. Wassenaar, J. M. H. Levelt, and W. de Graaf, Appl. Sci. Res. **4**, 381 (1954b).

Michels, A., H. Wouters, and J. DeBoer, Physica **3**(7), 585 (1936).

Miller, R. C., A. J. Kidnay, and M. J. Hiza, AIChE J. **19**(1), 145 (1973).

Narinskii, G. B., Kislorod **10**(3), 9 (1957).

Narinskii, G. B., Russ. J. Phys. Chem. **40**(9), 1093 (1966).

Narinskii, G. B., Zh. Fiz. Khim. **43**(2), 408 (1969).

Nellis, W. J., A. C. Mitchell, F. H. Ree, M. Ross, N. C. Holmes, R. J. Trainor, and D. J. Erskine, J. Chem. Phys. **95**(7), 5268 (1991).

Nesselmann, K., Z. Tech. Phys. **6**(4), 151 (1925).

Nowak, P., R. Kleinrahm, and W. Wagner, J. Chem. Thermodyn. **29**, 1137 (1997).

Olien, N. A., National Bureau of Standards, Boulder (private communication to R. T Jacobsen, 1987).

Palavra, A. M., Effect of pressure and temperature on excess properties in the system argon-nitrogen, M. S. thesis, Instituto Superior Tecnico Universidade Tecnica De Lisboa, 1979.

Panasiti, M. D., ''Thermophysical properties of air from 60 to 2000 K at pressures up to 2000 MPa,'' M. S. thesis, University of Idaho, Moscow, 1996.

Panasiti, M. D., E. W. Lemmon, S. G. Penoncello, R. T Jacobsen, and D. G. Friend, Int. J. Thermophys. **20**(1), 217 (1999).

Parikh, N. C. and J. A. Zollweg, Energy Week Proceedings, Houston, 1997, Vol. 7, p. 58.

Peng, D. Y. and D. B. Robinson, Ind. Eng. Chem. Fundam. **15**(1), 59 (1976).

Penning, F. M., Communs. Phys. Lab. Univ. Leiden, Number 166 (1923).

Poferl, D. J., R. A. Svehla, and K. Lewandowski, ''Thermodynamic and Transport Properties of Air and the Combustion Products of Natural Gas and of ASTM-A-1 Fuel with Air,'' NASA Tech. Note D-5452 (1959).

Pool, R. A. H., G. Saville, T. M. Herrington, B. D. C. Shields, and L. A. K. Staveley, Trans. Faraday Soc. **58**, 1692 (1962).

Prasad, D. H. L. and D. S. Viswanath, ''Generalized thermodynamic properties of real fluids using molar polarization at the critical temperature as the third parameter,'' Department of Chemical Engineering, Indian Institute of Science, Bangalore, 1974.

Preston-Thomas, H., Metrologia **27**, 3 (1990).

Quigley, T. H., Phys. Rev. **67**, 298 (1945).

Ricardo, A. A., S. F. Barreiros, M. Nunes da Ponte, G. M. N. Albuquerque, and J. C. G. Calado, J. Chem. Thermodyn. **24**, 1281 (1992).

Robertson, S. L. and S. E. Babb, J. Chem. Phys. **50**(10), 4560 (1969).

Rogovaya, I. A. and M. G. Kaganer, Russ. J. Phys. Chem. **34**(9), 917 (1960).
Romberg, H., VDI-Forsch., Dusseldorf, VDI-Verlag, Number 543 (1971).
Saji, Y. and T. Okuda, Adv. Cryo. Eng. **10**, 209 (1965).
Saurel, J., J. Recherche CNRS **42**, 22 (1958).
Schmidt, R. and W. Wagner, Fluid Phase Equilib. **19**, 175 (1985).
Shilling, W. G. and J. R. Partington, Philos. Mag. **6**(38), 920 (1928).
Smith, J. M. and H. C. Van Ness, *Introduction to Chemical Engineering Thermodynamics*, 3rd ed. (McGraw-Hill, New York, 1975).
Span, R., *Multiparameter Equations of State—An Accurate Source of Thermodynamic Property Data* (Springer, Berlin, 2000).
Span, R., E. W. Lemmon, R. T Jacobsen, and W. Wagner, 2000, *A Reference Equation of State for the Thermodynamic Properties of Nitrogen for Temperatures from 63.151 to 1000 K and Pressures to 2200 MPa* (in press, 2000), J. Phys. Chem. Ref. Data; Int. J. Thermophys. **14**(4), 1121 (1998).
Span, R. and W. Wagner, Int. J. Thermophys. **18**(6), 1415 (1997).
Sprow, F. B. and J. M. Prausnitz, AIChE J. **12**(4), 780 (1966).
Sychev, V. V., A. A. Vasserman, A. D. Kozlov, G. A. Spiridonov, and V. A. Tsymarny, *Thermodynamic Properties of Air* (Hemisphere, Washington, 1987), Volume 6.
Tegeler, C., R. Span, and W. Wagner, J. Phys. Chem. Ref. Data **28**(3), 779 (1999).
Thorogood, R. M. and G. G. Haselden, Br. Chem. Eng. **8**(9), 623 (1963).
Thorpe, P. L., Trans. Faraday Soc. **64**(549), 2273 (1968).
Townsend, P. W., ''Pressure-volume-temperature relationships of binary gaseous mixtures,'' Ph.D. dissertation, Faculty of Pure Science, Columbia University, New York, 1956.
Tucker, W. S., Philos. Mag. **34**, 217 (1943).
U.S. Standard Atmosphere (U.S. Government Printing, Washington, D.C., 1976).
Van Itterbeek, A. and W. de Rop, Appl. Sci. Res., Sec. A **6**, 21 (1955).
Van Ness, H. C. and M. M. Abbott, *Classical Thermodynamics of Nonelectrolyte Solutions with Applications to Phase Equilibria* (McGraw-Hill, New York, 1982).
Vasserman, A. A. and V. A. Rabinovich, *Thermophysical Properties of Liquid Air and its Components*, Series of Monographs No. 3 (Israel Program for Scientific Translations, Jerusalem, 1970).
Vasserman, A. A., E. A. Golovskii, E. P. Mitsevich, and V. A. Tsymarnyi, *Measurement of the Density of Air at Temperatures of 78 to 190 K up to Pressures of 600 Bars*, VINITI Deposition No. 2953 (Odessa Institute of Marine Engineering, Ukraine, 1976).
Vasserman, A. A., Ya. Z. Kazavchinskii, and V. A. Rabinovich, 1971, *Thermophysical Properties of Air and Air Components* (Israel Program Science Translations, Tech. 1971), Transl. TT70-50095, 397 pp.
Wagner, W., Fortschr.-Ber. VDI, Dusseldorf, VDI-Verlag **3**(39) (1974).
Wang, D. I. J., Adv. Cryo. Eng. **3**, 294 (1960).
Waxman, M. and H. Davis, J. Res. Natl. Bur. Stand. **83**(5), 415 (1978).
Weishaupt, J., Angew. Chem. **B20**(12), 321 (1948).
Wilson, G. M., P. M. Silverberg, and M.G. Zellner, Adv. Cryo. Eng. **10**, 192 (1965).
Yorizane, M., S. Yoshimura, H. Masuoka, A. Toyama, Y. Nakako, and I. Funada, Chem. Eng. Sci. **33**, 641 (1978).
Younglove, B. A. and N. V. Frederick, Int. J. Thermophys. **13**(6), 1033 (1992).
Zandbergen, P. and J. J. M. Beenakker, Physica **33**(2), 343 (1967).

9. Appendix: Tables of Properties of Air

9.1. Representative Tables of Thermodynamic Properties of Air

Properties of air along the dew and bubble-point curves were calculated using pressures from the appropriate ancillary equation at the specified temperature. The density was calculated using the air equation of state for the input temperature and pressure. Dew and bubble-point entries for the isobar tables were calculated using pressure as the input to Eq. (1) to determine the corresponding temperatures. The densities for these entries were calculated using the temperature and pressure as input variables in the equation of state.

TABLE A1. Thermodynamic properties of air on the dew and bubble lines

Temperature (K)	Pressure (MPa)	Density (mol/dm^3)	Enthalpy (J/mol)	Entropy J/(mol-K)	c_v J/(mol-K)	c_p J/(mol-K)	Speed of sound (m/s)
59.75[a]	0.005 265	33.067	−4713.1	70.902	34.01	55.06	1030.3
59.75[a]	0.002 43	0.004 91	1721.6	182.97	20.80	29.22	154.8
60	0.005 55	33.031	−4699.3	71.131	33.95	55.06	1028.3
60	0.002 58	0.005 19	1728.6	182.59	20.81	29.23	155.1
61	0.006 80	32.888	−4644.3	72.041	33.73	55.06	1020.3
61	0.003 27	0.006 47	1756.7	181.09	20.82	29.26	156.4
62	0.008 27	32.745	−4589.2	72.937	33.51	55.06	1012.2
62	0.004 11	0.008 00	1784.7	179.66	20.84	29.30	157.6
63	0.009 99	32.601	−4534.1	73.817	33.30	55.07	1004.0
63	0.005 12	0.009 82	1812.5	178.29	20.86	29.35	158.8
64	0.012 00	32.457	−4478.9	74.684	33.09	55.08	995.8
64	0.006 33	0.011 95	1840.1	176.97	20.89	29.40	160.0
65	0.014 32	32.312	−4423.8	75.538	32.88	55.10	987.5
65	0.007 76	0.014 44	1867.5	175.71	20.91	29.46	161.2
66	0.016 99	32.166	−4368.6	76.379	32.68	55.12	979.1
66	0.009 44	0.017 33	1894.7	174.50	20.94	29.52	162.3
67	0.020 04	32.020	−4313.4	77.208	32.49	55.15	970.7
67	0.011 42	0.020 66	1921.7	173.34	20.97	29.59	163.4
68	0.023 52	31.873	−4258.2	78.025	32.29	55.18	962.2
68	0.013 71	0.024 48	1948.5	172.22	21.00	29.66	164.5
69	0.027 46	31.725	−4202.9	78.830	32.11	55.22	953.7
69	0.016 37	0.028 84	1974.9	171.15	21.04	29.75	165.6
70	0.031 91	31.576	−4147.6	79.624	31.92	55.27	945.1
70	0.019 43	0.033 79	2001.1	170.12	21.07	29.84	166.7
71	0.036 91	31.427	−4092.2	80.408	31.74	55.32	936.4
71	0.022 93	0.039 38	2027.0	169.13	21.11	29.93	167.7
72	0.042 50	31.277	−4036.7	81.181	31.56	55.38	927.7
72	0.026 92	0.045 66	2052.6	168.17	21.16	30.04	168.7
73	0.048 73	31.126	−3981.2	81.944	31.39	55.44	918.9
73	0.031 44	0.052 70	2077.8	167.25	21.20	30.15	169.7
74	0.055 66	30.974	−3925.6	82.698	31.22	55.51	910.0
74	0.036 55	0.060 55	2102.7	166.36	21.25	30.28	170.6
75	0.063 33	30.821	−3869.8	83.442	31.05	55.59	901.1
75	0.042 28	0.069 27	2127.2	165.50	21.30	30.41	171.6
76	0.071 79	30.668	−3814.0	84.178	30.89	55.68	892.1
76	0.048 70	0.078 92	2151.3	164.67	21.36	30.55	172.5
77	0.081 09	30.513	−3758.1	84.905	30.73	55.78	883.0
77	0.055 86	0.089 56	2175.0	163.87	21.41	30.70	173.4
78	0.091 29	30.357	−3702.1	85.624	30.57	55.88	873.9
78	0.063 81	0.101 27	2198.3	163.09	21.47	30.86	174.2
79	0.102 45	30.200	−3645.9	86.334	30.41	56.00	864.7
79	0.072 61	0.114 10	2221.2	162.34	21.54	31.04	175.1
80	0.114 62	30.042	−3589.6	87.037	30.26	56.12	855.4
80	0.082 32	0.128 13	2243.6	161.61	21.60	31.22	175.8
81	0.127 85	29.883	−3533.2	87.733	30.11	56.26	846.1
81	0.093 00	0.143 43	2265.5	160.91	21.67	31.41	176.6
82	0.142 21	29.722	−3476.6	88.421	29.97	56.40	836.7
82	0.104 71	0.160 06	2286.9	160.22	21.75	31.62	177.4
83	0.157 75	29.560	−3419.8	89.103	29.83	56.56	827.2
83	0.117 51	0.178 11	2307.8	159.56	21.82	31.84	178.1
84	0.174 53	29.397	−3362.9	89.778	29.69	56.72	817.6
84	0.131 47	0.197 65	2328.1	158.91	21.90	32.07	178.8
85	0.192 62	29.232	−3305.8	90.447	29.55	56.90	808.0
85	0.146 65	0.218 75	2347.9	158.28	21.98	32.32	179.4
86	0.212 07	29.066	−3248.4	91.110	29.42	57.09	798.2
86	0.163 12	0.241 50	2367.1	157.67	22.07	32.58	180.0
87	0.232 95	28.898	−3190.9	91.767	29.29	57.30	788.4
87	0.180 94	0.265 98	2385.8	157.07	22.16	32.85	180.6
88	0.255 31	28.729	−3133.1	92.418	29.16	57.52	778.6
88	0.200 18	0.292 28	2403.8	156.49	22.25	33.14	181.2
89	0.279 22	28.558	−3075.1	93.065	29.03	57.76	768.6
89	0.220 91	0.320 48	2421.2	155.92	22.34	33.45	181.7
90	0.304 75	28.385	−3016.8	93.706	28.91	58.01	758.5

TABLE A1. Thermodynamic properties of air on the dew and bubble lines—Continued

Temperature (K)	Pressure (MPa)	Density (mol/dm^3)	Enthalpy (J/mol)	Entropy J/(mol-K)	c_v J/(mol-K)	c_p J/(mol-K)	Speed of sound (m/s)
90	0.243 20	0.350 68	2437.9	155.36	22.44	33.77	182.2
91	0.331 96	28.210	−2958.2	94.342	28.79	58.28	748.4
91	0.267 12	0.382 98	2454.0	154.82	22.54	34.11	182.6
92	0.360 91	28.033	−2899.4	94.974	28.68	58.57	738.2
92	0.292 73	0.417 47	2469.3	154.29	22.64	34.47	183.1
93	0.391 66	27.854	−2840.2	95.602	28.56	58.87	727.9
93	0.320 11	0.454 26	2484.0	153.77	22.74	34.85	183.5
94	0.424 29	27.673	−2780.8	96.225	28.45	59.20	717.5
94	0.349 34	0.493 45	2497.9	153.26	22.85	35.26	183.8
95	0.458 86	27.489	−2720.9	96.845	28.35	59.55	707.0
95	0.380 47	0.535 17	2511.0	152.75	22.96	35.68	184.2
96	0.495 43	27.304	−2660.8	97.461	28.24	59.93	696.5
96	0.413 59	0.579 53	2523.3	152.26	23.08	36.13	184.5
97	0.534 08	27.115	−2600.2	98.074	28.14	60.33	685.8
97	0.448 78	0.626 67	2534.8	151.78	23.20	36.61	184.7
98	0.574 86	26.924	−2539.2	98.684	28.04	60.76	675.0
98	0.486 09	0.676 71	2545.4	151.30	23.32	37.12	184.9
99	0.617 86	26.730	−2477.8	99.291	27.95	61.22	664.2
99	0.525 62	0.729 80	2555.2	150.83	23.44	37.65	185.1
100	0.663 13	26.533	−2416.0	99.896	27.86	61.71	653.3
100	0.567 42	0.786 09	2564.0	150.36	23.57	38.23	185.3
101	0.710 74	26.333	−2353.6	100.50	27.77	62.23	642.2
101	0.611 59	0.845 75	2571.9	149.90	23.70	38.83	185.4
102	0.760 77	26.130	−2290.8	101.10	27.68	62.80	631.1
102	0.658 20	0.908 95	2578.8	149.44	23.83	39.48	185.5
103	0.813 29	25.923	−2227.4	101.70	27.60	63.40	619.8
103	0.707 32	0.975 87	2584.6	148.99	23.97	40.18	185.6
104	0.868 36	25.713	−2163.4	102.29	27.53	64.05	608.5
104	0.759 03	1.0467	2589.4	148.54	24.11	40.92	185.6
105	0.926 06	25.499	−2098.9	102.89	27.45	64.75	597.1
105	0.813 41	1.1217	2593.0	148.10	24.26	41.71	185.5
106	0.986 45	25.281	−2033.7	103.49	27.38	65.51	585.5
106	0.870 55	1.2011	2595.5	147.65	24.41	42.57	185.5
107	1.049 61	25.058	−1967.8	104.08	27.32	66.32	573.9
107	0.930 52	1.2852	2596.7	147.21	24.56	43.49	185.4
108	1.115 61	24.831	−1901.2	104.68	27.26	67.21	562.1
108	0.993 40	1.3742	2596.6	146.77	24.72	44.49	185.2
109	1.184 53	24.598	−1833.8	105.27	27.20	68.16	550.2
109	1.059 28	1.4684	2595.1	146.33	24.89	45.57	185.1
110	1.256 42	24.361	−1765.6	105.87	27.15	69.20	538.2
110	1.128 24	1.5682	2592.2	145.89	25.06	46.75	184.9
111	1.331 38	24.118	−1696.5	106.47	27.10	70.34	526.1
111	1.200 36	1.6740	2587.7	145.45	25.23	48.04	184.6
112	1.409 47	23.868	−1626.4	107.06	27.06	71.58	513.9
112	1.275 74	1.7862	2581.7	145.00	25.42	49.45	184.3
113	1.490 77	23.613	−1555.4	107.67	27.03	72.95	501.5
113	1.354 45	1.9053	2573.8	144.55	25.61	51.01	184.0
114	1.575 34	23.350	−1483.2	108.27	27.00	74.46	489.0
114	1.436 60	2.0318	2564.2	144.10	25.81	52.73	183.6
115	1.663 27	23.080	−1409.9	108.88	26.98	76.13	476.3
115	1.522 26	2.1664	2552.5	143.64	26.01	54.64	183.2
116	1.754 62	22.801	−1335.2	109.49	26.97	78.00	463.5
116	1.611 54	2.3097	2538.7	143.18	26.23	56.79	182.7
117	1.849 47	22.514	−1259.2	110.11	26.96	80.09	450.5
117	1.704 52	2.4625	2522.7	142.70	26.46	59.21	182.2
118	1.947 89	22.217	−1181.6	110.73	26.97	82.46	437.3
118	1.801 32	2.6259	2504.0	142.22	26.70	61.96	181.7
119	2.049 95	21.908	−1102.4	111.36	26.98	85.16	423.9
119	1.902 02	2.8009	2482.7	141.73	26.96	65.10	181.1
120	2.155 73	21.588	−1021.2	112.00	27.01	88.28	410.2
120	2.006 74	2.9889	2458.3	141.22	27.23	68.74	180.4
121	2.265 29	21.253	−937.90	112.65	27.05	91.92	396.3
121	2.115 60	3.1913	2430.6	140.70	27.51	72.99	179.8

TABLE A1. Thermodynamic properties of air on the dew and bubble lines—Continued

Temperature (K)	Pressure (MPa)	Density (mol/dm^3)	Enthalpy (J/mol)	Entropy J/(mol-K)	c_v J/(mol-K)	c_p J/(mol-K)	Speed of sound (m/s)
122	2.378 71	20.903	−852.17	113.31	27.11	96.23	382.0
122	2.228 71	3.4103	2399.1	140.16	27.82	78.02	179.1
123	2.496 04	20.534	−763.63	113.98	27.19	101.4	367.4
123	2.346 20	3.6481	2363.3	139.59	28.16	84.05	178.3
124	2.617 34	20.144	−671.82	114.68	27.30	107.8	352.3
124	2.468 23	3.9078	2322.6	139.00	28.52	91.43	177.5
125	2.742 67	19.727	−576.07	115.40	27.44	115.9	336.7
125	2.594 95	4.1934	2276.3	138.38	28.91	100.6	176.7
126	2.872 07	19.278	−475.47	116.15	27.62	126.5	320.4
126	2.726 56	4.5101	2223.2	137.71	29.34	112.4	175.8
127	3.005 54	18.788	−368.72	116.93	27.85	140.9	303.2
127	2.863 31	4.8653	2161.9	137.00	29.83	128.0	174.9
128	3.143 06	18.242	−253.75	117.78	28.17	161.9	285.0
128	3.005 51	5.2697	2090.3	136.22	30.37	149.6	174.0
129	3.284 48	17.616	−127.06	118.70	28.61	195.2	265.4
129	3.153 61	5.7405	2004.9	135.34	30.99	181.3	173.0
130	3.429 47	16.863	18.109	119.76	29.24	256.2	243.7
130	3.308 35	6.3074	1899.9	134.33	31.73	232.6	171.9
131	3.576 98	15.869	198.35	121.07	30.27	401.5	219.1
131	3.471 16	7.0343	1763.0	133.10	32.62	329.9	170.8
132	3.722 84	14.198	478.83	123.13	32.34	1015.	189.1
132	3.646 25	8.1273	1553.9	131.33	33.81	598.0	169.4
132.6312[b]	3.785 02	10.4477	1111.3	127.87	35.26	2196.	168.0

[a]Solidification point.
[b]Maxcondentherm.

TABLE A2. Thermodynamic properties of air

Temperature (K)	Density (mol/dm^3)	Internal energy (J/mol)	Enthalpy (J/mol)	Entropy J/(mol-K)	c_v J/(mol-K)	c_p J/(mol-K)	Speed of sound (m/s)
0.101 325 MPa isobar							
59.77	33.069	−4713.1	−4710.0	70.905	34.01	55.05	1030.6
60	33.036	−4700.3	−4697.2	71.119	33.96	55.05	1028.8
62	32.750	−4590.2	−4587.1	72.924	33.52	55.05	1012.6
64	32.462	−4480.1	−4477.0	74.672	33.09	55.07	996.3
66	32.171	−4369.9	−4366.8	76.367	32.69	55.11	979.6
68	31.878	−4259.7	−4256.5	78.013	32.30	55.17	962.7
70	31.581	−4149.3	−4146.1	79.614	31.92	55.25	945.5
72	31.281	−4038.7	−4035.5	81.172	31.56	55.37	928.1
74	30.978	−3927.9	−3924.6	82.691	31.22	55.51	910.4
76	30.670	−3816.7	−3813.4	84.173	30.89	55.68	892.3
78	30.358	−3705.2	−3701.9	85.622	30.57	55.88	874.0
78.90	30.215	−3654.7	−3651.4	86.266	30.43	55.99	865.6
81.72	0.155 27	1628.3	2280.9	160.41	21.73	31.56	177.2
82	0.154 67	1634.6	2289.8	160.52	21.71	31.52	177.5
84	0.150 53	1679.4	2352.5	161.28	21.58	31.26	180.0
86	0.146 63	1723.8	2414.8	162.01	21.48	31.04	182.4
88	0.142 95	1767.9	2476.7	162.72	21.40	30.85	184.8
90	0.139 47	1811.7	2538.2	163.41	21.33	30.69	187.1
92	0.136 17	1855.4	2599.5	164.09	21.27	30.55	189.4
94	0.133 03	1898.8	2660.4	164.74	21.22	30.42	191.7
96	0.130 05	1942.1	2721.2	165.38	21.17	30.32	193.9
98	0.127 21	1985.2	2781.7	166.00	21.13	30.22	196.1
100	0.124 49	2028.2	2842.1	166.61	21.09	30.13	198.2
102	0.121 90	2071.0	2902.2	167.21	21.06	30.05	200.3
104	0.119 42	2113.8	2962.3	167.79	21.03	29.98	202.4
106	0.117 04	2156.4	3022.2	168.36	21.01	29.92	204.5
108	0.114 76	2199.0	3082.0	168.92	20.98	29.86	206.5
110	0.112 57	2241.5	3141.6	169.47	20.96	29.81	208.6
112	0.110 47	2284.0	3201.2	170.01	20.94	29.76	210.5
114	0.108 44	2326.3	3260.7	170.53	20.93	29.72	212.5
116	0.106 49	2368.6	3320.1	171.05	20.91	29.68	214.5
118	0.104 62	2410.9	3379.4	171.56	20.90	29.64	216.4
120	0.102 81	2453.1	3438.7	172.05	20.89	29.61	218.3
122	0.101 06	2495.3	3497.8	172.54	20.87	29.58	220.2
124	0.099 377	2537.4	3557.0	173.02	20.86	29.55	222.1
126	0.097 748	2579.5	3616.0	173.50	20.85	29.52	223.9
128	0.096 174	2621.5	3675.1	173.96	20.84	29.50	225.8
130	0.094 650	2663.5	3734.0	174.42	20.84	29.48	227.6
132	0.093 175	2705.5	3793.0	174.87	20.83	29.45	229.4
134	0.091 747	2747.5	3851.9	175.31	20.82	29.43	231.2
136	0.090 363	2789.4	3910.7	175.75	20.82	29.42	232.9
138	0.089 021	2831.3	3969.5	176.18	20.81	29.40	234.7
140	0.087 718	2873.2	4028.3	176.60	20.81	29.38	236.4
142	0.086 455	2915.1	4087.1	177.02	20.80	29.37	238.2
144	0.085 227	2956.9	4145.8	177.43	20.80	29.35	239.9
146	0.084 035	2998.7	4204.5	177.83	20.79	29.34	241.6
148	0.082 877	3040.5	4263.1	178.23	20.79	29.33	243.3
150	0.081 750	3082.3	4321.8	178.62	20.78	29.32	244.9
155	0.079 065	3186.8	4468.3	179.59	20.78	29.29	249.1
160	0.076 553	3291.1	4614.7	180.51	20.77	29.27	253.1
165	0.074 198	3395.4	4761.0	181.41	20.76	29.25	257.1
170	0.071 985	3499.6	4907.2	182.29	20.76	29.23	261.1
175	0.069 902	3603.8	5053.3	183.13	20.75	29.22	264.9
180	0.067 937	3707.9	5199.3	183.96	20.75	29.20	268.7
185	0.066 081	3812.0	5345.3	184.76	20.75	29.19	272.5
190	0.064 324	3916.0	5491.2	185.54	20.75	29.18	276.2
195	0.062 659	4020.0	5637.1	186.29	20.75	29.17	279.8
200	0.061 079	4124.0	5782.9	187.03	20.74	29.16	283.4
210	0.058 147	4331.9	6074.5	188.45	20.74	29.15	290.5
220	0.055 486	4539.8	6365.9	189.81	20.74	29.14	297.4
230	0.053 059	4747.6	6657.3	191.11	20.74	29.13	304.1
240	0.050 836	4955.4	6948.6	192.35	20.75	29.13	310.7

TABLE A2. Thermodynamic properties of air—Continued

Temperature (K)	Density (mol/dm^3)	Internal energy (J/mol)	Enthalpy (J/mol)	Entropy J/(mol-K)	c_v J/(mol-K)	c_p J/(mol-K)	Speed of sound (m/s)
250	0.048 793	5163.2	7239.9	193.53	20.75	29.13	317.1
260	0.046 908	5371.1	7531.1	194.68	20.76	29.13	323.4
270	0.045 164	5578.9	7822.4	195.78	20.76	29.13	329.6
280	0.043 546	5786.8	8113.7	196.84	20.77	29.13	335.6
290	0.042 040	5994.8	8405.1	197.86	20.78	29.14	341.5
300	0.040 634	6203.0	8696.5	198.85	20.80	29.15	347.4
310	0.039 320	6411.2	8988.1	199.80	20.81	29.16	353.1
320	0.038 089	6619.5	9279.8	200.73	20.83	29.18	358.7
330	0.036 932	6828.1	9571.6	201.63	20.85	29.19	364.2
340	0.035 844	7036.8	9863.6	202.50	20.87	29.21	369.7
350	0.034 818	7245.7	10 156.0	203.34	20.89	29.23	375.0
360	0.033 850	7454.9	10 448.0	204.17	20.92	29.26	380.3
370	0.032 933	7664.3	10 741.0	204.97	20.94	29.28	385.4
380	0.032 066	7874.0	11 034.0	205.75	20.97	29.31	390.5
390	0.031 243	8084.0	11 327.0	206.51	21.01	29.34	395.5
400	0.030 461	8294.3	11 621.0	207.26	21.04	29.38	400.5
450	0.027 074	9351.8	13 094.0	210.73	21.25	29.58	424.2
500	0.024 365	10 421.0	14 579.0	213.86	21.50	29.83	446.4
550	0.022 149	11 503.0	16 078.0	216.71	21.80	30.13	467.3
600	0.020 303	12 602.0	17 592.0	219.35	22.13	30.45	487.1
650	0.018 742	13 717.0	19 123.0	221.80	22.47	30.79	505.9
700	0.017 403	14 849.0	20 671.0	224.09	22.82	31.14	523.9
750	0.016 243	15 999.0	22 237.0	226.25	23.17	31.48	541.2
800	0.015 228	17 166.0	23 820.0	228.30	23.51	31.82	557.8
900	0.013 536	19 549.0	27 035.0	232.08	24.15	32.47	589.6
1000	0.012 183	21 994.0	30 311.0	235.53	24.73	33.05	619.6
1100	0.011 075	24 494.0	33 642.0	238.71	25.25	33.57	648.1
1200	0.010 153	27 042.0	37 022.0	241.65	25.70	34.02	675.5
1300	0.009 372	29 633.0	40 444.0	244.39	26.10	34.42	701.7
1400	0.008 703	32 261.0	43 904.0	246.95	26.45	34.77	727.0
1500	0.008 122	34 922.0	47 397.0	249.36	26.76	35.08	751.5
1600	0.007 615	37 612.0	50 919.0	251.63	27.04	35.35	775.2
1700	0.007 167	40 329.0	54 466.0	253.79	27.29	35.60	798.2
1800	0.006 769	43 069.0	58 038.0	255.83	27.51	35.82	820.5
1900	0.006 413	45 830.0	61 630.0	257.77	27.71	36.03	842.3
2000	0.006 092	48 610.0	65 242.0	259.62	27.90	36.21	863.5
			0.2 MPa isobar				
59.78	33.072	−4712.9	−4706.8	70.908	34.01	55.05	1031.0
60	33.041	−4701.0	−4695.0	71.106	33.96	55.04	1029.3
62	32.756	−4591.0	−4584.9	72.911	33.52	55.04	1013.2
64	32.468	−4481.0	−4474.8	74.659	33.10	55.06	996.8
66	32.177	−4370.9	−4364.6	76.353	32.69	55.10	980.2
68	31.884	−4260.7	−4254.4	77.999	32.30	55.16	963.3
70	31.588	−4150.3	−4144.0	79.599	31.93	55.24	946.1
72	31.288	−4039.8	−4033.4	81.157	31.57	55.35	928.7
74	30.985	−3929.1	−3922.6	82.675	31.22	55.49	911.0
76	30.678	−3818.0	−3811.5	84.157	30.89	55.65	893.0
78	30.366	−3706.5	−3700.0	85.605	30.57	55.86	874.7
80	30.050	−3594.7	−3588.0	87.022	30.27	56.10	856.1
82	29.728	−3482.3	−3475.5	88.411	29.97	56.38	837.2
84	29.400	−3369.2	−3362.4	89.773	29.69	56.71	817.8
85.39	29.168	−3290.4	−3283.6	90.705	29.50	56.98	804.2
87.99	0.292 03	1718.8	2403.6	156.49	22.25	33.14	181.2
88	0.291 99	1719.0	2403.9	156.50	22.24	33.14	181.2
90	0.284 13	1765.8	2469.7	157.24	22.05	32.70	183.8
92	0.276 75	1812.1	2534.8	157.95	21.90	32.33	186.3
94	0.269 81	1857.9	2599.1	158.64	21.77	32.03	188.7
96	0.263 27	1903.2	2662.9	159.32	21.66	31.77	191.1
98	0.257 08	1948.2	2726.2	159.97	21.57	31.54	193.5
100	0.251 21	1993.0	2789.1	160.60	21.49	31.34	195.8
102	0.245 64	2037.4	2851.6	161.22	21.42	31.17	198.0
104	0.240 33	2081.6	2913.8	161.83	21.36	31.01	200.3
106	0.235 27	2125.6	2975.7	162.42	21.30	30.87	202.4

TABLE A2. Thermodynamic properties of air—Continued

Temperature (K)	Density (mol/dm^3)	Internal energy (J/mol)	Enthalpy (J/mol)	Entropy J/(mol-K)	c_v J/(mol-K)	c_p J/(mol-K)	Speed of sound (m/s)
108	0.230 44	2169.4	3037.3	162.99	21.26	30.75	204.6
110	0.225 83	2213.0	3098.7	163.55	21.21	30.64	206.7
112	0.221 41	2256.5	3159.8	164.11	21.17	30.53	208.8
114	0.217 17	2299.9	3220.8	164.65	21.14	30.44	210.9
116	0.213 11	2343.1	3281.6	165.17	21.11	30.36	212.9
118	0.209 20	2386.2	3342.2	165.69	21.08	30.28	214.9
120	0.205 45	2429.2	3402.7	166.20	21.06	30.21	216.9
122	0.201 83	2472.2	3463.1	166.70	21.03	30.14	218.8
124	0.198 35	2515.0	3523.3	167.19	21.01	30.08	220.8
126	0.194 99	2557.8	3583.4	167.67	20.99	30.03	222.7
128	0.191 75	2600.4	3643.4	168.14	20.97	29.98	224.6
130	0.188 63	2643.0	3703.3	168.61	20.96	29.93	226.5
132	0.185 61	2685.6	3763.2	169.06	20.94	29.89	228.3
134	0.182 68	2728.1	3822.9	169.51	20.93	29.85	230.1
136	0.179 86	2770.5	3882.5	169.95	20.92	29.81	232.0
138	0.177 12	2812.9	3942.1	170.39	20.90	29.77	233.8
140	0.174 47	2855.3	4001.6	170.82	20.89	29.74	235.5
142	0.171 90	2897.6	4061.1	171.24	20.88	29.71	237.3
144	0.169 40	2939.8	4120.5	171.65	20.87	29.68	239.1
146	0.166 98	2982.1	4179.8	172.06	20.87	29.65	240.8
148	0.164 63	3024.3	4239.1	172.47	20.86	29.63	242.5
150	0.162 35	3066.4	4298.3	172.86	20.85	29.60	244.2
155	0.156 93	3171.7	4446.2	173.83	20.83	29.55	248.4
160	0.151 86	3276.8	4593.8	174.77	20.82	29.50	252.6
165	0.147 12	3381.8	4741.2	175.68	20.81	29.46	256.6
170	0.142 67	3486.6	4888.5	176.56	20.80	29.43	260.6
175	0.138 49	3591.4	5035.5	177.41	20.79	29.40	264.5
180	0.134 55	3696.0	5182.4	178.24	20.78	29.37	268.4
185	0.130 83	3800.6	5329.2	179.04	20.78	29.35	272.2
190	0.127 32	3905.1	5475.9	179.82	20.77	29.32	275.9
195	0.124 00	4009.5	5622.5	180.59	20.77	29.31	279.6
200	0.120 84	4113.9	5768.9	181.33	20.77	29.29	283.2
210	0.115 00	4322.5	6061.7	182.76	20.76	29.26	290.4
220	0.109 70	4531.0	6354.2	184.12	20.76	29.24	297.3
230	0.104 87	4739.3	6646.4	185.42	20.76	29.22	304.0
240	0.100 46	4947.6	6938.6	186.66	20.76	29.21	310.7
250	0.096 399	5155.9	7230.6	187.85	20.76	29.20	317.1
260	0.092 660	5364.1	7522.5	189.00	20.77	29.19	323.4
270	0.089 203	5572.3	7814.4	190.10	20.77	29.19	329.6
280	0.085 996	5780.6	8106.3	191.16	20.78	29.19	335.7
290	0.083 012	5988.9	8398.1	192.18	20.79	29.19	341.6
300	0.080 230	6197.2	8690.1	193.17	20.80	29.20	347.5
310	0.077 629	6405.7	8982.0	194.13	20.82	29.20	353.2
320	0.075 193	6614.3	9274.1	195.06	20.83	29.21	358.8
330	0.072 905	6823.0	9566.3	195.96	20.85	29.23	364.4
340	0.070 753	7032.0	9858.7	196.83	20.87	29.24	369.8
350	0.068 725	7241.1	10 151.0	197.68	20.90	29.26	375.2
360	0.066 810	7450.4	10 444.0	198.50	20.92	29.29	380.4
370	0.064 999	7660.0	10 737.0	199.31	20.95	29.31	385.6
380	0.063 285	7869.9	11 030.0	200.09	20.98	29.34	390.7
390	0.061 658	8080.0	11 324.0	200.85	21.01	29.37	395.7
400	0.060 114	8290.5	11 618.0	201.59	21.04	29.40	400.7
450	0.053 424	9348.5	13 092.0	205.07	21.25	29.59	424.4
500	0.048 077	10 418.0	14 578.0	208.20	21.51	29.84	446.6
550	0.043 704	11 501.0	16 077.0	211.06	21.80	30.14	467.5
600	0.040 061	12 600.0	17 592.0	213.69	22.13	30.46	487.3
650	0.036 980	13 715.0	19 123.0	216.14	22.47	30.80	506.1
700	0.034 338	14 847.0	20 672.0	218.44	22.82	31.14	524.1
750	0.032 049	15 997.0	22 238.0	220.60	23.17	31.49	541.4
800	0.030 047	17 164.0	23 821.0	222.64	23.51	31.83	558.1
900	0.026 709	19 548.0	27 036.0	226.43	24.15	32.47	589.8
1000	0.024 039	21 993.0	30 313.0	229.88	24.73	33.05	619.8
1100	0.021 855	24 493.0	33 644.0	233.05	25.25	33.57	648.3

TABLE A2. Thermodynamic properties of air—Continued

Temperature (K)	Density (mol/dm^3)	Internal energy (J/mol)	Enthalpy (J/mol)	Entropy J/(mol-K)	c_v J/(mol-K)	c_p J/(mol-K)	Speed of sound (m/s)
1200	0.020 034	27 041.0	37 024.0	235.99	25.70	34.02	675.7
1300	0.018 494	29 632.0	40 447.0	238.73	26.10	34.42	701.9
1400	0.017 173	32 261.0	43 906.0	241.30	26.45	34.77	727.2
1500	0.016 029	34 922.0	47 399.0	243.71	26.76	35.08	751.7
1600	0.015 027	37 612.0	50 921.0	245.98	27.04	35.35	775.4
1700	0.014 144	40 329.0	54 469.0	248.13	27.29	35.60	798.3
1800	0.013 358	43 069.0	58 040.0	250.17	27.51	35.82	820.7
1900	0.012 656	45 830.0	61 633.0	252.12	27.71	36.03	842.5
2000	0.012 023	48 610.0	65 245.0	253.97	27.90	36.21	863.7
			0.5 MPa isobar				
59.84	33.080	−4712.3	−4697.1	70.919	34.01	55.02	1032.1
60	33.057	−4703.4	−4688.2	71.067	33.98	55.02	1030.8
62	32.772	−4593.5	−4578.2	72.871	33.54	55.01	1014.7
64	32.485	−4483.6	−4468.2	74.618	33.11	55.02	998.4
66	32.195	−4373.6	−4358.1	76.311	32.71	55.06	981.9
68	31.903	−4263.6	−4247.9	77.956	32.32	55.11	965.1
70	31.608	−4153.5	−4137.6	79.554	31.94	55.19	948.0
72	31.309	−4043.1	−4027.2	81.111	31.59	55.30	930.7
74	31.007	−3932.6	−3916.4	82.627	31.24	55.43	913.1
76	30.701	−3821.7	−3805.4	84.108	30.91	55.59	895.2
78	30.391	−3710.5	−3694.1	85.554	30.59	55.79	877.0
80	30.076	−3598.9	−3582.3	86.969	30.28	56.02	858.5
82	29.755	−3486.8	−3469.9	88.356	29.99	56.29	839.7
84	29.429	−3374.0	−3357.1	89.716	29.70	56.61	820.5
86	29.096	−3260.7	−3243.5	91.052	29.43	56.98	801.0
88	28.756	−3146.5	−3129.1	92.367	29.17	57.41	781.0
90	28.408	−3031.4	−3013.8	93.663	28.92	57.91	760.6
92	28.051	−2915.2	−2897.4	94.942	28.68	58.49	739.8
94	27.683	−2797.8	−2779.8	96.207	28.46	59.15	718.4
96	27.304	−2679.0	−2660.7	97.460	28.24	59.92	696.5
96.12	27.281	−2671.8	−2653.4	97.535	28.23	59.98	695.2
98.36	0.695 38	1830.0	2549.0	151.13	23.36	37.31	185.0
100	0.678 71	1872.9	2609.6	151.74	23.07	36.53	187.4
102	0.659 81	1924.1	2681.9	152.45	22.79	35.75	190.3
104	0.642 25	1974.2	2752.7	153.14	22.56	35.11	193.0
106	0.625 86	2023.5	2822.4	153.80	22.37	34.57	195.7
108	0.610 51	2072.0	2891.0	154.45	22.21	34.10	198.2
110	0.596 06	2120.0	2958.8	155.07	22.07	33.70	200.7
112	0.582 43	2167.4	3025.9	155.67	21.95	33.35	203.2
114	0.569 54	2214.4	3092.3	156.26	21.85	33.04	205.5
116	0.557 31	2260.9	3158.1	156.83	21.76	32.77	207.9
118	0.545 69	2307.1	3223.4	157.39	21.68	32.52	210.1
120	0.534 63	2352.9	3288.2	157.93	21.61	32.30	212.4
122	0.524 08	2398.5	3352.6	158.47	21.54	32.10	214.6
124	0.514 00	2443.8	3416.6	158.99	21.48	31.92	216.7
126	0.504 35	2488.9	3480.3	159.50	21.43	31.75	218.8
128	0.495 11	2533.8	3543.6	160.00	21.38	31.60	220.9
130	0.486 25	2578.4	3606.7	160.48	21.34	31.46	223.0
132	0.477 73	2622.9	3669.5	160.96	21.30	31.34	225.0
134	0.469 55	2667.2	3732.0	161.43	21.26	31.22	227.0
136	0.461 67	2711.3	3794.4	161.90	21.23	31.11	229.0
138	0.454 08	2755.3	3856.5	162.35	21.20	31.01	230.9
140	0.446 76	2799.2	3918.4	162.80	21.17	30.91	232.8
142	0.439 69	2843.0	3980.1	163.23	21.14	30.83	234.7
144	0.432 87	2886.6	4041.7	163.66	21.12	30.75	236.6
146	0.426 28	2930.2	4103.1	164.09	21.10	30.67	238.4
148	0.419 89	2973.6	4164.4	164.50	21.08	30.60	240.3
150	0.413 72	3017.0	4225.5	164.91	21.06	30.53	242.1
155	0.399 10	3125.0	4377.8	165.91	21.02	30.39	246.5
160	0.385 55	3232.6	4529.4	166.88	20.98	30.26	250.9
165	0.372 95	3339.8	4680.4	167.80	20.95	30.15	255.1
170	0.361 19	3446.6	4830.9	168.70	20.93	30.05	259.3
175	0.350 19	3553.2	4981.0	169.57	20.90	29.97	263.4

TABLE A2. Thermodynamic properties of air—Continued

Temperature (K)	Density (mol/dm^3)	Internal energy (J/mol)	Enthalpy (J/mol)	Entropy J/(mol-K)	c_v J/(mol-K)	c_p J/(mol-K)	Speed of sound (m/s)
180	0.339 87	3659.5	5130.6	170.42	20.89	29.90	267.4
185	0.330 17	3765.6	5280.0	171.24	20.87	29.83	271.3
190	0.321 04	3871.5	5429.0	172.03	20.86	29.78	275.1
195	0.312 41	3977.3	5577.7	172.80	20.85	29.72	278.9
200	0.304 25	4082.9	5726.2	173.55	20.84	29.68	282.6
210	0.289 19	4293.7	6022.6	175.00	20.82	29.60	289.9
220	0.275 59	4504.0	6318.3	176.38	20.81	29.54	297.0
230	0.263 25	4714.1	6613.4	177.69	20.80	29.49	303.9
240	0.251 99	4923.9	6908.1	178.94	20.80	29.45	310.6
250	0.241 67	5133.4	7202.4	180.14	20.80	29.41	317.1
260	0.232 18	5342.9	7496.4	181.30	20.80	29.39	323.5
270	0.223 42	5552.2	7790.1	182.41	20.80	29.37	329.8
280	0.215 31	5761.4	8083.7	183.47	20.81	29.35	335.9
290	0.207 77	5970.6	8377.1	184.50	20.81	29.34	341.9
300	0.200 75	6179.8	8670.5	185.50	20.82	29.33	347.8
310	0.194 20	6389.1	8963.8	186.46	20.84	29.33	353.6
320	0.188 06	6598.4	9257.1	187.39	20.85	29.33	359.3
330	0.182 31	6807.8	9550.4	188.29	20.87	29.34	364.8
340	0.176 89	7017.3	9843.9	189.17	20.89	29.35	370.3
350	0.171 80	7227.0	10 137.0	190.02	20.91	29.36	375.7
360	0.166 99	7436.9	10 431.0	190.85	20.93	29.37	381.0
370	0.162 45	7647.0	10 725.0	191.65	20.96	29.39	386.2
380	0.158 15	7857.3	11 019.0	192.44	20.99	29.41	391.3
390	0.154 07	8067.9	11 313.0	193.20	21.02	29.44	396.3
400	0.150 20	8278.8	11 608.0	193.95	21.06	29.47	401.3
450	0.133 45	9338.5	13 085.0	197.43	21.26	29.65	425.1
500	0.120 07	10 409.0	14 573.0	200.56	21.51	29.89	447.3
550	0.109 14	11 494.0	16 075.0	203.42	21.81	30.17	468.2
600	0.100 04	12 593.0	17 591.0	206.06	22.13	30.48	488.0
650	0.092 347	13 709.0	19 123.0	208.52	22.47	30.82	506.8
700	0.085 752	14 842.0	20 673.0	210.81	22.82	31.16	524.8
750	0.080 038	15 993.0	22 240.0	212.97	23.17	31.51	542.1
800	0.075 038	17 160.0	23 823.0	215.02	23.51	31.84	558.7
900	0.066 707	19 545.0	27 040.0	218.81	24.15	32.48	590.5
1000	0.060 042	21 990.0	30 318.0	222.26	24.74	33.06	620.4
1100	0.054 589	24 491.0	33 650.0	225.43	25.25	33.57	648.9
1200	0.050 045	27 039.0	37 030.0	228.37	25.71	34.03	676.2
1300	0.046 199	29 631.0	40 453.0	231.11	26.10	34.42	702.5
1400	0.042 902	32 259.0	43 914.0	233.68	26.46	34.77	727.8
1500	0.040 045	34 921.0	47 407.0	236.09	26.76	35.08	752.2
1600	0.037 544	37 611.0	50 929.0	238.36	27.04	35.36	775.9
1700	0.035 338	40 328.0	54 477.0	240.51	27.29	35.60	798.8
1800	0.033 377	43 068.0	58 049.0	242.55	27.51	35.83	821.2
1900	0.031 621	45 829.0	61 641.0	244.50	27.71	36.03	842.9
2000	0.030 042	48 610.0	65 254.0	246.35	27.90	36.21	864.1
			1.0 MPa isobar				
59.93	33.094	−4711.2	−4681.0	70.936	34.02	54.97	1033.8
60	33.083	−4707.2	−4677.0	71.002	34.00	54.97	1033.3
62	32.800	−4597.6	−4567.1	72.804	33.56	54.96	1017.3
64	32.514	−4487.9	−4457.2	74.549	33.14	54.97	1001.1
66	32.225	−4378.2	−4347.2	76.241	32.73	55.00	984.7
68	31.934	−4268.5	−4237.2	77.884	32.34	55.05	968.0
70	31.641	−4158.6	−4127.0	79.480	31.97	55.12	951.1
72	31.344	−4048.6	−4016.7	81.034	31.61	55.21	933.9
74	31.044	−3938.4	−3906.1	82.549	31.27	55.33	916.5
76	30.740	−3827.9	−3795.3	84.026	30.93	55.49	898.8
78	30.431	−3717.0	−3684.2	85.470	30.62	55.67	880.8
80	30.119	−3605.8	−3572.6	86.882	30.31	55.89	862.5
82	29.801	−3494.2	−3460.6	88.265	30.01	56.15	843.8
84	29.478	−3381.9	−3348.0	89.622	29.73	56.45	824.9
86	29.148	−3269.1	−3234.8	90.954	29.46	56.80	805.6
88	28.812	−3155.5	−3120.8	92.264	29.20	57.20	786.0
90	28.467	−3041.1	−3005.9	93.555	28.95	57.67	765.9

TABLE A2. Thermodynamic properties of air—Continued

Temperature (K)	Density (mol/dm^3)	Internal energy (J/mol)	Enthalpy (J/mol)	Entropy J/(mol-K)	c_v J/(mol-K)	c_p J/(mol-K)	Speed of sound (m/s)
92	28.115	−2925.6	−2890.1	94.828	28.71	58.21	745.4
94	27.752	−2809.1	−2773.1	96.086	28.48	58.83	724.4
96	27.379	−2691.2	−2654.7	97.332	28.26	59.55	702.9
98	26.993	−2571.8	−2534.8	98.568	28.06	60.38	680.9
100	26.593	−2450.7	−2413.1	99.798	27.87	61.36	658.2
102	26.177	−2327.5	−2289.3	101.02	27.69	62.50	634.9
104	25.742	−2201.8	−2162.9	102.25	27.53	63.85	610.8
106	25.284	−2073.2	−2033.7	103.48	27.38	65.48	585.8
106.22	25.232	−2059.0	−2019.3	103.62	27.37	65.68	583.0
108.10	1.3836	1873.7	2596.5	146.73	24.74	44.60	185.2
110	1.3382	1931.9	2679.2	147.49	24.21	42.69	188.7
112	1.2951	1990.8	2763.0	148.24	23.78	41.11	192.1
114	1.2559	2047.6	2843.9	148.96	23.43	39.85	195.3
116	1.2200	2102.9	2922.5	149.64	23.15	38.81	198.3
118	1.1870	2156.7	2999.2	150.30	22.91	37.94	201.2
120	1.1563	2209.5	3074.3	150.93	22.71	37.20	204.0
122	1.1276	2261.3	3148.1	151.54	22.54	36.56	206.8
124	1.1009	2312.2	3220.6	152.13	22.39	36.00	209.4
126	1.0757	2362.5	3292.1	152.70	22.26	35.52	211.9
128	1.0519	2412.1	3362.7	153.25	22.15	35.08	214.4
130	1.0295	2461.1	3432.5	153.79	22.05	34.69	216.8
132	1.0082	2509.7	3501.5	154.32	21.95	34.34	219.2
134	0.988 04	2557.8	3569.9	154.84	21.87	34.03	221.5
136	0.968 81	2605.5	3637.7	155.34	21.80	33.74	223.8
138	0.950 48	2652.8	3704.9	155.83	21.73	33.48	226.0
140	0.932 97	2699.8	3771.6	156.31	21.66	33.24	228.2
142	0.916 22	2746.4	3837.9	156.78	21.61	33.02	230.3
144	0.900 18	2792.8	3903.7	157.24	21.55	32.82	232.4
146	0.884 78	2838.9	3969.2	157.69	21.51	32.64	234.5
148	0.869 99	2884.8	4034.3	158.13	21.46	32.46	236.5
150	0.855 77	2930.5	4099.0	158.57	21.42	32.30	238.5
155	0.822 47	3043.8	4259.6	159.62	21.33	31.95	243.4
160	0.792 01	3156.0	4418.6	160.63	21.26	31.66	248.1
165	0.763 99	3267.4	4576.3	161.60	21.20	31.41	252.7
170	0.738 11	3377.9	4732.8	162.53	21.14	31.19	257.1
175	0.714 11	3487.9	4888.2	163.44	21.10	31.00	261.5
180	0.691 76	3597.2	5042.8	164.31	21.06	30.84	265.7
185	0.670 90	3706.1	5196.6	165.15	21.03	30.70	269.8
190	0.651 36	3814.6	5349.8	165.97	21.00	30.57	273.9
195	0.633 01	3922.6	5502.4	166.76	20.98	30.46	277.9
200	0.615 74	4030.4	5654.4	167.53	20.95	30.36	281.7
210	0.584 06	4245.0	5957.2	169.01	20.92	30.19	289.3
220	0.555 66	4458.7	6258.4	170.41	20.90	30.06	296.6
230	0.530 03	4671.7	6558.4	171.74	20.88	29.95	303.7
240	0.506 76	4884.0	6857.4	173.01	20.86	29.85	310.6
250	0.485 53	5095.9	7155.5	174.23	20.85	29.78	317.3
260	0.466 07	5307.4	7453.0	175.40	20.85	29.72	323.8
270	0.448 16	5518.5	7749.9	176.52	20.85	29.66	330.2
280	0.431 62	5729.5	8046.3	177.60	20.85	29.62	336.4
290	0.416 30	5940.2	8342.3	178.64	20.85	29.59	342.5
300	0.402 05	6150.8	8638.1	179.64	20.86	29.56	348.4
310	0.388 76	6361.4	8933.6	180.61	20.87	29.54	354.3
320	0.376 35	6571.9	9229.0	181.54	20.88	29.53	360.0
330	0.364 72	6782.4	9524.2	182.45	20.90	29.52	365.6
340	0.353 80	6992.9	9819.4	183.33	20.91	29.52	371.1
350	0.343 53	7203.6	10 115.0	184.19	20.93	29.52	376.6
360	0.333 85	7414.4	10 410.0	185.02	20.96	29.52	381.9
370	0.324 71	7625.3	10 705.0	185.83	20.98	29.53	387.1
380	0.316 06	7836.4	11 000.0	186.62	21.01	29.54	392.3
390	0.307 87	8047.7	11 296.0	187.39	21.04	29.56	397.3
400	0.300 09	8259.3	11 592.0	188.13	21.07	29.58	402.3
450	0.266 51	9322.0	13 074.0	191.63	21.27	29.73	426.2
500	0.239 74	10 395.0	14 566.0	194.77	21.53	29.95	448.5

TABLE A2. Thermodynamic properties of air—Continued

Temperature (K)	Density (mol/dm^3)	Internal energy (J/mol)	Enthalpy (J/mol)	Entropy J/(mol-K)	c_v J/(mol-K)	c_p J/(mol-K)	Speed of sound (m/s)
550	0.217 90	11 481.0	16 070.0	197.64	21.82	30.22	469.4
600	0.199 72	12 582.0	17 589.0	200.28	22.14	30.53	489.2
650	0.184 35	13 699.0	19 124.0	202.74	22.48	30.86	508.0
700	0.171 19	14 834.0	20 675.0	205.04	22.83	31.19	526.0
750	0.159 79	15 985.0	22 243.0	207.20	23.18	31.53	543.2
800	0.149 81	17 153.0	23 828.0	209.25	23.52	31.87	559.9
900	0.133 19	19 539.0	27 047.0	213.04	24.16	32.50	591.5
1000	0.119 90	21 986.0	30 326.0	216.49	24.74	33.07	621.5
1100	0.109 02	24 487.0	33 659.0	219.67	25.26	33.58	650.0
1200	0.099 953	27 036.0	37 041.0	222.61	25.71	34.03	677.2
1300	0.092 279	29 628.0	40 465.0	225.35	26.11	34.43	703.4
1400	0.085 701	32 257.0	43 925.0	227.91	26.46	34.78	728.7
1500	0.079 999	34 919.0	47 419.0	230.32	26.77	35.09	753.1
1600	0.075 008	37 610.0	50 942.0	232.60	27.04	35.36	776.7
1700	0.070 604	40 327.0	54 490.0	234.75	27.29	35.61	799.7
1800	0.066 689	43 067.0	58 062.0	236.79	27.51	35.83	822.0
1900	0.063 185	45 829.0	61 655.0	238.73	27.71	36.03	843.7
2000	0.060 031	48 609.0	65 268.0	240.59	27.90	36.22	864.9
			2.0 MPa isobar				
60.11	33.121	−4709.1	−4648.7	70.970	34.02	54.88	1037.4
62	32.854	−4605.7	−4544.8	72.673	33.61	54.86	1022.4
64	32.570	−4496.5	−4435.1	74.414	33.18	54.86	1006.5
66	32.285	−4387.3	−4325.3	76.103	32.78	54.88	990.3
68	31.997	−4278.1	−4215.6	77.741	32.39	54.91	973.8
70	31.706	−4168.8	−4105.7	79.334	32.02	54.97	957.2
72	31.412	−4059.3	−3995.7	80.884	31.66	55.05	940.3
74	31.116	−3949.7	−3885.5	82.393	31.32	55.15	923.1
76	30.815	−3839.9	−3775.0	83.866	30.99	55.29	905.7
78	30.511	−3729.9	−3664.3	85.304	30.67	55.45	888.1
80	30.203	−3619.4	−3553.2	86.710	30.36	55.64	870.2
82	29.891	−3508.6	−3441.7	88.087	30.07	55.87	852.0
84	29.573	−3397.4	−3329.7	89.436	29.78	56.13	833.5
86	29.249	−3285.5	−3217.2	90.760	29.51	56.44	814.7
88	28.919	−3173.1	−3103.9	92.062	29.25	56.80	795.6
90	28.583	−3059.9	−2989.9	93.343	29.00	57.21	776.1
92	28.238	−2945.9	−2875.0	94.606	28.76	57.69	756.2
94	27.885	−2830.9	−2759.1	95.852	28.53	58.23	736.0
96	27.522	−2714.7	−2642.1	97.084	28.31	58.86	715.3
98	27.149	−2597.3	−2523.6	98.305	28.10	59.57	694.1
100	26.763	−2478.4	−2403.7	99.517	27.90	60.41	672.5
102	26.364	−2357.8	−2281.9	100.72	27.72	61.37	650.2
104	25.948	−2235.2	−2158.1	101.92	27.55	62.49	627.4
106	25.514	−2110.2	−2031.8	103.13	27.40	63.82	603.9
108	25.058	−1982.5	−1902.7	104.33	27.26	65.40	579.6
110	24.577	−1851.4	−1770.0	105.55	27.14	67.31	554.3
112	24.065	−1716.2	−1633.1	106.78	27.04	69.66	528.0
114	23.513	−1576.0	−1491.0	108.04	26.97	72.64	500.4
116	22.913	−1429.3	−1342.0	109.34	26.94	76.56	470.9
118	22.245	−1273.6	−1183.7	110.69	26.96	82.02	439.1
118.52	22.059	−1231.7	−1141.0	111.05	26.97	83.81	430.4
119.94	2.9766	1788.0	2459.9	141.25	27.21	68.49	180.5
120	2.9709	1791.1	2464.3	141.29	27.17	68.18	180.7
122	2.8114	1880.8	2592.2	142.35	26.12	60.34	186.1
124	2.6809	1961.3	2707.4	143.28	25.36	55.18	190.8
126	2.5702	2035.7	2813.8	144.13	24.78	51.49	195.1
128	2.4740	2105.5	2913.9	144.92	24.33	48.71	199.0
130	2.3888	2171.9	3009.1	145.66	23.96	46.54	202.6
132	2.3124	2235.5	3100.4	146.36	23.66	44.78	206.1
134	2.2432	2296.8	3188.4	147.02	23.40	43.33	209.3
136	2.1799	2356.4	3273.8	147.65	23.18	42.11	212.4
138	2.1217	2414.3	3357.0	148.26	22.99	41.07	215.4
140	2.0678	2470.9	3438.2	148.84	22.83	40.16	218.3
142	2.0176	2526.4	3517.7	149.41	22.68	39.38	221.0

TABLE A2. Thermodynamic properties of air—Continued

Temperature (K)	Density (mol/dm^3)	Internal energy (J/mol)	Enthalpy (J/mol)	Entropy J/(mol-K)	c_v J/(mol-K)	c_p J/(mol-K)	Speed of sound (m/s)
144	1.9707	2580.9	3595.7	149.95	22.55	38.68	223.7
146	1.9267	2634.4	3672.5	150.48	22.43	38.06	226.3
148	1.8853	2687.2	3748.0	151.00	22.32	37.51	228.8
150	1.8462	2739.2	3822.5	151.50	22.22	37.01	231.3
155	1.7572	2866.7	4004.9	152.69	22.02	35.96	237.2
160	1.6785	2991.0	4182.5	153.82	21.85	35.12	242.7
165	1.6082	3112.7	4356.3	154.89	21.71	34.44	248.1
170	1.5448	3232.4	4527.1	155.91	21.60	33.87	253.1
175	1.4872	3350.4	4695.2	156.88	21.50	33.39	258.0
180	1.4345	3466.9	4861.1	157.82	21.42	32.99	262.8
185	1.3861	3582.3	5025.2	158.72	21.35	32.64	267.3
190	1.3413	3696.5	5187.6	159.58	21.29	32.34	271.8
195	1.2997	3809.9	5348.6	160.42	21.24	32.08	276.1
200	1.2610	3922.4	5508.4	161.23	21.19	31.84	280.3
210	1.1909	4145.5	5824.9	162.77	21.12	31.46	288.4
220	1.1291	4366.5	6137.9	164.23	21.07	31.15	296.2
230	1.0739	4585.7	6448.1	165.61	21.02	30.90	303.6
240	1.0243	4803.5	6756.1	166.92	20.99	30.70	310.8
250	0.979 42	5020.2	7062.2	168.17	20.97	30.53	317.8
260	0.938 59	5236.0	7366.9	169.36	20.95	30.39	324.6
270	0.901 25	5451.0	7670.2	170.51	20.94	30.28	331.2
280	0.866 94	5665.4	7972.4	171.61	20.93	30.18	337.6
290	0.835 28	5879.3	8273.8	172.67	20.93	30.09	343.8
300	0.805 97	6092.8	8574.3	173.68	20.93	30.03	349.9
310	0.778 73	6306.0	8874.3	174.67	20.93	29.97	355.9
320	0.753 36	6519.0	9173.7	175.62	20.94	29.92	361.7
330	0.729 65	6731.7	9472.7	176.54	20.95	29.88	367.4
340	0.707 45	6944.4	9771.4	177.43	20.97	29.85	373.0
350	0.686 60	7156.9	10 070.0	178.30	20.98	29.83	378.5
360	0.666 99	7369.5	10 368.0	179.14	21.00	29.82	383.9
370	0.648 50	7582.1	10 666.0	179.95	21.03	29.81	389.2
380	0.631 04	7794.8	10 964.0	180.75	21.05	29.80	394.4
390	0.614 51	8007.6	11 262.0	181.52	21.08	29.80	399.5
400	0.598 86	8220.6	11 560.0	182.28	21.11	29.81	404.5
450	0.531 41	9289.2	13 053.0	185.79	21.30	29.91	428.5
500	0.477 83	10 367.0	14 552.0	188.95	21.55	30.09	450.8
550	0.434 20	11 457.0	16 063.0	191.83	21.84	30.33	471.8
600	0.397 94	12 561.0	17 586.0	194.48	22.16	30.62	491.5
650	0.367 32	13 680.0	19 125.0	196.94	22.50	30.93	510.3
700	0.34 112	14 816.0	20 680.0	199.25	22.84	31.26	528.3
750	0.31 842	15 970.0	22 251.0	201.42	23.19	31.58	545.5
800	0.298 57	17 139.0	23 838.0	203.47	23.53	31.91	562.1
900	0.265 50	19 528.0	27 061.0	207.26	24.17	32.53	593.7
1000	0.239 05	21 976.0	30 343.0	210.72	24.75	33.10	623.6
1100	0.217 40	24 479.0	33 679.0	213.90	25.26	33.61	652.0
1200	0.199 36	27 030.0	37 062.0	216.84	25.72	34.05	679.2
1300	0.184 08	29 623.0	40 487.0	219.58	26.11	34.44	705.3
1400	0.170 99	32 253.0	43 949.0	222.15	26.46	34.79	730.5
1500	0.159 63	34 915.0	47 444.0	224.56	26.77	35.10	754.8
1600	0.149 69	37 607.0	50 967.0	226.83	27.05	35.37	778.4
1700	0.140 92	40 324.0	54 517.0	228.98	27.29	35.61	801.3
1800	0.133 12	43 065.0	58 089.0	231.03	27.52	35.83	823.6
1900	0.126 14	45 827.0	61 683.0	232.97	27.72	36.04	845.3
2000	0.119 85	48 608.0	65 296.0	234.82	27.90	36.22	866.4
			5.0 MPa isobar				
60.64	33.200	−4702.6	−4552.0	71.073	34.04	54.61	1047.7
62	33.012	−4629.1	−4477.6	72.287	33.75	54.58	1037.3
64	32.736	−4521.2	−4368.5	74.019	33.33	54.55	1021.9
66	32.458	−4413.4	−4259.4	75.698	32.93	54.54	1006.3
68	32.178	−4305.7	−4150.3	77.326	32.54	54.55	990.5
70	31.895	−4198.0	−4041.2	78.907	32.17	54.57	974.6
72	31.611	−4090.2	−3932.0	80.445	31.82	54.61	958.5
74	31.324	−3982.4	−3822.8	81.942	31.48	54.67	942.2

TABLE A2. Thermodynamic properties of air—Continued

Temperature (K)	Density (mol/dm^3)	Internal energy (J/mol)	Enthalpy (J/mol)	Entropy J/(mol-K)	c_v J/(mol-K)	c_p J/(mol-K)	Speed of sound (m/s)
76	31.034	−3874.5	−3713.4	83.401	31.15	54.75	925.7
78	30.742	−3766.4	−3603.8	84.824	30.83	54.85	909.0
80	30.446	−3658.2	−3493.9	86.214	30.52	54.98	892.1
82	30.146	−3549.7	−3383.8	87.574	30.23	55.13	875.0
84	29.843	−3441.0	−3273.4	88.904	29.94	55.31	857.7
86	29.535	−3331.9	−3162.6	90.208	29.67	55.52	840.2
88	29.223	−3222.4	−3051.3	91.488	29.41	55.77	822.4
90	28.906	−3112.4	−2939.5	92.744	29.15	56.06	804.4
92	28.582	−3002.0	−2827.0	93.980	28.91	56.38	786.2
94	28.253	−2890.9	−2713.9	95.196	28.68	56.75	767.7
96	27.917	−2779.1	−2600.0	96.395	28.45	57.17	748.9
98	27.574	−2666.5	−2485.2	97.579	28.24	57.64	729.9
100	27.222	−2553.1	−2369.4	98.748	28.03	58.18	710.6
102	26.861	−2438.6	−2252.4	99.906	27.84	58.79	690.9
104	26.490	−2322.9	−2134.2	101.05	27.66	59.48	671.0
106	26.108	−2206.0	−2014.5	102.19	27.48	60.26	650.7
108	25.713	−2087.5	−1893.1	103.33	27.32	61.15	630.0
110	25.304	−1967.4	−1769.8	104.46	27.17	62.17	609.0
112	24.879	−1845.3	−1644.3	105.59	27.03	63.34	587.6
114	24.436	−1720.9	−1516.3	106.72	26.90	64.69	565.7
116	23.972	−1594.0	−1385.4	107.86	26.79	66.26	543.3
118	23.483	−1464.0	−1251.1	109.01	26.70	68.12	520.4
120	22.966	−1330.4	−1112.7	110.17	26.62	70.34	496.8
122	22.415	−1192.4	−969.37	111.36	26.57	73.05	472.5
124	21.822	−1049.1	−820.02	112.57	26.55	76.44	447.2
126	21.176	−899.10	−662.99	113.83	26.57	80.80	420.8
128	20.462	−740.19	−495.84	115.14	26.63	86.66	393.0
130	19.654	−569.09	−314.69	116.55	26.78	95.03	363.1
132	18.706	−380.05	−112.75	118.09	27.04	107.94	330.4
134	17.533	−162.02	123.16	119.86	27.53	130.20	294.1
136	15.954	108.31	421.72	122.07	28.44	173.22	253.7
138	13.686	470.13	835.47	125.09	29.89	241.20	216.2
140	11.096	892.71	1343.3	128.75	30.37	246.60	199.5
142	9.2688	1229.6	1769.0	131.77	29.21	178.44	199.2
144	8.1721	1462.3	2074.2	133.90	27.96	131.40	202.8
146	7.4446	1636.9	2308.5	135.52	26.99	105.29	206.9
148	6.9126	1778.7	2502.1	136.83	26.24	89.47	211.0
150	6.4975	1900.3	2669.9	137.96	25.66	78.99	214.9
155	5.7485	2152.4	3022.2	140.27	24.63	63.74	223.8
160	5.2273	2362.0	3318.5	142.15	23.95	55.49	231.8
165	4.8317	2547.3	3582.1	143.78	23.46	50.29	239.1
170	4.5153	2716.8	3824.1	145.22	23.08	46.71	245.9
175	4.2532	2875.2	4050.8	146.54	22.78	44.09	252.2
180	4.0305	3025.5	4266.1	147.75	22.54	42.09	258.2
185	3.8376	3169.5	4472.4	148.88	22.35	40.51	263.9
190	3.6681	3308.6	4671.7	149.94	22.18	39.24	269.3
195	3.5173	3443.6	4865.2	150.95	22.04	38.19	274.5
200	3.3819	3575.4	5053.8	151.90	21.92	37.31	279.4
210	3.1473	3831.0	5419.6	153.69	21.72	35.92	288.8
220	2.9500	4078.5	5773.4	155.34	21.58	34.88	297.7
230	2.7806	4319.9	6118.1	156.87	21.46	34.08	306.0
240	2.6330	4556.6	6455.6	158.30	21.37	33.45	314.0
250	2.5028	4789.7	6787.4	159.66	21.31	32.94	321.5
260	2.3868	5019.7	7114.6	160.94	21.25	32.52	328.8
270	2.2825	5247.4	7438.0	162.16	21.21	32.17	335.9
280	2.1880	5473.0	7758.2	163.33	21.17	31.88	342.7
290	2.1020	5697.0	8075.7	164.44	21.15	31.63	349.2
300	2.0232	5919.6	8390.9	165.51	21.13	31.42	355.6
310	1.9507	6141.1	8704.2	166.54	21.12	31.24	361.8
320	1.8837	6361.6	9015.9	167.53	21.11	31.09	367.9
330	1.8216	6581.2	9326.2	168.48	21.11	30.96	373.8
340	1.7637	6800.3	9635.2	169.40	21.12	30.85	379.6
350	1.7097	7018.8	9943.3	170.30	21.12	30.76	385.2

TABLE A2. Thermodynamic properties of air—Continued

Temperature (K)	Density (mol/dm^3)	Internal energy (J/mol)	Enthalpy (J/mol)	Entropy J/(mol-K)	c_v J/(mol-K)	c_p J/(mol-K)	Speed of sound (m/s)
360	1.6591	7236.8	10 250.0	171.16	21.13	30.68	390.7
370	1.6117	7454.5	10 557.0	172.00	21.15	30.61	396.1
380	1.5671	7672.0	10 863.0	172.82	21.17	30.56	401.4
390	1.5250	7889.3	11 168.0	173.61	21.19	30.51	406.6
400	1.4852	8106.4	11 473.0	174.38	21.22	30.47	411.7
450	1.3152	9192.6	12 994.0	177.97	21.39	30.41	435.9
500	1.1814	10 284.0	14 516.0	181.17	21.62	30.48	458.3
550	1.0731	11 384.0	16 044.0	184.08	21.90	30.64	479.2
600	0.983 39	12 497.0	17 581.0	186.76	22.21	30.87	498.9
650	0.907 81	13 624.0	19 131.0	189.24	22.54	31.14	517.6
700	0.843 21	14 766.0	20 696.0	191.56	22.89	31.43	535.4
750	0.787 32	15 924.0	22 275.0	193.74	23.23	31.74	552.5
800	0.738 47	17 099.0	23 869.0	195.80	23.56	32.04	569.0
900	0.657 11	19 494.0	27 103.0	199.61	24.20	32.63	600.3
1000	0.592 03	21 949.0	30 394.0	203.07	24.77	33.18	629.9
1100	0.538 74	24 456.0	33 737.0	206.26	25.29	33.67	658.1
1200	0.494 31	27 011.0	37 126.0	209.21	25.74	34.10	685.1
1300	0.456 67	29 607.0	40 556.0	211.95	26.13	34.48	711.0
1400	0.424 38	32 239.0	44 021.0	214.52	26.48	34.82	736.0
1500	0.396 36	34 904.0	47 519.0	216.93	26.79	35.12	760.1
1600	0.371 82	37 598.0	51 045.0	219.21	27.06	35.39	783.6
1700	0.350 15	40 317.0	54 596.0	221.36	27.30	35.63	806.3
1800	0.330 88	43 059.0	58 171.0	223.40	27.53	35.85	828.4
1900	0.313 61	45 823.0	61 766.0	225.35	27.73	36.05	850.0
2000	0.298 06	48 605.0	65 380.0	227.20	27.91	36.23	871.0
			10.0 MPa isobar				
61.52	33.329	−4691.3	−4391.2	71.245	34.08	54.19	1064.0
62	33.264	−4665.6	−4364.9	71.671	33.98	54.18	1060.5
64	32.998	−4559.7	−4256.7	73.390	33.57	54.12	1046.0
66	32.731	−4454.0	−4148.5	75.054	33.17	54.07	1031.3
68	32.462	−4348.4	−4040.4	76.668	32.79	54.03	1016.5
70	32.192	−4243.0	−3932.4	78.233	32.43	54.00	1001.6
72	31.921	−4137.6	−3824.4	79.755	32.07	53.99	986.5
74	31.648	−4032.4	−3716.4	81.234	31.74	53.99	971.4
76	31.373	−3927.1	−3608.4	82.674	31.41	54.01	956.1
78	31.096	−3821.9	−3500.3	84.077	31.09	54.04	940.7
80	30.817	−3716.7	−3392.2	85.446	30.79	54.09	925.2
82	30.536	−3611.5	−3284.0	86.782	30.50	54.15	909.6
84	30.253	−3506.1	−3175.6	88.088	30.21	54.24	893.8
86	29.966	−3400.7	−3067.0	89.366	29.94	54.34	877.9
88	29.677	−3295.2	−2958.2	90.616	29.68	54.47	861.9
90	29.384	−3189.5	−2849.1	91.842	29.42	54.61	845.8
92	29.088	−3083.5	−2739.7	93.044	29.18	54.78	829.6
94	28.788	−2977.4	−2630.0	94.224	28.94	54.97	813.2
96	28.484	−2870.9	−2519.8	95.384	28.71	55.19	796.8
98	28.176	−2764.1	−2409.2	96.524	28.49	55.44	780.2
100	27.863	−2656.9	−2298.1	97.647	28.28	55.72	763.5
102	27.546	−2549.4	−2186.3	98.753	28.08	56.02	746.7
104	27.222	−2441.3	−2073.9	99.844	27.89	56.36	729.7
106	26.893	−2332.7	−1960.8	100.92	27.70	56.74	712.7
108	26.558	−2223.5	−1846.9	101.99	27.52	57.16	695.5
110	26.215	−2113.6	−1732.2	103.04	27.35	57.61	678.3
112	25.866	−2003.1	−1616.5	104.08	27.19	58.12	661.0
114	25.509	−1891.7	−1499.7	105.11	27.03	58.67	643.6
116	25.143	−1779.5	−1381.8	106.14	26.89	59.27	626.2
118	24.768	−1666.3	−1262.6	107.16	26.75	59.93	608.7
120	24.383	−1552.1	−1142.0	108.17	26.62	60.65	591.1
122	23.988	−1436.8	−1019.9	109.18	26.50	61.44	573.6
124	23.582	−1320.2	−896.19	110.19	26.39	62.30	556.0
126	23.164	−1202.4	−770.65	111.19	26.28	63.25	538.4
128	22.732	−1083.1	−643.14	112.20	26.19	64.28	520.9
130	22.287	−962.17	−513.47	113.20	26.10	65.41	503.5
132	21.826	−839.59	−381.42	114.21	26.03	66.66	486.1

TABLE A2. Thermodynamic properties of air—Continued

Temperature (K)	Density (mol/dm^3)	Internal energy (J/mol)	Enthalpy (J/mol)	Entropy J/(mol-K)	c_v J/(mol-K)	c_p J/(mol-K)	Speed of sound (m/s)
134	21.349	−715.17	−246.76	115.22	25.96	68.02	468.8
136	20.855	−588.77	−109.26	116.24	25.90	69.51	451.7
138	20.342	−460.24	31.349	117.27	25.86	71.13	434.8
140	19.810	−329.46	175.34	118.30	25.82	72.88	418.1
142	19.257	−196.33	322.96	119.35	25.79	74.76	401.9
144	18.684	−60.807	474.42	120.41	25.77	76.71	386.1
146	18.090	77.041	629.83	121.48	25.76	78.69	371.0
148	17.478	217.00	789.15	122.56	25.75	80.60	356.7
150	16.851	358.66	952.10	123.66	25.73	82.31	343.4
155	15.253	715.54	1371.2	126.41	25.65	84.77	316.0
160	13.709	1064.0	1793.4	129.09	25.45	83.46	297.6
165	12.331	1388.9	2199.9	131.59	25.11	78.69	287.3
170	11.170	1682.4	2577.7	133.84	24.70	72.33	282.7
175	10.218	1944.8	2923.4	135.85	24.30	66.09	281.8
180	9.4390	2180.7	3240.1	137.63	23.94	60.75	283.1
185	8.7946	2395.5	3532.6	139.24	23.62	56.38	285.6
190	8.2534	2593.7	3805.4	140.69	23.35	52.86	288.8
195	7.7920	2778.9	4062.3	142.03	23.11	50.01	292.4
200	7.3931	2953.7	4306.3	143.26	22.90	47.67	296.3
210	6.7353	3279.3	4764.1	145.50	22.56	44.10	304.3
220	6.2116	3581.7	5191.5	147.49	22.30	41.53	312.4
230	5.7819	3867.3	5596.8	149.29	22.10	39.62	320.3
240	5.4208	4140.6	5985.3	150.94	21.93	38.14	328.0
250	5.1116	4404.4	6360.7	152.47	21.80	36.98	335.4
260	4.8429	4660.8	6725.7	153.91	21.70	36.04	342.7
270	4.6064	4911.3	7082.2	155.25	21.61	35.28	349.7
280	4.3961	5157.0	7431.7	156.52	21.54	34.64	356.5
290	4.2075	5398.7	7775.4	157.73	21.49	34.11	363.1
300	4.0370	5637.1	8114.2	158.88	21.44	33.66	369.5
310	3.8819	5872.8	8448.9	159.97	21.41	33.28	375.7
320	3.7400	6106.2	8780.0	161.03	21.38	32.95	381.8
330	3.6096	6337.7	9108.1	162.04	21.36	32.67	387.7
340	3.4891	6567.4	9433.5	163.01	21.35	32.42	393.5
350	3.3774	6795.8	9756.7	163.94	21.34	32.21	399.1
360	3.2735	7023.0	10 078.0	164.85	21.34	32.03	404.6
370	3.1765	7249.1	10 397.0	165.72	21.34	31.87	410.0
380	3.0857	7474.4	10 715.0	166.57	21.35	31.73	415.3
390	3.0004	7699.0	11 032.0	167.39	21.37	31.61	420.5
400	2.9202	7923.0	11 347.0	168.19	21.38	31.50	425.6
450	2.5803	9037.7	12 913.0	171.88	21.52	31.18	449.6
500	2.3157	10 151.0	14 469.0	175.16	21.73	31.08	471.8
550	2.1029	11 268.0	16 023.0	178.12	22.00	31.12	492.5
600	1.9274	12 395.0	17 583.0	180.84	22.30	31.27	511.9
650	1.7800	13 533.0	19 151.0	183.35	22.62	31.47	530.3
700	1.6542	14 685.0	20 730.0	185.69	22.95	31.71	547.8
750	1.5454	15 852.0	22 322.0	187.88	23.29	31.97	564.6
800	1.4504	17 033.0	23 928.0	189.96	23.62	32.24	580.8
900	1.2922	19 441.0	27 179.0	193.79	24.24	32.79	611.6
1000	1.1655	21 904.0	30 484.0	197.27	24.81	33.30	640.7
1100	1.0618	24 419.0	33 837.0	200.46	25.32	33.76	668.5
1200	0.975 11	26 980.0	37 235.0	203.42	25.77	34.18	695.0
1300	0.901 65	29 581.0	40 672.0	206.17	26.16	34.55	720.6
1400	0.838 54	32 218.0	44 143.0	208.74	26.50	34.88	745.2
1500	0.783 74	34 886.0	47 646.0	211.16	26.81	35.17	769.1
1600	0.735 69	37 583.0	51 176.0	213.44	27.08	35.43	792.2
1700	0.693 21	40 305.0	54 731.0	215.59	27.32	35.66	814.7
1800	0.655 39	43 050.0	58 308.0	217.64	27.54	35.88	836.5
1900	0.621 49	45 815.0	61 906.0	219.58	27.74	36.07	857.9
2000	0.590 94	48 600.0	65 522.0	221.44	27.93	36.25	878.6
			20.0 MPa isobar				
63.24	33.574	−4666.7	−4071.0	71.587	34.18	53.48	1094.3
64	33.480	−4627.8	−4030.5	72.224	34.03	53.44	1089.3
66	33.230	−4525.5	−3923.7	73.867	33.64	53.33	1076.1

TABLE A2. Thermodynamic properties of air—Continued

Temperature (K)	Density (mol/dm^3)	Internal energy (J/mol)	Enthalpy (J/mol)	Entropy J/(mol-K)	c_v J/(mol-K)	c_p J/(mol-K)	Speed of sound (m/s)
68	32.981	−4423.5	−3817.1	75.457	33.27	53.24	1062.8
70	32.730	−4321.8	−3710.7	76.999	32.91	53.15	1049.4
72	32.480	−4220.3	−3604.5	78.496	32.57	53.07	1036.0
74	32.228	−4119.0	−3498.4	79.949	32.23	53.00	1022.6
76	31.976	−4017.9	−3392.5	81.361	31.91	52.94	1009.1
78	31.724	−3917.1	−3286.7	82.736	31.60	52.88	995.6
80	31.470	−3816.5	−3180.9	84.074	31.30	52.84	982.1
82	31.216	−3716.0	−3075.3	85.378	31.02	52.80	968.6
84	30.961	−3615.7	−2969.7	86.650	30.74	52.77	955.0
86	30.705	−3515.6	−2864.2	87.892	30.47	52.76	941.4
88	30.447	−3415.6	−2758.7	89.105	30.20	52.75	927.8
90	30.189	−3315.7	−2653.2	90.290	29.95	52.75	914.2
92	29.929	−3215.9	−2547.7	91.450	29.71	52.76	900.5
94	29.667	−3116.3	−2442.1	92.585	29.47	52.79	886.9
96	29.405	−3016.7	−2336.5	93.696	29.24	52.82	873.2
98	29.140	−2917.2	−2230.9	94.786	29.02	52.86	859.6
100	28.874	−2817.7	−2125.1	95.854	28.81	52.91	846.0
102	28.606	−2718.3	−2019.2	96.903	28.60	52.98	832.4
104	28.337	−2619.0	−1913.2	97.932	28.40	53.05	818.8
106	28.065	−2519.6	−1807.0	98.943	28.21	53.13	805.2
108	27.791	−2420.3	−1700.6	99.937	28.02	53.23	791.7
110	27.516	−2320.9	−1594.1	100.91	27.84	53.33	778.2
112	27.238	−2221.6	−1487.3	101.88	27.67	53.44	764.8
114	26.958	−2122.2	−1380.3	102.82	27.50	53.57	751.5
116	26.675	−2022.8	−1273.0	103.76	27.34	53.70	738.2
118	26.390	−1923.4	−1165.5	104.68	27.18	53.84	725.0
120	26.103	−1823.9	−1057.7	105.58	27.03	53.99	711.9
122	25.813	−1724.4	−949.55	106.48	26.88	54.14	699.0
124	25.520	−1624.8	−841.10	107.36	26.74	54.31	686.1
126	25.225	−1525.2	−732.32	108.23	26.61	54.48	673.4
128	24.928	−1425.5	−623.18	109.09	26.48	54.65	660.9
130	24.628	−1325.8	−513.69	109.94	26.35	54.84	648.5
132	24.325	−1226.0	−403.84	110.77	26.23	55.02	636.3
134	24.020	−1126.3	−293.61	111.60	26.11	55.21	624.3
136	23.712	−1026.4	−183.00	112.42	26.00	55.40	612.5
138	23.402	−926.63	−72.016	113.23	25.89	55.59	601.0
140	23.090	−826.82	39.349	114.03	25.79	55.78	589.6
142	22.776	−727.03	151.09	114.83	25.69	55.96	578.5
144	22.460	−627.28	263.20	115.61	25.59	56.15	567.7
146	22.142	−527.60	375.68	116.39	25.50	56.33	557.2
148	21.822	−428.01	488.50	117.15	25.41	56.50	546.9
150	21.501	−328.54	601.66	117.91	25.32	56.66	536.9
155	20.693	−80.620	885.87	119.78	25.12	57.01	513.3
160	19.884	165.72	1171.6	121.59	24.92	57.25	491.8
165	19.077	409.75	1458.1	123.35	24.74	57.34	472.4
170	18.280	650.59	1744.7	125.07	24.56	57.24	455.3
175	17.500	887.32	2030.2	126.72	24.39	56.91	440.5
180	16.745	1119.0	2313.4	128.32	24.22	56.35	428.0
185	16.021	1344.9	2593.3	129.85	24.06	55.58	417.6
190	15.332	1564.4	2868.9	131.32	23.89	54.62	409.1
195	14.683	1777.1	3139.3	132.72	23.74	53.52	402.4
200	14.074	1982.9	3403.9	134.06	23.58	52.34	397.2
210	12.978	2374.1	3915.2	136.56	23.30	49.90	390.6
220	12.034	2740.3	4402.3	138.83	23.04	47.56	387.6
230	11.221	3084.8	4867.1	140.89	22.81	45.45	387.3
240	10.519	3410.9	5312.2	142.79	22.62	43.61	388.7
250	9.9093	3721.9	5740.2	144.53	22.45	42.03	391.3
260	9.3749	4020.3	6153.6	146.16	22.31	40.69	394.7
270	8.9032	4308.2	6554.6	147.67	22.19	39.54	398.6
280	8.4837	4587.4	6944.9	149.09	22.09	38.55	402.8
290	8.1078	4859.3	7326.1	150.43	22.00	37.71	407.3
300	7.7690	5125.0	7699.4	151.69	21.93	36.97	412.0
310	7.4616	5385.5	8065.9	152.89	21.86	36.34	416.7

TABLE A2. Thermodynamic properties of air—Continued

Temperature (K)	Density (mol/dm^3)	Internal energy (J/mol)	Enthalpy (J/mol)	Entropy J/(mol-K)	c_v J/(mol-K)	c_p J/(mol-K)	Speed of sound (m/s)
320	7.1814	5641.5	8426.5	154.04	21.81	35.79	421.5
330	6.9246	5893.6	8781.8	155.13	21.77	35.30	426.3
340	6.6882	6142.3	9132.7	156.18	21.74	34.87	431.1
350	6.4698	6388.2	9479.5	157.19	21.71	34.50	435.9
360	6.2673	6631.6	9822.8	158.15	21.69	34.17	440.6
370	6.0788	6872.8	10 163.0	159.08	21.68	33.87	445.3
380	5.9028	7112.2	10 500.0	159.98	21.67	33.61	450.0
390	5.7380	7349.9	10 835.0	160.85	21.67	33.38	454.6
400	5.5834	7586.1	11 168.0	161.70	21.68	33.18	459.2
450	4.9320	8752.1	12 807.0	165.56	21.76	32.46	481.1
500	4.4288	9904.1	14 420.0	168.96	21.94	32.09	501.8
550	4.0260	11 053.0	16 020.0	172.01	22.17	31.95	521.2
600	3.6950	12 204.0	17 617.0	174.79	22.45	31.95	539.5
650	3.4173	13 364.0	19 216.0	177.35	22.76	32.04	557.0
700	3.1804	14 533.0	20 822.0	179.73	23.08	32.20	573.7
750	2.9756	15 715.0	22 436.0	181.96	23.40	32.39	589.8
800	2.7966	16 910.0	24 061.0	184.05	23.72	32.61	605.2
900	2.4982	19 339.0	27 345.0	187.92	24.33	33.07	634.8
1000	2.2588	21 820.0	30 674.0	191.43	24.89	33.52	662.8
1100	2.0621	24 349.0	34 047.0	194.64	25.39	33.94	689.6
1200	1.8975	26 921.0	37 461.0	197.61	25.83	34.32	715.2
1300	1.7576	29 532.0	40 911.0	200.37	26.21	34.67	740.0
1400	1.6372	32 177.0	44 393.0	202.95	26.55	34.97	764.0
1500	1.5323	34 852.0	47 904.0	205.38	26.85	35.25	787.2
1600	1.4402	37 555.0	51 442.0	207.66	27.12	35.50	809.7
1700	1.3586	40 282.0	55 003.0	209.82	27.36	35.72	831.6
1800	1.2858	43 032.0	58 586.0	211.87	27.58	35.93	853.0
1900	1.2205	45 802.0	62 189.0	213.81	27.78	36.12	873.8
2000	1.1615	48 590.0	65 809.0	215.67	27.96	36.29	894.2
			50.0 MPa isobar				
68.21	34.238	−4581.8	−3121.4	72.575	34.51	51.91	1172.7
70	34.049	−4497.3	−3028.8	73.915	34.20	51.77	1163.3
72	33.837	−4403.1	−2925.4	75.371	33.87	51.60	1152.9
74	33.626	−4309.3	−2822.4	76.783	33.55	51.45	1142.5
76	33.416	−4216.0	−2719.7	78.153	33.24	51.29	1132.1
78	33.206	−4123.0	−2617.2	79.483	32.94	51.14	1121.8
80	32.997	−4030.4	−2515.1	80.776	32.65	50.99	1111.6
82	32.789	−3938.2	−2413.3	82.033	32.37	50.84	1101.4
84	32.581	−3846.4	−2311.7	83.257	32.10	50.70	1091.2
86	32.374	−3754.9	−2210.5	84.448	31.84	50.56	1081.1
88	32.167	−3663.9	−2109.5	85.609	31.59	50.42	1071.1
90	31.961	−3573.2	−2008.8	86.740	31.34	50.29	1061.2
92	31.756	−3482.9	−1908.3	87.844	31.10	50.16	1051.3
94	31.551	−3392.9	−1808.1	88.922	30.87	50.04	1041.5
96	31.346	−3303.3	−1708.2	89.974	30.65	49.91	1031.7
98	31.142	−3214.0	−1608.5	91.002	30.43	49.79	1022.0
100	30.939	−3125.1	−1509.0	92.007	30.22	49.68	1012.4
102	30.736	−3036.5	−1409.8	92.989	30.01	49.56	1002.9
104	30.534	−2948.3	−1310.8	93.950	29.81	49.45	993.4
106	30.332	−2860.4	−1212.0	94.891	29.62	49.34	984.1
108	30.130	−2772.9	−1113.4	95.813	29.43	49.23	974.8
110	29.929	−2685.6	−1015.0	96.715	29.25	49.13	965.6
112	29.729	−2598.8	−916.88	97.599	29.07	49.03	956.4
114	29.529	−2512.2	−818.93	98.466	28.90	48.93	947.4
116	29.329	−2426.0	−721.17	99.316	28.73	48.83	938.5
118	29.130	−2340.0	−623.60	100.15	28.57	48.74	929.6
120	28.932	−2254.4	−526.23	100.97	28.41	48.64	920.9
122	28.733	−2169.2	−429.04	101.77	28.26	48.55	912.3
124	28.536	−2084.2	−332.03	102.56	28.11	48.46	903.7
126	28.339	−1999.6	−235.21	103.34	27.96	48.37	895.3
128	28.142	−1915.3	−138.56	104.10	27.82	48.28	887.0
130	27.946	−1831.3	−42.096	104.84	27.68	48.19	878.8
132	27.750	−1747.6	54.197	105.58	27.55	48.10	870.7

TABLE A2. Thermodynamic properties of air—Continued

Temperature (K)	Density (mol/dm^3)	Internal energy (J/mol)	Enthalpy (J/mol)	Entropy J/(mol-K)	c_v J/(mol-K)	c_p J/(mol-K)	Speed of sound (m/s)
134	27.555	−1664.2	150.32	106.30	27.42	48.02	862.7
136	27.361	−1581.2	246.26	107.01	27.29	47.93	854.8
138	27.167	−1498.4	342.03	107.71	27.17	47.84	847.1
140	26.974	−1416.0	437.64	108.40	27.05	47.76	839.4
142	26.781	−1333.9	533.07	109.08	26.94	47.67	831.9
144	26.589	−1252.1	628.33	109.74	26.82	47.59	824.6
146	26.398	−1170.7	723.42	110.40	26.71	47.50	817.3
148	26.207	−1089.6	818.33	111.04	26.60	47.42	810.2
150	26.017	−1008.7	913.08	111.68	26.50	47.33	803.2
155	25.545	−808.12	1149.2	113.23	26.25	47.11	786.3
160	25.079	−609.54	1384.2	114.72	26.01	46.89	770.2
165	24.618	−413.01	1618.0	116.16	25.79	46.66	754.9
170	24.163	−218.56	1850.8	117.55	25.59	46.42	740.5
175	23.714	−26.212	2082.3	118.89	25.39	46.18	726.9
180	23.272	164.03	2312.6	120.19	25.21	45.93	714.1
185	22.837	352.15	2541.6	121.44	25.04	45.68	702.1
190	22.410	538.13	2769.3	122.66	24.88	45.41	690.9
195	21.990	721.98	2995.7	123.83	24.72	45.14	680.4
200	21.579	903.69	3220.7	124.97	24.58	44.87	670.6
210	20.783	1260.7	3666.6	127.15	24.31	44.29	653.1
220	20.022	1609.4	4106.6	129.20	24.07	43.70	638.1
230	19.299	1949.7	4540.6	131.13	23.86	43.10	625.4
240	18.613	2282.1	4968.5	132.95	23.66	42.49	614.7
250	17.963	2606.8	5390.3	134.67	23.49	41.88	605.8
260	17.350	2924.2	5806.0	136.30	23.33	41.27	598.5
270	16.773	3234.7	6215.8	137.85	23.19	40.68	592.7
280	16.228	3538.8	6619.8	139.32	23.06	40.12	588.0
290	15.716	3836.8	7018.2	140.71	22.95	39.57	584.4
300	15.234	4129.2	7411.3	142.05	22.85	39.06	581.7
310	14.780	4416.5	7799.4	143.32	22.76	38.57	579.7
320	14.353	4699.1	8182.8	144.54	22.68	38.11	578.4
330	13.950	4977.3	8561.7	145.70	22.61	37.68	577.7
340	13.569	5251.6	8936.4	146.82	22.55	37.28	577.4
350	13.210	5522.3	9307.3	147.90	22.50	36.91	577.6
360	12.870	5789.7	9674.6	148.93	22.45	36.56	578.1
370	12.549	6054.1	10 039.0	149.93	22.42	36.24	578.9
380	12.244	6315.8	10 399.0	150.89	22.39	35.94	580.0
390	11.955	6575.1	10 758.0	151.82	22.36	35.67	581.4
400	11.680	6832.1	11 113.0	152.72	22.35	35.42	582.9
450	10.489	8090.6	12 858.0	156.83	22.34	34.44	592.4
500	9.5353	9319.0	14 563.0	160.42	22.44	33.81	604.1
550	8.7536	10 531.0	16 243.0	163.63	22.62	33.44	616.6
600	8.0999	11 737.0	17 910.0	166.53	22.85	33.25	629.5
650	7.5440	12 943.0	19 571.0	169.19	23.11	33.19	642.5
700	7.0646	14 153.0	21 230.0	171.65	23.40	33.21	655.5
750	6.6465	15 370.0	22 892.0	173.94	23.69	33.29	668.3
800	6.2780	16 595.0	24 559.0	176.09	23.99	33.40	681.0
900	5.6573	19 076.0	27 915.0	180.04	24.57	33.71	705.9
1000	5.1533	21 599.0	31 302.0	183.61	25.09	34.04	730.0
1100	4.7351	24 163.0	34 722.0	186.87	25.57	34.37	753.6
1200	4.3818	26 764.0	38 175.0	189.88	25.99	34.68	776.5
1300	4.0790	29 400.0	41 658.0	192.66	26.36	34.97	798.8
1400	3.8164	32 066.0	45 168.0	195.27	26.69	35.23	820.6
1500	3.5862	34 760.0	48 703.0	197.70	26.98	35.47	841.8
1600	3.3828	37 479.0	52 260.0	200.00	27.23	35.68	862.5
1700	3.2015	40 221.0	55 839.0	202.17	27.47	35.88	882.8
1800	3.0389	42 983.0	59 436.0	204.23	27.68	36.07	902.6
1900	2.8923	45 764.0	63 051.0	206.18	27.87	36.23	922.0
2000	2.7593	48 562.0	66 683.0	208.04	28.04	36.39	941.1
			100.0 MPa isobar				
75.92	35.183	−4416.8	−1574.5	74.060	34.95	50.34	1281.8
76	35.176	−4413.2	−1570.4	74.114	34.94	50.34	1281.5
78	35.002	−4326.8	−1469.9	75.419	34.65	50.15	1273.7

TABLE A2. Thermodynamic properties of air—Continued

Temperature (K)	Density (mol/dm^3)	Internal energy (J/mol)	Enthalpy (J/mol)	Entropy J/(mol-K)	c_v J/(mol-K)	c_p J/(mol-K)	Speed of sound (m/s)
80	34.829	−4240.9	−1369.8	76.686	34.37	49.96	1265.9
82	34.658	−4155.4	−1270.0	77.918	34.10	49.78	1258.3
84	34.487	−4070.3	−1170.7	79.115	33.83	49.60	1250.6
86	34.318	−3985.6	−1071.6	80.280	33.58	49.42	1243.1
88	34.150	−3901.3	−972.99	81.414	33.33	49.24	1235.6
90	33.982	−3817.4	−874.69	82.518	33.09	49.06	1228.3
92	33.816	−3733.9	−776.74	83.595	32.85	48.89	1220.9
94	33.651	−3650.8	−679.13	84.644	32.63	48.72	1213.7
96	33.486	−3568.2	−581.87	85.668	32.40	48.55	1206.5
98	33.323	−3485.8	−484.94	86.668	32.19	48.38	1199.4
100	33.161	−3403.9	−388.34	87.644	31.98	48.22	1192.4
102	33.000	−3322.4	−292.06	88.597	31.78	48.06	1185.4
104	32.839	−3241.2	−196.11	89.528	31.58	47.90	1178.5
106	32.680	−3160.4	−100.48	90.439	31.39	47.74	1171.7
108	32.522	−3080.0	−5.1555	91.330	31.20	47.58	1165.0
110	32.365	−2999.9	89.857	92.202	31.02	47.43	1158.3
112	32.208	−2920.2	184.56	93.055	30.84	47.28	1151.7
114	32.053	−2840.9	278.97	93.891	30.66	47.13	1145.2
116	31.898	−2761.9	373.08	94.709	30.50	46.98	1138.7
118	31.745	−2683.2	466.90	95.511	30.33	46.84	1132.3
120	31.592	−2604.9	560.44	96.297	30.17	46.69	1126.0
122	31.440	−2527.0	653.68	97.067	30.01	46.55	1119.8
124	31.289	−2449.3	746.65	97.823	29.86	46.41	1113.6
126	31.139	−2372.0	839.34	98.565	29.71	46.28	1107.5
128	30.990	−2295.1	931.76	99.293	29.57	46.14	1101.5
130	30.842	−2218.4	1023.9	100.01	29.43	46.01	1095.5
132	30.695	−2142.1	1115.8	100.71	29.29	45.88	1089.7
134	30.548	−2066.1	1207.4	101.40	29.15	45.75	1083.9
136	30.403	−1990.4	1298.8	102.07	29.02	45.62	1078.1
138	30.258	−1915.0	1389.9	102.74	28.90	45.49	072.5
140	30.114	−1840.0	1480.7	103.39	28.77	45.36	1066.9
142	29.971	−1765.2	1571.4	104.04	28.65	45.24	1061.4
144	29.829	−1690.7	1661.7	104.67	28.53	45.12	1055.9
146	29.688	−1616.6	1751.8	105.29	28.41	45.00	1050.6
148	29.547	−1542.7	1841.7	105.90	28.30	44.88	1045.3
150	29.408	−1469.1	1931.3	106.50	28.19	44.76	1040.1
155	29.062	−1286.5	2154.4	107.96	27.92	44.47	1027.3
160	28.722	−1105.6	2376.1	109.37	27.67	44.19	1015.0
165	28.387	−926.45	2596.3	110.73	27.43	43.91	1003.2
170	28.057	−748.99	2815.2	112.03	27.20	43.65	991.7
175	27.732	−573.18	3032.8	113.30	26.99	43.38	980.8
180	27.412	−398.99	3249.0	114.51	26.78	43.13	970.2
185	27.097	−226.38	3464.1	115.69	26.59	42.88	960.0
190	26.787	−55.313	3677.9	116.83	26.41	42.64	950.3
195	26.482	114.25	3890.4	117.94	26.23	42.40	941.0
200	26.182	282.34	4101.8	119.01	26.07	42.16	932.0
210	25.596	614.24	4521.2	121.05	25.76	41.71	915.2
220	25.029	940.66	4936.1	122.98	25.48	41.27	899.9
230	24.481	1261.9	5346.7	124.81	25.23	40.86	885.9
240	23.951	1578.1	5753.2	126.54	24.99	40.45	873.2
250	23.440	1889.6	6155.8	128.18	24.78	40.07	861.6
260	22.946	2196.6	6554.6	129.75	24.59	39.70	851.2
270	22.469	2499.3	6949.8	131.24	24.42	39.34	841.7
280	22.009	2798.0	7341.5	132.66	24.26	39.00	833.1
290	21.566	3092.9	7729.9	134.03	24.11	38.68	825.4
300	21.138	3384.3	8115.1	135.33	23.98	38.37	818.5
310	20.725	3672.2	8497.3	136.59	23.86	38.07	812.2
320	20.327	3956.9	8876.6	137.79	23.75	37.78	806.7
330	19.942	4238.6	9253.0	138.95	23.65	37.51	801.7
340	19.572	4517.5	9626.9	140.06	23.57	37.26	797.3
350	19.214	4793.8	9998.2	141.14	23.49	37.01	793.3
360	18.869	5067.6	10 367.0	142.18	23.42	36.78	789.9
370	18.536	5339.1	10 734.0	143.19	23.35	36.56	786.8

TABLE A2. Thermodynamic properties of air—Continued

Temperature (K)	Density (mol/dm^3)	Internal energy (J/mol)	Enthalpy (J/mol)	Entropy J/(mol-K)	c_v J/(mol-K)	c_p J/(mol-K)	Speed of sound (m/s)
380	18.214	5608.4	11 099.0	144.16	23.30	36.36	784.1
390	17.904	5875.7	11 461.0	145.10	23.25	36.16	781.8
400	17.604	6141.2	11 822.0	146.01	23.21	35.98	779.8
450	16.245	7445.0	13 601.0	150.20	23.10	35.22	773.7
500	15.089	8720.1	15 347.0	153.88	23.12	34.69	772.4
550	14.095	9977.4	17 072.0	157.17	23.22	34.34	774.3
600	13.231	11 225.0	18 784.0	160.15	23.39	34.13	778.2
650	12.473	12 470.0	20 487.0	162.88	23.61	34.03	783.7
700	11.803	13 716.0	22 188.0	165.40	23.86	34.01	790.1
750	11.206	14 966.0	23 889.0	167.75	24.11	34.05	797.4
800	10.671	16 222.0	25 593.0	169.95	24.38	34.12	805.1
900	9.7481	18 757.0	29 015.0	173.98	24.90	34.33	821.8
1000	8.9805	21 326.0	32 461.0	177.61	25.39	34.59	839.3
1100	8.3307	23 929.0	35 933.0	180.92	25.83	34.85	857.4
1200	7.7726	26 565.0	39 430.0	183.96	26.23	35.10	875.6
1300	7.2877	29 230.0	42 952.0	186.78	26.58	35.34	893.9
1400	6.8619	31 923.0	46 497.0	189.40	26.89	35.55	912.2
1500	6.4847	34 641.0	50 062.0	191.86	27.16	35.75	930.3
1600	6.1481	37 381.0	53 647.0	194.18	27.40	35.94	948.2
1700	5.8456	40 142.0	57 249.0	196.36	27.62	36.10	965.9
1800	5.5723	42 921.0	60 867.0	198.43	27.82	36.26	983.4
1900	5.3239	45 717.0	64 501.0	200.39	28.01	36.41	1000.6
2000	5.0972	48 530.0	68 148.0	202.26	28.17	36.55	1017.7
			200.0 MPa isobar				
89.73	36.712	−4043.0	1404.9	76.473	35.48	48.75	1462.1
90	36.693	−4032.4	1418.2	76.622	35.45	48.72	1461.4
92	36.561	−3954.8	1515.5	77.691	35.22	48.54	1456.1
94	36.430	−3877.6	1612.4	78.733	35.00	48.37	1450.9
96	36.299	−3800.8	1708.9	79.749	34.78	48.19	1445.8
98	36.170	−3724.3	1805.2	80.741	34.56	48.02	1440.7
100	36.042	−3648.1	1901.0	81.710	34.36	47.85	1435.7
102	35.914	−3572.3	1996.6	82.655	34.15	47.68	1430.7
104	35.788	−3496.8	2091.7	83.580	33.96	47.51	1425.8
106	35.662	−3421.6	2186.6	84.483	33.76	47.35	1420.9
108	35.538	−3346.7	2281.1	85.366	33.58	47.18	1416.1
110	35.414	−3272.1	2375.3	86.231	33.39	47.02	1411.4
112	35.291	−3197.9	2469.2	87.076	33.21	46.86	1406.6
114	35.170	−3124.0	2562.8	87.904	33.04	46.70	1402.0
116	35.049	−3050.3	2656.0	88.715	32.87	46.54	1397.4
118	34.929	−2977.0	2748.9	89.510	32.70	46.39	1392.8
120	34.810	−2904.0	2841.6	90.288	32.54	46.24	1388.3
122	34.691	−2831.3	2933.9	91.051	32.38	46.09	1383.8
124	34.574	−2758.8	3025.9	91.799	32.22	45.94	1379.4
126	34.457	−2686.6	3117.6	92.533	32.07	45.79	1375.0
128	34.342	−2614.8	3209.1	93.253	31.92	45.65	1370.7
130	34.227	−2543.2	3300.2	93.960	31.77	45.50	1366.4
132	34.113	−2471.8	3391.1	94.653	31.63	45.36	1362.2
134	33.999	−2400.8	3481.7	95.334	31.49	45.22	1358.0
136	33.887	−2330.0	3572.0	96.003	31.35	45.08	1353.9
138	33.775	−2259.5	3662.0	96.661	31.22	44.95	1349.8
140	33.664	−2189.2	3751.8	97.306	31.09	44.81	1345.8
142	33.554	−2119.2	3841.3	97.941	30.96	44.68	1341.8
144	33.445	−2049.5	3930.5	98.565	30.84	44.55	1337.8
146	33.336	−1980.0	4019.5	99.179	30.71	44.42	1333.9
148	33.228	−1910.8	4108.2	99.782	30.59	44.30	1330.0
150	33.121	−1841.8	4196.7	100.38	30.47	44.17	1326.2
155	32.856	−1670.3	4416.7	101.82	30.19	43.86	1316.8
160	32.596	−1500.4	4635.3	103.21	29.92	43.57	1307.7
165	32.340	−1331.8	4852.4	104.54	29.66	43.28	1298.8
170	32.088	−1164.7	5068.1	105.83	29.42	43.00	1290.2
175	31.841	−998.86	5282.4	107.07	29.18	42.73	1281.9
180	31.597	−834.33	5495.4	108.27	28.96	42.47	1273.7
185	31.357	−671.06	5707.1	109.43	28.74	42.21	1265.8

TABLE A2. Thermodynamic properties of air—Continued

Temperature (K)	Density (mol/dm^3)	Internal energy (J/mol)	Enthalpy (J/mol)	Entropy J/(mol-K)	c_v J/(mol-K)	c_p J/(mol-K)	Speed of sound (m/s)
190	31.121	−509.01	5917.5	110.56	28.54	41.97	1258.1
195	30.888	−348.14	6126.8	111.64	28.34	41.73	1250.7
200	30.660	−188.42	6334.8	112.70	28.16	41.50	1243.4
210	30.212	127.71	6747.6	114.71	27.81	41.05	1229.6
220	29.778	439.64	7156.0	116.61	27.48	40.64	1216.5
230	29.357	747.62	7560.4	118.41	27.19	40.25	1204.2
240	28.947	1051.9	7961.0	120.11	26.91	39.87	1192.5
250	28.549	1352.6	8358.0	121.73	26.66	39.52	1181.6
260	28.163	1650.0	8751.5	123.28	26.43	39.19	1171.3
270	27.787	1944.3	9141.9	124.75	26.21	38.88	1161.6
280	27.421	2235.6	9529.3	126.16	26.01	38.59	1152.5
290	27.065	2524.1	9913.7	127.51	25.83	38.31	1143.9
300	26.718	2810.0	10 295.0	128.80	25.66	38.05	1135.8
310	26.381	3093.4	10 675.0	130.05	25.50	37.80	1128.2
320	26.052	3374.5	11 052.0	131.24	25.36	37.56	1121.0
330	25.731	3653.4	11 426.0	132.40	25.23	37.34	1114.3
340	25.419	3930.3	11 798.0	133.51	25.10	37.13	1107.9
350	25.114	4205.2	12 169.0	134.58	24.99	36.94	1101.9
360	24.817	4478.3	12 537.0	135.62	24.89	36.75	1096.3
370	24.527	4749.7	12 904.0	136.62	24.80	36.58	1091.0
380	24.245	5019.5	13 269.0	137.60	24.71	36.41	1086.1
390	23.968	5287.8	13 632.0	138.54	24.63	36.26	1081.4
400	23.699	5554.8	13 994.0	139.46	24.57	36.12	1077.0
450	22.441	6872.0	15 784.0	143.67	24.32	35.53	1058.7
500	21.316	8167.3	17 550.0	147.39	24.22	35.12	1045.4
550	20.305	9449.0	19 299.0	150.73	24.23	34.86	1035.9
600	19.391	10 723.0	21 037.0	153.75	24.32	34.70	1029.4
650	18.562	11 995.0	22 770.0	156.53	24.46	34.64	1025.3
700	17.804	13 269.0	24 502.0	159.10	24.64	34.63	1023.1
750	17.111	14 545.0	26 234.0	161.49	24.84	34.67	1022.5
800	16.473	15 828.0	27 969.0	163.72	25.06	34.74	1023.1
900	15.338	18 412.0	31 452.0	167.83	25.50	34.93	1027.4
1000	14.359	21 027.0	34 955.0	171.52	25.92	35.15	1034.5
1100	13.505	23 671.0	38 481.0	174.88	26.31	35.37	1043.7
1200	12.752	26 345.0	42 029.0	177.97	26.66	35.59	1054.4
1300	12.083	29 045.0	45 598.0	180.82	26.97	35.79	1066.0
1400	11.484	31 770.0	49 186.0	183.48	27.24	35.97	1078.4
1500	10.944	34 517.0	52 791.0	185.97	27.49	36.13	1091.3
1600	10.455	37 284.0	56 412.0	188.30	27.71	36.29	1104.5
1700	10.010	40 069.0	60 048.0	190.51	27.91	36.43	1118.0
1800	9.6027	42 870.0	63 698.0	192.60	28.09	36.56	1131.6
1900	9.2283	45 688.0	67 360.0	194.58	28.26	36.68	1145.2
2000	8.8829	48 519.0	71 034.0	196.46	28.41	36.80	1158.9
			500.0 MPa isobar				
123.66	39.920	−2818.8	9706.4	81.122	36.30	47.19	1860.1
124	39.905	−2807.3	9722.5	81.252	36.27	47.17	1859.6
126	39.820	−2739.8	9816.7	82.006	36.12	47.04	1856.8
128	39.736	−2672.5	9910.6	82.745	35.97	46.90	1853.9
130	39.652	−2605.5	10 004.0	83.472	35.82	46.77	1851.0
132	39.569	−2538.6	10 098.0	84.185	35.67	46.64	1848.2
134	39.486	−2471.9	10 191.0	84.885	35.53	46.51	1845.4
136	39.404	−2405.3	10 284.0	85.573	35.39	46.38	1842.7
138	39.322	−2339.0	10 376.0	86.249	35.25	46.25	1839.9
140	39.241	−2272.9	10 469.0	86.914	35.12	46.13	1837.2
142	39.161	−2206.9	10 561.0	87.567	34.98	46.00	1834.5
144	39.081	−2141.1	10 653.0	88.210	34.85	45.88	1831.8
146	39.002	−2075.5	10 744.0	88.842	34.72	45.75	1829.1
148	38.923	−2010.1	10 836.0	89.464	34.59	45.63	1826.5
150	38.845	−1944.8	10 927.0	90.075	34.47	45.51	1823.9
155	38.651	−1782.4	11 154.0	91.563	34.17	45.21	1817.5
160	38.461	−1621.1	11 379.0	92.994	33.87	44.92	1811.2
165	38.274	−1460.8	11 603.0	94.372	33.60	44.64	1805.0
170	38.089	−1301.6	11 826.0	95.700	33.33	44.37	1799.0

TABLE A2. Thermodynamic properties of air—Continued

Temperature (K)	Density (mol/dm^3)	Internal energy (J/mol)	Enthalpy (J/mol)	Entropy J/(mol-K)	c_v J/(mol-K)	c_p J/(mol-K)	Speed of sound (m/s)
175	37.908	−1143.2	12 047.0	96.982	33.07	44.10	1793.1
180	37.729	−985.89	12 267.0	98.221	32.82	43.84	1787.4
185	37.553	−829.45	12 485.0	99.419	32.58	43.58	1781.7
190	37.380	−673.92	12 702.0	100.58	32.35	43.33	1776.2
195	37.209	−519.26	12 918.0	101.70	32.13	43.09	1770.8
200	37.041	−365.46	13 133.0	102.79	31.91	42.86	1765.5
210	36.711	−60.311	13 560.0	104.87	31.51	42.40	1755.2
220	36.391	241.69	13 981.0	106.83	31.13	41.98	1745.3
230	36.079	540.72	14 399.0	108.69	30.78	41.57	1735.8
240	35.776	836.94	14 813.0	110.45	30.45	41.19	1726.7
250	35.480	1130.5	15 223.0	112.12	30.14	40.82	1718.0
260	35.192	1421.5	15 629.0	113.72	29.85	40.47	1709.5
270	34.911	1710.2	16 032.0	115.24	29.58	40.15	1701.4
280	34.636	1996.6	16 432.0	116.69	29.33	39.84	1693.6
290	34.368	2280.8	16 829.0	118.09	29.10	39.54	1686.1
300	34.106	2563.1	17 223.0	119.42	28.88	39.27	1678.8
310	33.850	2843.4	17 615.0	120.70	28.67	39.00	1671.8
320	33.599	3122.0	18 003.0	121.94	28.47	38.75	1665.0
330	33.354	3398.9	18 390.0	123.13	28.29	38.52	1658.5
340	33.114	3674.2	18 774.0	124.27	28.12	38.30	1652.2
350	32.878	3948.0	19 156.0	125.38	27.96	38.09	1646.0
360	32.648	4220.5	19 536.0	126.45	27.82	37.89	1640.1
370	32.421	4491.6	19 913.0	127.49	27.68	37.70	1634.4
380	32.200	4761.5	20 290.0	128.49	27.55	37.52	1628.8
390	31.982	5030.3	20 664.0	129.46	27.43	37.36	1623.4
400	31.769	5298.0	21 037.0	130.41	27.32	37.20	1618.2
450	30.756	6623.2	22 880.0	134.75	26.89	36.56	1594.3
500	29.826	7932.1	24 696.0	138.58	26.61	36.11	1573.6
550	28.965	9231.2	26 494.0	142.00	26.47	35.81	1555.7
600	28.164	10 526.0	28 279.0	145.11	26.41	35.63	1540.0
650	27.416	11 820.0	30 058.0	147.96	26.43	35.53	1526.5
700	26.714	13 116.0	31 833.0	150.59	26.50	35.49	1514.8
750	26.054	14 417.0	33 608.0	153.04	26.60	35.51	1504.7
800	25.431	15 724.0	35 384.0	155.33	26.72	35.55	1496.1
900	24.283	18 356.0	38 947.0	159.53	26.99	35.70	1482.8
1000	23.247	21 018.0	42 526.0	163.30	27.27	35.89	1473.8
1100	22.305	23 707.0	46 124.0	166.73	27.54	36.08	1468.3
1200	21.443	26 424.0	49 741.0	169.87	27.79	36.26	1465.5
1300	20.651	29 164.0	53 375.0	172.78	28.01	36.43	1465.0
1400	19.921	31 926.0	57 026.0	175.49	28.21	36.58	1466.3
1500	19.243	34 708.0	60 691.0	178.02	28.39	36.72	1469.2
1600	18.614	37 508.0	64 370.0	180.39	28.55	36.85	1473.2
1700	18.027	40 324.0	68 061.0	182.63	28.70	36.97	1478.2
1800	17.478	43 155.0	71 763.0	184.74	28.83	37.08	1484.0
1900	16.963	46 000.0	75 476.0	186.75	28.95	37.18	1490.5
2000	16.480	48 857.0	79 198.0	188.66	29.07	37.27	1497.6
			1000.0 MPa isobar				
167.86	43.415	−736.70	22 297.0	85.397	37.29	46.74	2313.2
170	43.352	−670.08	22 397.0	85.987	37.17	46.63	2311.1
175	43.208	−514.75	22 629.0	87.335	36.90	46.38	2306.4
180	43.065	−360.10	22 860.0	88.639	36.65	46.14	2301.7
185	42.925	−206.12	23 091.0	89.899	36.40	45.90	2297.0
190	42.786	−52.792	23 319.0	91.120	36.15	45.66	2292.5
195	42.649	99.887	23 547.0	92.303	35.92	45.43	2288.0
200	42.514	251.93	23 774.0	93.451	35.69	45.20	2283.6
210	42.249	554.16	24 224.0	95.645	35.25	44.76	2275.0
220	41.990	853.98	24 669.0	97.718	34.84	44.33	2266.7
230	41.738	1151.5	25 110.0	99.679	34.45	43.92	2258.6
240	41.493	1446.8	25 548.0	101.54	34.08	43.53	2250.8
250	41.252	1740.0	25 981.0	103.31	33.74	43.16	2243.3
260	41.018	2031.1	26 411.0	105.00	33.41	42.80	2235.9
270	40.789	2320.3	26 837.0	106.60	33.10	42.45	2228.8
280	40.565	2607.7	27 260.0	108.14	32.81	42.12	2221.8

TABLE A2. Thermodynamic properties of air—Continued

Temperature (K)	Density (mol/dm^3)	Internal energy (J/mol)	Enthalpy (J/mol)	Entropy J/(mol-K)	c_v J/(mol-K)	c_p J/(mol-K)	Speed of sound (m/s)
290	40.345	2893.3	27 679.0	109.61	32.53	41.81	2215.1
300	40.130	3177.3	28 096.0	111.03	32.27	41.51	2208.5
310	39.920	3459.6	28 510.0	112.38	32.02	41.22	2202.1
320	39.714	3740.5	28 921.0	113.69	31.79	40.95	2195.9
330	39.512	4019.9	29 329.0	114.94	31.57	40.69	2189.8
340	39.314	4297.9	29 734.0	116.15	31.36	40.44	2183.9
350	39.119	4574.7	30 138.0	117.32	31.17	40.21	2178.1
360	38.928	4850.3	30 539.0	118.45	30.98	39.98	2172.4
370	38.741	5124.8	30 937.0	119.55	30.81	39.77	2166.9
380	38.557	5398.2	31 334.0	120.60	30.65	39.57	2161.5
390	38.376	5670.7	31 729.0	121.63	30.49	39.38	2156.2
400	38.198	5942.2	32 122.0	122.62	30.35	39.19	2151.1
450	37.351	7288.1	34 061.0	127.19	29.75	38.42	2126.8
500	36.567	8619.7	35 967.0	131.21	29.33	37.84	2104.7
550	35.836	9942.8	37 848.0	134.80	29.06	37.42	2084.6
600	35.150	11 262.0	39 711.0	138.04	28.88	37.13	2066.2
650	34.505	12 581.0	41 562.0	141.00	28.79	36.93	2049.3
700	33.895	13 902.0	43 405.0	143.73	28.75	36.80	2033.9
750	33.316	15 228.0	45 243.0	146.27	28.76	36.73	2019.9
800	32.765	16 559.0	47 079.0	148.64	28.80	36.69	2007.0
900	31.736	19 238.0	50 748.0	152.96	28.92	36.70	1984.7
1000	30.791	21 944.0	54 421.0	156.83	29.07	36.77	1966.3
1100	29.916	24 676.0	58 103.0	160.34	29.22	36.86	1951.2
1200	29.101	27 431.0	61 794.0	163.55	29.36	36.96	1939.0
1300	28.338	30 207.0	65 495.0	166.51	29.49	37.06	1929.2
1400	27.622	33 003.0	69 206.0	169.26	29.60	37.16	1921.4
1500	26.946	35 816.0	72 927.0	171.83	29.70	37.25	1915.5
1600	26.307	38 644.0	76 656.0	174.24	29.79	37.34	1911.0
1700	25.701	41 486.0	80 395.0	176.50	29.88	37.42	1908.0
1800	25.125	44 341.0	84 141.0	178.65	29.95	37.51	1906.1
1900	24.577	47 208.0	87 896.0	180.68	30.02	37.58	1905.2
2000	24.054	50 085.0	91 658.0	182.60	30.08	37.66	1905.3
			2000.0 MPa isobar				
236.19	47.967	3353.0	45 048.0	90.033	38.84	46.92	2923.5
240	47.893	3466.7	45 227.0	90.783	38.69	46.79	2920.7
250	47.700	3764.2	45 693.0	92.685	38.33	46.43	2913.6
260	47.512	4060.2	46 155.0	94.499	37.98	46.08	2906.7
270	47.327	4354.8	46 614.0	96.232	37.64	45.74	2899.8
280	47.145	4648.0	47 070.0	97.890	37.32	45.41	2893.2
290	46.968	4939.9	47 522.0	99.477	37.01	45.09	2886.7
300	46.793	5230.5	47 972.0	101.00	36.72	44.78	2880.3
310	46.622	5519.8	48 418.0	102.46	36.44	44.49	2874.1
320	46.454	5808.0	48 862.0	103.87	36.17	44.20	2867.9
330	46.289	6094.9	49 302.0	105.23	35.92	43.92	2861.9
340	46.126	6380.8	49 740.0	106.54	35.68	43.66	2856.1
350	45.967	6665.7	50 175.0	107.80	35.44	43.40	2850.3
360	45.810	6949.6	50 608.0	109.02	35.22	43.15	2844.6
370	45.656	7232.5	51 038.0	110.20	35.02	42.92	2839.0
380	45.504	7514.5	51 466.0	111.34	34.82	42.69	2833.6
390	45.355	7795.7	51 892.0	112.44	34.63	42.48	2828.2
400	45.208	8076.2	52 316.0	113.52	34.45	42.27	2822.9
450	44.506	9468.3	54 406.0	118.44	33.68	41.36	2797.6
500	43.852	10 848.0	56 455.0	122.76	33.11	40.65	2774.1
550	43.240	12 220.0	58 473.0	126.61	32.68	40.09	2752.1
600	42.664	13 588.0	60 466.0	130.07	32.37	39.66	2731.6
650	42.120	14 956.0	62 440.0	133.23	32.15	39.32	2712.4
700	41.603	16 326.0	64 400.0	136.14	32.00	39.07	2694.4
750	41.111	17 700.0	66 349.0	138.83	31.90	38.88	2677.5
800	40.641	19 078.0	68 289.0	141.33	31.84	38.73	2661.8
900	39.760	21 849.0	72 151.0	145.88	31.78	38.53	2633.2
1000	38.945	24 643.0	75 998.0	149.94	31.77	38.41	2608.2
1100	38.184	27 458.0	79 835.0	153.59	31.79	38.34	2586.1
1200	37.471	30 292.0	83 666.0	156.93	31.80	38.29	2566.7

TABLE A2. Thermodynamic properties of air—Continued

Temperature (K)	Density (mol/dm^3)	Internal energy (J/mol)	Enthalpy (J/mol)	Entropy J/(mol-K)	c_v J/(mol-K)	c_p J/(mol-K)	Speed of sound (m/s)
1300	36.799	33 143.0	87 493.0	159.99	31.82	38.25	2549.5
1400	36.162	36 010.0	91 317.0	162.82	31.83	38.22	2534.2
1500	35.556	38 889.0	95 138.0	165.46	31.84	38.21	2520.6
1600	34.978	41 780.0	98 958.0	167.93	31.85	38.20	2508.5
1700	34.425	44 680.0	102 780.0	170.24	31.85	38.19	2497.8
1800	33.894	475 90.0	106 600.0	172.42	31.85	38.19	2488.2
1900	33.384	505 07.0	110 420.0	174.49	31.86	38.20	2479.6
2000	32.893	534 33.0	114 240.0	176.45	31.86	38.21	2472.1